

Supporting Information

**Stable Meisenheimer Complexes as Powerful Photoreductants
Readily Obtained from Aza-Hetero Aromatic Compounds**

F. Calogero, L. Wilczek, E. Pinosa, A. Gualandi, R. Dorta, A. Herrera, Y. Dai, A. Rossignol,
F. Negri*, Z. Ziani, A. Fermi, P. Ceroni*, P. G. Cozzi**

Supporting Information: Stable Meisenheimer Complexes as Powerful Photoreductants Readily Obtained from Aza-Hetero Aromatic Compounds

Francesco Calogero,^[a,b] Leonie Wilczek,^[a] Emanuele Pinosa,^[a,b] Andrea Gualandi,^{*,[a,b]} Romano Dorta,^[c] Alberto Herrera,^[c] Yasi Dai,^[a,b] Arthur Rossignol,^[a] Fabrizia Negri,^{*,[a,b]} Zakaria Ziani,^[a,b] Andrea Fermi,^[a,b] Paola Ceroni,^{*,[a,b]} and Pier Giorgio Cozzi^{*,[a,b]}

-
- [a] Dr. F. Calogero, Ms. L. Wilczek, Mr. E. Pinosa, Prof. A. Gualandi, Dr. Y. Dai, Mr. A. Rossignol, Prof. F. Negri, Dr. Z. Ziani, Dr. A. Fermi, Prof. P. Ceroni, Prof. P. G. Cozzi
Dipartimento di Chimica “Giacomo Ciamician”
Alma Mater Studiorum – Università di Bologna
Via Gobetti 85, 40129 Bologna, Italy
E-mail: andrea.gualandi10@unibo.it; paola.ceroni@unibo.it; fabrizia.negri@unibo.it, piergiorgio.cozzi@unibo.it
- [b] Dr. F. Calogero, Mr. E. Pinosa, Prof. A. Gualandi, Dr. Y. Dai, Prof. F. Negri, Dr. Z. Ziani, Dr. A. Fermi, Prof. P. Ceroni, Prof. P. G. Cozzi
Center for Chemical Catalysis – C3
Alma Mater Studiorum – Università di Bologna
Via Gobetti 85, 40129 Bologna, Italy
- [C] Prof. R. Dorta, Dr. A. Herrera
Department of Chemistry and Pharmacy
Friedrich-Alexander-Universität
Egerlandstr. 1, 91058 Erlangen

Synthetic details.	3
Synthesis of unreported starting materials.	9
General Procedures.	10
Characterization of the products.	19
Optimization for photoinduced detosylation of amines.	24
Photophysical investigation.	25
Computational details.	32
References.	47
NMR Traces.	48

Organic Synthesis details.

¹H-NMR spectra were recorded on Varian Mercury 400, Inova 600, or Bruker 600 spectrometers. Chemical shifts are reported in ppm from TMS with the residual solvent resonance as the internal standard (CHCl₃: δ = 7.26 ppm). Data are reported as follows: chemical shift, multiplicity (s = singlet, d = duplet, t = triplet, q = quartet, dd = double duplet, m = multiplet), coupling constants (Hz). ¹³C-NMR spectra were recorded on Varian Mercury 400, Inova 600, or Bruker 600 spectrometers. Chemical shifts are reported in ppm from TMS with the solvent as the internal standard (CDCl₃: δ = 77.0 ppm). LC-electrospray ionization mass spectra (ESI-MS) were obtained with Agilent Technologies MSD1100 equipped with a single-quadrupole mass spectrometer. Chromatographic purifications were done with 240-400 mesh silica gel. HRMS spectra were obtained with a G2XS QToF mass spectrometer using either ESI or APCI ionization techniques, as specified case by case.

All the reagents were purchased from commercial sources (Sigma-Aldrich, Alfa Aesar, Fluorochem, Strem Chemicals, TCI) and used without further purification unless specified.

All reactions requiring an inert atmosphere were set up under argon in heat gun-dried glassware using standard Schlenk techniques unless specified.

Anhydrous solvents were supplied by Aldrich in Sureseal[®] bottles and, unless specified, were used without further treatment.

Anhydrous tetrahydrofuran (THF), diethyl ether (DET), and 1,2-dimethoxyethane (DME) were obtained by standard sodium/benzophenone ketyl distillation starting from reagent grade solvent, supplied by TCI[®] or Sigma Aldrich[®].

Freshly distilled THF, DET, and DME were stored under an argon atmosphere in a dry Schlenk tube, equipped with a Rotaflo[®] stopcock with activated 3Å molecular sieves (*ca.* 5 g of MS for 100 mL of solvent). 3Å molecular sieves were supplied by Sigma-Aldrich. Activation of the MS was performed through five 6-minute cycles in a microwave (750 W). Once the cycles are completed the MS is rapidly inserted in a dry Schlenk tube, equipped with a Rotaflo[®] stopcock, and then heat gun-dried for 5 minutes under vacuum before starting the distillation.

Photocatalytic reactions were irradiated with Kessil[®] PR160L@456 nm and Kessil[®] PR160L@525 nm.^[1]

***n*BuLi 1.6 M in hexane or 2.5 M in hexane** was purchased by Sigma Aldrich[®] and used without further purification. Before its first usage, it is stored at room temperature. Following its first use, it is kept refrigerated at a temperature between 2° and 8° C.

1 was purchased by Fluorochem[®] or Sigma Aldrich[®] and used without further purification.

2 was purchased by Sigma Aldrich[®]. and was stirred one day over KOH and distilled before its use.

3 was purchased by Sigma Aldrich[®] and used without further purification.

4 was purchased by Sigma Aldrich[®]. and was distilled under reduced pressure before its use.

5 was purchased by Sigma Aldrich[®]. and was distilled under reduced pressure before its use.

Substrate **6** was purchased by Sigma Aldrich[®] and used without further purification.

Substrates **7** was purchased by TCI[®] and used without further purification.

Substrate **8** was purchased by Sigma Aldrich[®] and used without further purification.

Substrates **14a-j**, **16a**, **17a**, and **19a-f** were prepared according to previously reported synthetic protocol. Spectroscopic data match with what has already been reported in the literature.^[2-11]

Figure S1. The emission profile of the Kessil® PR160L@456 and PR160L@525 nm was used to irradiate the solutions (from the Kessil® website⁽¹⁾).

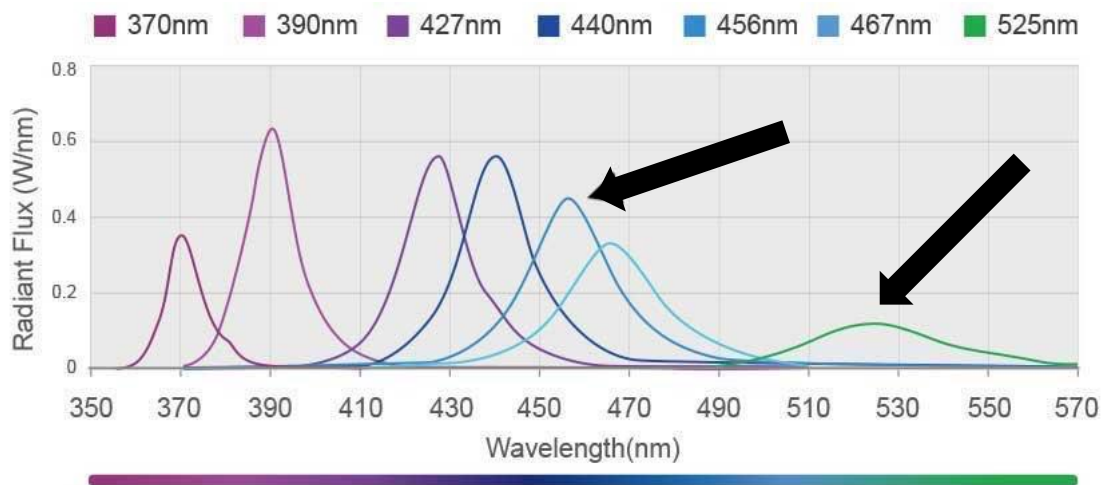


Figure S2. On the left 1 in THF; on the right 1•nBuLi in THF.

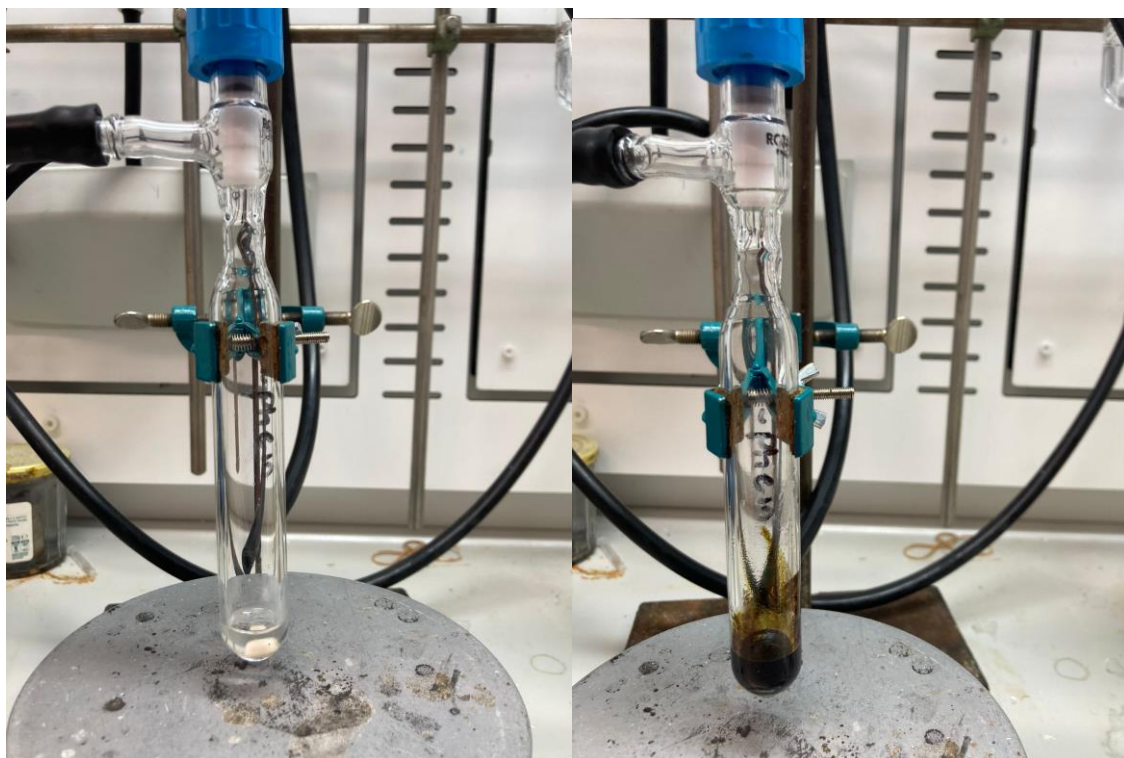


Figure S3. On the left 2 in DET; on the right 2-*n*BuLi in DET.



Figure S4. Reaction set-up for radical cyclization before and during irradiation with Kessil® PR160L@456 nm lamp.

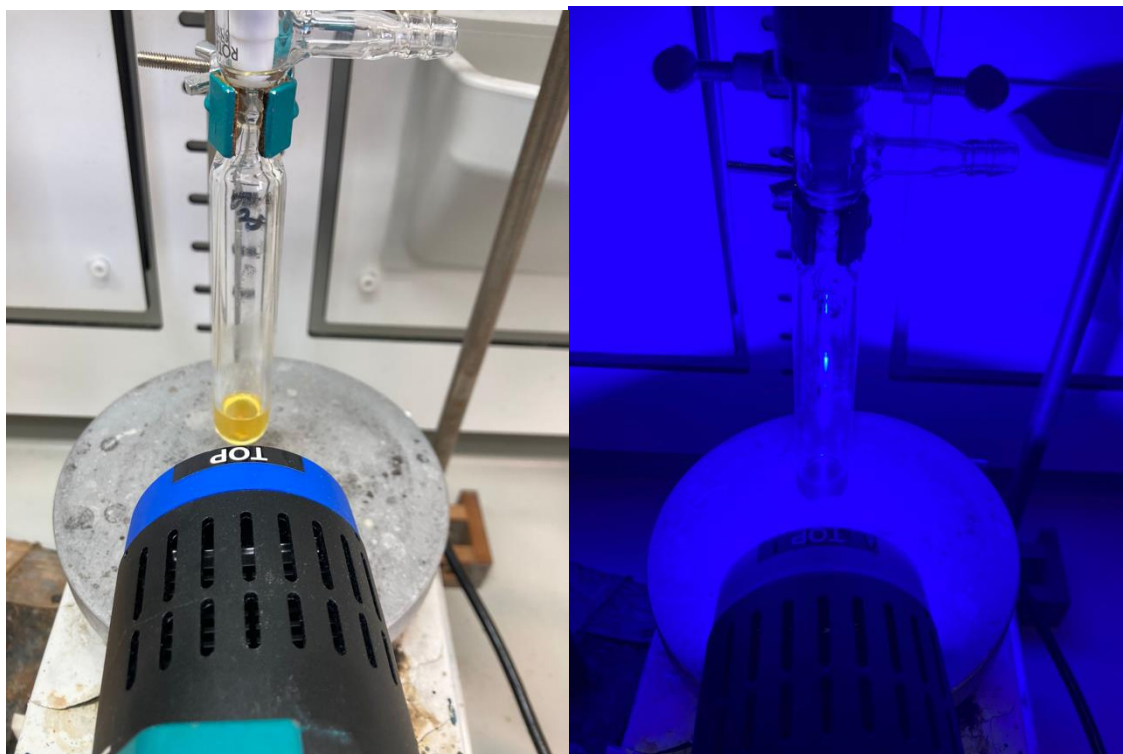
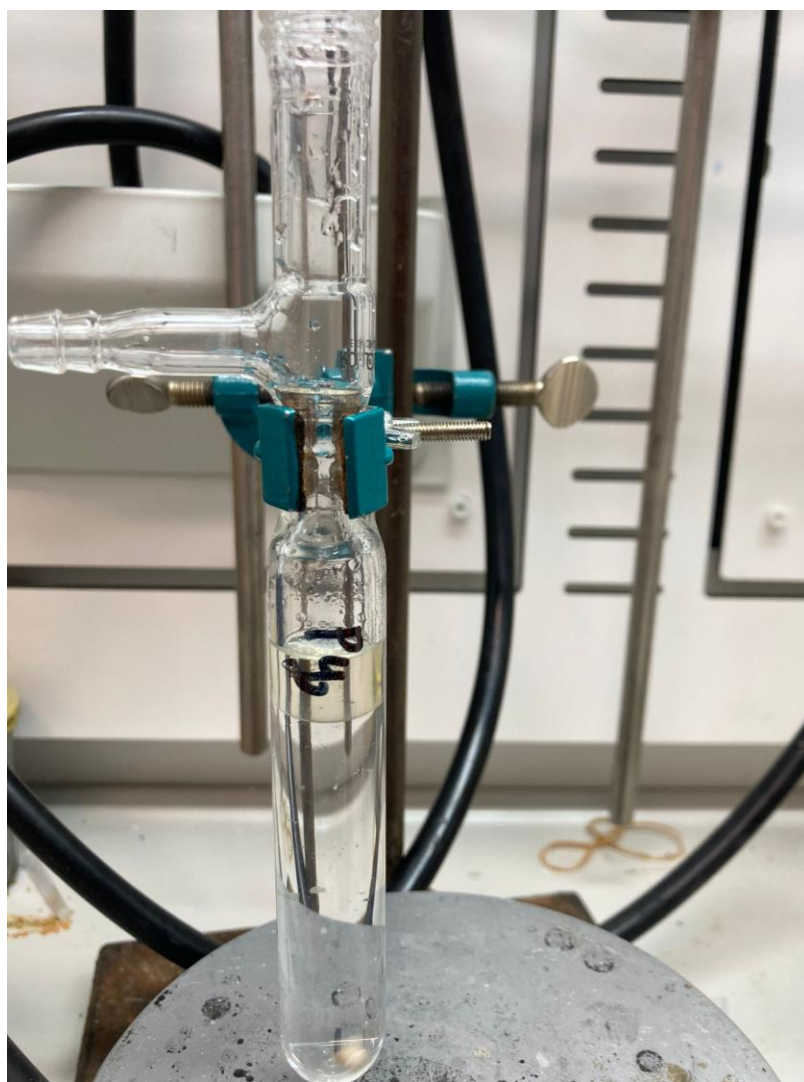
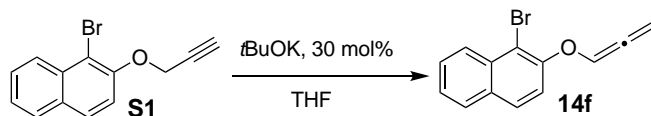


Figure S5. Reaction crude for radical cyclization after irradiation and acidic quenching.



Synthesis of unreported starting materials.

Synthesis of **14f**

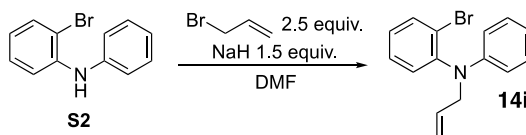


S1 was prepared according to the reported literature procedure. Spectroscopic data agree with those reported in the literature.^[2] In a two-necked 25 mL round bottom flask equipped with a magnetic stirring bar, **S1** (3 mmol, 1 equiv., 783 mg) was dissolved in 9 mL of dry THF. The solution was cooled down at 0°C and potassium *tert*-butoxide (1 mmol, 0.33 equiv., 112 mg) was added portion-wise. The reaction was allowed to warm up at room temperature and stirred for 5 h. The reaction was quenched with water (5 mL) and extracted with EtOAc (3 x 10 mL). The organic phases were combined and dried over Na₂SO₄, and the solvent was removed under reduced pressure. **14f** was isolated as a pale-yellow solid after column chromatography (SiO₂, 3% EtOAc in hexane) in 71% yield (556 mg, 3.12 mmol).

¹H NMR (600 MHz, CDCl₃) δ = 8.30 – 8.23 (m, 1H), 7.84 – 7.76 (m, 2H), 7.63 – 7.56 (m, 1H), 7.50 – 7.44 (m, 1H), 7.42 – 7.36 (m, 1H), 6.98 (t, *J* = 5.9 Hz, 1H), 5.43 (d, *J* = 5.9 Hz, 2H).

¹³C NMR (150 MHz, CDCl₃) δ = 202.4, 151.7, 133.4, 131.5, 129.0, 128.5, 128.1, 127.1, 125.7, 119.9, 119.1, 112.1, 91.4.

Synthesis of **14i**



S2 was prepared according to the reported literature procedure. Spectroscopic data agree with those reported in the literature.^[12]

In a flame-dried two-necked flask **S2** (3 mmol, 1.0 equiv., 744 mg) was added under an inert atmosphere and dissolved in dry DMF (9 mL). At 0 °C NaH (60% in mineral oil, 4.5 mmol, 1.5 equiv., 180 mg) was added and stirred for 15 min at 0 °C and 45 min at room temperature. The solution was cooled to 0 °C and allyl bromide (540 mg, 2.5 equiv., 7.5 mmol) was added, and it was stirred for 1.5 h. After all starting material was consumed (monitored via TLC), the reaction was quenched with H₂O at 0 °C, and the aqueous phase was extracted with EtOAc (3 x 10 mL). The combined organic phases were washed H₂O (5 x 10 mL), dried over Na₂SO₄, and concentrated under reduced pressure. The product was isolated as a colorless liquid in 67% yield (2.01 mmol, 580 mg) via column chromatography (SiO₂, 10% EtOAc in cyclohexane).

¹H NMR (600 MHz, CDCl₃) δ = 7.70 (dd, *J* = 8.0, 1.5 Hz, 1H), 7.29 (dd, *J* = 7.9, 1.7 Hz, 1H), 7.20 – 7.13 (m, 3H), 6.78 – 6.71 (m, 1H), 6.59 – 6.53 (m, 2H), 6.12 – 5.68 (m, 1H), 5.31 (dd, *J* = 17.3, 1.6 Hz, 1H), 5.18 (dd, *J* = 10.3, 1.6 Hz, 1H), 4.25 (dt, *J* = 5.3, 1.7 Hz, 2H).

¹³C NMR (150 MHz, CDCl₃) δ = 148.1, 145.8, 134.6, 134.1, 132.1, 129.3, 129.2, 128.3, 125.2, 118.1, 117.2, 114.1.

General Procedures.

Preparation of preformed $2\cdot n\text{BuLi}$, $5\cdot n\text{BuLi}$

$2\cdot n\text{BuLi}$: A heat-gun dried 100 mL Schlenk tube, magnetic stirring bar, and an argon supply tube, were firstly charged under vigorous argon flux with the azaarene of interest **2** (10 mmol, 1 equiv., 790 mg). Then, inhibitor-free and freshly distilled Et_2O (10 mL to obtain a 1 M substrate solution) was added to the reaction mixture. The solution was cooled to 0°C with an ice bath and $n\text{BuLi}$ 2.5 M in hexanes (10.05 mmol, 2.5 equiv., 4.04 mL) was added dropwise over 5 minutes. The reaction mixture rapidly turned from colorless to yellow. The solution was allowed to stir for 10 min. at 0°C and 15 min. at room temperature. The crude reaction mixture was vacuum-dried overnight until a finely dispersed yellow/orange powdery solid was obtained. Due to its high reactivity, the product was stored under argon for photoinduced cyclizations or in a glovebox for photophysical studies. Any purification attempt has led to the degradation of the target product. Considering this, the yield of $2\cdot n\text{BuLi}$ is considered quantitative.

$4\cdot n\text{BuLi}$: A heat-gun dried 100 mL Schlenk tube, magnetic stirring bar, and an argon supply tube, were firstly charged under vigorous argon flux with the azaarene of interest **5** (10 mmol, 1 equiv., 1290 mg). Then, inhibitor-free and freshly distilled THF (10 mL to obtain a 1 M substrate solution) was added to the reaction mixture. The solution was cooled to 0°C with an ice bath and $n\text{BuLi}$ 2.5 M in hexanes (10.05 mmol, 2.5 equiv., 4.04 mL) was added dropwise over 5 minutes. The reaction mixture rapidly turned from colorless to orange. The solution was allowed to stir for 10 min. at 0°C and 15 min. at room temperature. The crude reaction mixture was vacuum-dried overnight until a finely dispersed yellow/orange powdery solid was obtained. Due to its high reactivity, the product was stored under argon for photoinduced cyclizations or in a glovebox for photophysical studies. Any purification attempt has led to the degradation of the target product. Considering this, the yield of $4\cdot n\text{BuLi}$ is considered quantitative.

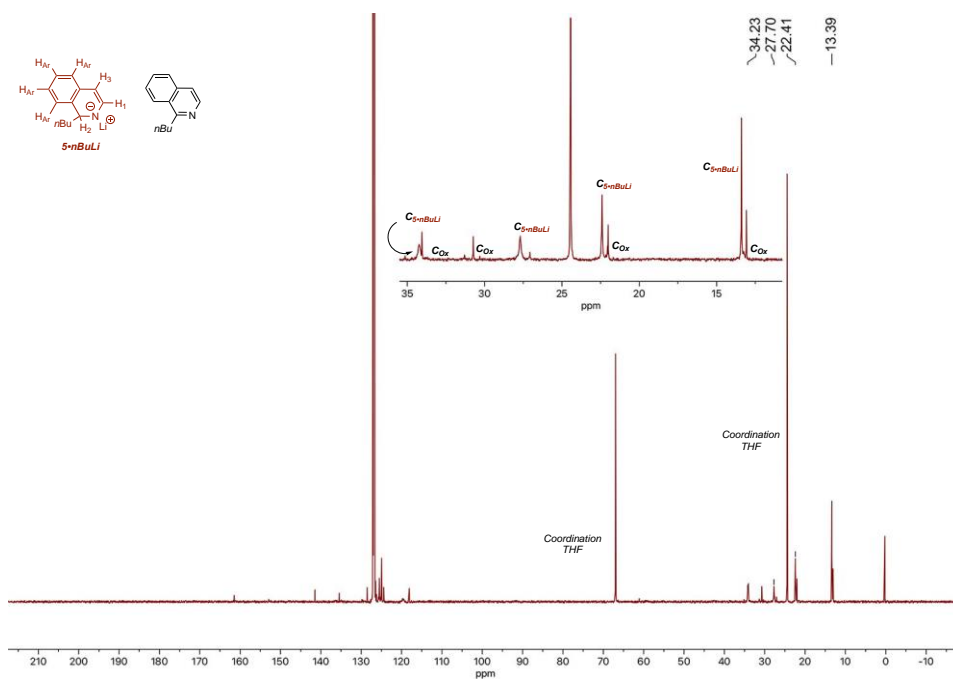
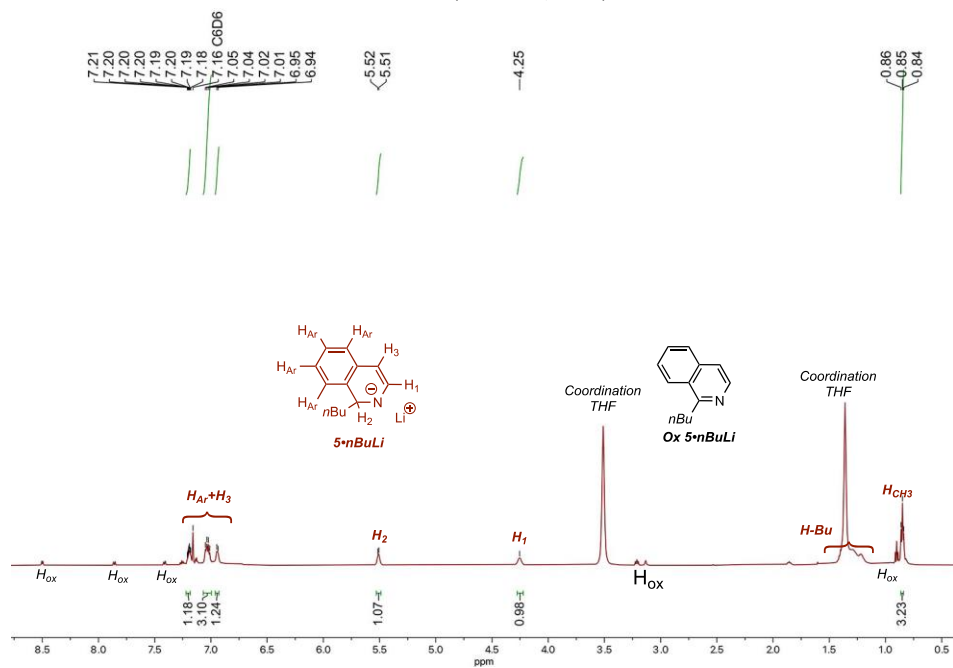
$5\cdot n\text{BuLi}$: A heat-gun dried 100 mL Schlenk tube, magnetic stirring bar, and an argon supply tube, was firstly charged under vigorous argon flux with the azaarene of interest **5** (10 mmol, 1 equiv., 1290 mg). Then, inhibitor-free and freshly distilled THF (10 mL to obtain a 1 M substrate solution) was added to the reaction mixture. The solution was cooled to 0°C with an ice bath and $n\text{BuLi}$ 2.5 M in hexanes (10.05 mmol, 2.5 equiv., 4.04 mL) was added dropwise over 5 minutes. The reaction mixture rapidly turned from colorless to reddish/orange. The solution was allowed to stir for 10 min. at 0°C and 15 min. at room temperature. The crude reaction mixture was vacuum-dried overnight until a finely dispersed yellow/orange powdery solid was obtained. Due to its high reactivity, the product was stored under argon for photoinduced cyclizations or in a glovebox for photophysical studies. Any purification attempt has led to the degradation of the target product. Considering this, the yield of $5\cdot n\text{BuLi}$ is considered quantitative.

$5\cdot n\text{BuLi}$ was also selected as the model adduct for the ^1H - and ^{13}C NMR characterization. Given the high reactivity of the adducts for the characterization, the preparation of **$5\cdot n\text{BuLi}$** was accomplished in analogy with the above-described procedure on a reduced scale (0.3 mmol of **5**). After evaporation of the solvent, the reaction crude was dissolved in dry deuterated benzene (C_6D_6) trying to keep as much as possible the solution under an inert atmosphere. The ^1H - and ^{13}C NMR characterization reported below shows the typical broad signal observed in the case of anionic species. Moreover, the initial formation of the oxidized/rearomatized product (indicated as **Ox- $5\cdot n\text{BuLi}$**) is detectable in minor amounts. To the best of our knowledge, we believe that the formation **Ox- $5\cdot n\text{BuLi}$** depends on traces of oxygen.

Similarly, due to the high reactivity of the product, obtaining a conclusive ^{13}C NMR spectrum is very challenging. To prevent complete degradation of the sample, a limited number of scans were performed. As shown in the following figure, the coexistence of two butylated species can be observed: one with sharp peaks and the other with broad peaks. We suppose that the broad peaks correspond to **$5\cdot n\text{BuLi}$** .

^1H NMR (600 MHz, C_6D_6) δ 7.19 (td, $J = 6.7, 4.1$ Hz, 1H), 7.06 – 7.00 (m, 3H), 6.94 (d, $J = 7.1$ Hz, 1H), 5.51 (d, $J = 6.4$ Hz, 1H), 4.26–4.23 (m, 1H), 1.37 – 1.23 (br m, 6H overlapped with coordination THF signal) 0.85 (t, $J = 7.1$ Hz, 3H).

¹H NMR (600 MHz, C₆D₆)



¹³C NMR (150 MHz, C₆D₆)

Photoinduced reduction of 4-halo-Anisole derivatives.

All the reactions were performed on a 0.2 mmol scale of 4-halo-anisole derivative. A heat-gun dried 10 mL Schlenk tube, equipped with a Rotaflo® stopcock, magnetic stirring bar, and an argon supply tube, was firstly charged under vigorous argon flux with the azaarene of interest **1-5** (0.4 mmol, 2 equiv.). Then, inhibitor-free and freshly distilled dry solvent (THF or DME, 2 mL to obtain a 0.1 M substrate solution) was added to the reaction mixture. The solution was cooled to 0°C with an ice bath and *n*BuLi 2.5 M in hexanes (0.36 mmol, 1.8 equiv., 144 µL) was added dropwise. The reaction mixture rapidly turned from colorless to yellow for derivative **2** and from colorless to orange/red for **1, 3-5**. The solution was allowed to stir for 10 min. at 0 °C and 5 min. at room temperature. Finally, the substrate **6-8** (1 equiv. 0.2 mmol) was added to the solution that was further subjected to a freeze-pump-thaw procedure (three cycles, 5 min. per cycle) and then refilled with argon. The degassed reaction mixture was irradiated under vigorous stirring for the stated time (See Infra).

Determination of HPCL yield of anisole from the photoinduced reduction of 4-halo-anisole derivatives.

For the determination of the yield of the photoinduced reduction promoted by photoactive Meisenheimer adducts in the presence of 4-halo anisole derivatives, trichloroethene was chosen as the internal standard (IS). After the desired irradiation time, an equimolar amount (0.2 mmol, 26.2 mg, 18µL) of IS was added to the reaction mixture. A 20 µL aliquot of the reaction solution was withdrawn and diluted to a total volume of 1 mL with acetonitrile HPLC-grade. This solution was then injected into the HPLC, and the ratio between the areas of **9** and of the internal standard was evaluated by analyzing the chromatogram at a wavelength of 230 nm. Using the prepared calibration curve it is possible to determine the ratio between the known concentration of the IS and the product **9**. Then, the yield of the reaction was determined by the integration of HPLC traces.

HPLC conditions:

The column employed is HPLC Column ZORBAX Eclipse, XDB-C18, 80Å, 5 µm, 4,6 x 250 mm. Retention time **9**: **12.313 min** Retention time IS: **15.097 min** Separation conditions: **25 minutes run** flux: **0.5 mil/min gradient run from H₂O/MeCN 20:80 to H₂O/MeCN80:20.**

Yields for various 4-halo-anisole derivatives (**6-8**) in the presence of different Azarenes evaluated (**1-5**) were obtained by interpolation using a calibration curve. Below the experimental values obtained from the injections and the corresponding yields obtained by interpolation are reported.

Calibration curve

To build the calibration curve, trichloroethylene was selected as the internal standard. Maintaining a constant concentration of the product (*approximately 1 mg/mL*), solutions of known concentration of both the internal standard and the product were prepared.

Solution A: Internal Standard to Product ratio 1:0

Product Concentration= 0.76 mM (*approximately 1 mg/mL*)

Solution B: Internal Standard to Product ratio 1:0.25

Product Concentration = 0.76 mM Internal Standard Concentration = 0.19 mM

Solution C: Internal Standard to Product ratio 1:0.5

Internal Product = 0.76 mM Internal Standard Concentration = 0.38 mM

Solution D: Internal Standard to Product ratio 1:0.75

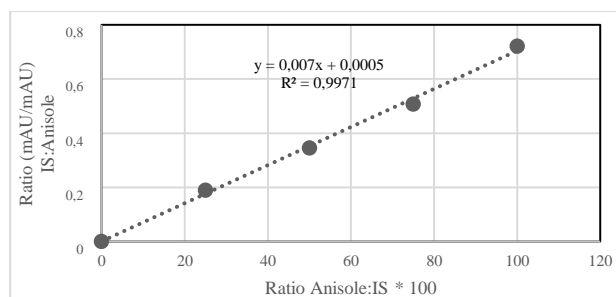
Product Concentration = 0.76 mM Internal Standard Concentration = 0.57 mM

Solution E: Internal Standard to Product ratio 1:1

Product Concentration = 0.76 mM Internal Standard Concentration = 0.76 mM

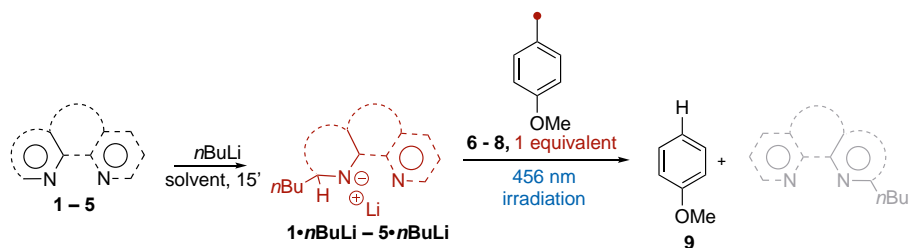
Below are the experimental values obtained from the injections which allow for the construction of the calibration curve. The slope of the curve within it enables the exclusion of the difference between the molar extinction coefficients of the product and the internal standard at the analysis wavelength (230 nm).

Entry	Ratio (mmol/mmol) Anisole:IS	Area IS (mAU)	Area Anisole(mAU)	Ratio (mAU/mAU) IS:Anisole
A	1:0	0	689,34567	–
B	1:0.25	203,38487	603,21472	0,33716828
C	1:0.5	416,00864	644,73395	0,64524078
D	1:0.75	580,91339	683,73187	0,84962164
E	1:1	691,85284	700,48828	0,98767226

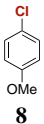


Results for Photoinduced reduction of 4-Halo-Anisole derivatives.

Table S1.



Entry	Haloanisole ^[a]	Heterocycle ^[b]	Solvent	9 (%) ^[c]	Area $SI^{[d]}$ (mAU)	Area 9 ^[d] (mAU)
1		(2.0)	THF	76	274.9	226.4
2	6	(2.0)	THF	60	2081.9	1335.7
3	6	(3.0) ^[e]	THF	55	783.9	465.5
4	6	(2.0)	THF	68	2775.3	2047.6
5	6	(2.0)	THF	38	792.9	324.0
6	6	(2.0)	THF	50	1140.0	618.7
7	6	(3.0) ^[e]	THF	66	1279.6	918.4
8		1 (2.0)	THF	traces	–	–
9	7	2 (2.0)	THF	50	2389.5	1409.0
10	7	3 (2.0)	THF	51	7346.0	4037.7
11	7	4 (2.0)	THF	30	728.4	234.9
12	7	5 (2.0)	THF	49	1261.1	665.5

13		1 (2.0)	THF	No reaction	–	–
14	8	2 (2.0)	THF	48	1252.2	649.3
15	8	2 (3.0) ^[e]	THF	47	764.2	388.6
16	8	2 (2.0)	Et ₂ O	Traces	–	–
17	8	2 (3.0) ^[e]	Et ₂ O	6	685.5	41.2
18	8	3 (3.0) ^[e]	Et ₂ O	No reaction	–	–
19	8	4(2.0)	THF	Traces	–	–
20	8	5 (2.0)	THF	42	2257.9	1024.8
21	8	5 (3.0) ^[e,f]	THF	51	934.9	515.5

[a] Reaction performed on 0.2 mmol of starting material. [b] Unless otherwise noted 0.4 mmol, 2.0 equiv. of azaarene and 0.36 mmol, 1.8 equivalent of *n*BuLi used. [c] HPLC yield is given. [d] Please refer to the calibration curve described above for extrapolating yields to correct the ratio between the areas. [e] 0.6 mmol, 3.0 equiv. of azaarene and 0.5 mmol, 2.5 equiv. of *n*BuLi. [f] 60 h irradiation time.

Photoinduced reduction of 4-chloro-4'-methoxy-1,1'-biphenyl 10.

The reaction was on a 0.2 mmol scale of 4-chloro-4'-methoxy-1,1'-biphenyl. A heat-gun dried 10 mL Schlenk tube, equipped with a Rotaflo[®] stopcock, magnetic stirring bar, and an argon supply tube, was firstly charged under vigorous argon flux with the azaarene of interest **2** or **5** (0.6 mmol, 3 equiv.). Then, inhibitor-free and freshly distilled dry solvent (THF or Et₂O, 2 mL to obtain a 0.1 M substrate solution) was added to the reaction mixture. The solution was cooled to 0 °C with an ice bath and *n*BuLi 2.5 M in hexanes (0.50 mmol, 2.5 equiv., 200 μL) was added dropwise. The reaction mixture rapidly turned from colorless to yellow for derivative **2** and from colorless to orange/red for **5**. The solution was allowed to stir for 10 min. at 0 °C and 5 min. at room temperature. Finally, 4-chloro-4'-methoxy-1,1'-biphenyl (1 equiv. 0.2 mmol 43.6 mg) was added to the solution that was further subjected to a freeze-pump-thaw procedure (three cycles, 5 min. per cycle) and then refilled with argon. The degassed reaction mixture was irradiated under vigorous stirring for 72 h. After that, the reaction mixture was quenched with HCl 2 M aq. (approx. 15 mL) and extracted with EtOAc (10 x 3 mL). The combined organic layers were dried over anhydrous Na₂SO₄ and the solvent was removed under reduced pressure. The reaction crude was purified by flash column chromatography (SiO₂, 1% EtOAc in Hexane) to afford 4-methoxy-1,1'-biphenyl **11**. Spectroscopical data following the reported literature.^[13]

From **5**•*n*BuLi: 4-methoxy-1,1'-biphenyl **11** was isolated in 35% yield (0.07 mmol, 13 mg)

From **2**•*n*BuLi 4-methoxy-1,1'-biphenyl **11** was isolated in 75% yield (0.15 mmol 27.5 mg)

Photoinduced reduction of 6-chloro-1-methyl-1H-indole 12.

The reaction was on a 0.2 mmol scale of 6-chloro-1-methyl-1H-indole. A heat-gun dried 10 mL Schlenk tube, equipped with a Rotaflo® stopcock, magnetic stirring bar, and an argon supply tube, was firstly charged under vigorous argon flux with the azaarene of interest **2** or **5** (0.6 mmol, 3 equiv.). Then, inhibitor-free and freshly distilled dry solvent (THF or Et₂O, 2 mL to obtain a 0.1 M substrate solution) was added to the reaction mixture. The solution was cooled to 0 °C with an ice bath and *n*BuLi 2.5 M in hexanes (0.50 mmol, 2.5 equiv., 200 μL) was added dropwise. The reaction mixture rapidly turned from colorless to yellow for derivative **2** and from colorless to orange/red for **5**. The solution was allowed to stir for 10 min. at 0 °C and 5 min. at room temperature. Finally, 6-chloro-*N*-methyl-indole **12** (1 equiv. 0.2 mmol 33 mg) was added to the solution that was further subjected to a freeze-pump-thaw procedure (three cycles, 5 min. per cycle) and then refilled with argon. The degassed reaction mixture was irradiated under vigorous stirring for 72 h. After that, the reaction mixture was quenched with HCl 2 M aq. (approx. 15 mL) and extracted with EtOAc (10 x 3 mL). The combined organic layers were dried over anhydrous Na₂SO₄ and the solvent was removed under reduced pressure. The reaction crude was purified by flash column chromatography (SiO₂, 1% EtOAc in hexane) to afford *N*-methyl-indole **13**. Spectroscopical data following the reported literature. ^[14]

From **5**·*n*BuLi: 1-methyl-1H-indole **13** was obtained in traces.

From **2**·*n*BuLi 1-methyl-1H-indole **13** was isolated in 58% yield (0.12 mmol 15.2 mg).

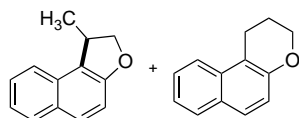
Photoinduced reductive radical cyclization.

Unless otherwise specified, all the reactions were performed on a 0.2 mmol scale. A heat-gun dried 10 mL Schlenk tube, equipped with a Rotaflo[®] stopcock, magnetic stirring bar, and an argon supply tube, was firstly charged under vigorous argon flux with freshly distilled pyridine **2** (0.4 mmol, 2 equiv., 31.8 mg, 32 μ L). Then, inhibitor-free and freshly distilled dry Et₂O (2 mL to obtain a 0.1 M substrate solution) was added to the reaction mixture. The solution was cooled to 0°C with an ice bath and *n*BuLi 2.5 M in hexanes (0.36 mmol, 1.8 equiv., 144 μ L) was added dropwise. The reaction mixture rapidly turned from colorless to yellow. The solution was allowed to stir for 10 min. at 0°C and 5 min. at room temperature. Finally, substrate **14a-j**, **16a**, **17a**, (1 equiv. 0.2 mmol) was added to the solution that was further subjected to a freeze-pump-thaw procedure (three cycles, 5 minutes per cycle) and then refilled with argon. The degassed reaction mixture was irradiated under vigorous stirring for the stated time (See Infra). After that, the reaction mixture was quenched with HCl 2 M aq. (approx. 15 mL) and extracted with EtOAc (10 x 3 mL). The combined organic layers were dried over anhydrous Na₂SO₄ and the solvent was removed under reduced pressure. The reaction crude was analyzed by ¹H-NMR for the evaluation of the regioisomeric/diastereomeric ratio. The NMR sample was carefully recovered, the solvent was removed under reduced pressure and, unless otherwise noted, purified by flash column chromatography (SiO₂) to afford products **15a-j** in the stated yields.

Photoinduced deprotection of tosyl amines.

Unless otherwise specified, all the reactions were performed on a 0.2 mmol scale. A heat-gun dried 10 mL Schlenk tube, equipped with a Rotaflo® stopcock, magnetic stirring bar, and an argon supply tube, was firstly charged under vigorous argon flux with freshly distilled isoquinoline **5** (0.4 mmol, 2 equiv., 51.6 mg). Then, inhibitor-free and freshly distilled dry DME (2 mL to obtain a 0.1 M substrate solution) was added to the reaction mixture. The solution was cooled to 0°C with an ice bath and *n*BuLi 1.6 M in hexanes (0.36 mmol, 1.8 equiv., 225 µL) was added dropwise. The reaction mixture rapidly turned from colorless to deep orange. The solution was allowed to stir for 10 min. at 0°C and 5 min. at room temperature. Finally, substrate **18a-f**, (1 equiv. 0.2 mmol) was added to the solution that was further subjected to a freeze-pump-thaw procedure (three cycles, 5 minutes per cycle) and then refilled with argon. The degassed reaction mixture was irradiated under vigorous stirring for the stated time. After that, the reaction mixture was quenched with water (approx. 15 mL) and extracted with Et₂O (10 x 3 mL). The combined organic layers were dried over anhydrous Na₂SO₄ and the solvent was removed under reduced pressure. The solvent was removed under reduced pressure and, unless otherwise noted, purified by flash column chromatography (SiO₂) to afford products **19a-f** in the stated yields.

Characterization of the products.



1-methyl-1,2-dihydronaphtho[2,1-b]furan 15a and 2,3-dihydro-1H-benzo[f]chromene 15a'

Yield (15a+ 15a') >95% from **14a** (0.195 mmol, 35.3 mg)

Yield (15a+ 15a') >95% from **16a** (0.195 mmol, 35.3 mg)

Yield (15a+ 15a') 55% from **17a** (0.11 mmol, 20.2 mg); irradiation time 50 h

Physical form: Pale yellow oil

15a:15a' = 13:1 from **14a**

15a:15a' > 95:5 from **16a**

15a:15a' = 5:1 from **17a**

Determined from ¹H-NMR of the reaction crude by integration of the proton(s) in benzylic position.

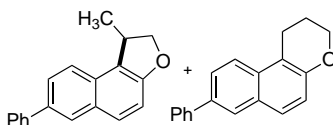
Case 1: **15a** was obtained following the general procedure as stated above employing 0.2 mmol (52.6 mg, 1 equiv.) of **14a**.

Case 2: **15a** was obtained following the general procedure as stated above employing 0.2 mmol (62.0 mg, 1 equiv.) of **16a**.

Case 3: **15a** was obtained following the general procedure as stated above employing 0.2 mmol (43.6 mg, 1 equiv.) of **17a**.

The title compound was isolated by flash column chromatography (SiO₂, 3-5% EtOAc in hexane).

Spectroscopical data are in agreement with the reported literature.^[2]



1-methyl-7-phenyl-1,2-dihydronaphtho[2,1-b]furan 15b and 8-phenyl-2,3-dihydro-1H-benzo[f]chromene 15b'

Yield >95% (0.195 mmol, 50.7 mg)

Physical form: Yellow solid.

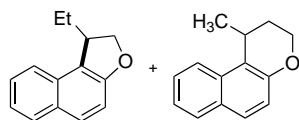
15b:15b' > 20:1 Determined from ¹H-NMR of the reaction crude by integration of the proton(s) in benzylic position.

15b was obtained following the general procedure as stated above employing 0.2 mmol (67.8 mg, 1 equiv.) of **14b**.

The title compound was isolated by flash column chromatography (SiO₂, 3-5% EtOAc in hexane).

¹H NMR (400 MHz, CDCl₃) δ = 7.93 – 7.88 (m, 2H), 7.80 – 7.66 (m, 3H), 7.58 (dd, *J* = 8.5, 1.9 Hz, 1H), 7.54 – 7.47 (m, 2H), 7.44 – 7.34 (m, 1H), 7.14 (d, *J* = 8.8 Hz, 1H), 4.81 (t, *J* = 8.7 Hz, 1H), 4.40 (dd, *J* = 8.7, 3.9 Hz, 1H), 4.03 – 3.91 (m, 1H), 1.52 (d, *J* = 6.9 Hz, 3H).

¹³CNMR (100 MHz, CDCl₃) δ = 157.6, 141.6, 139.5, 130.9, 129.6, 129.1, 129.0, 128.9, 128.9, 127.6, 127.5, 123.9, 122.7, 120.4, 112.4, 79.5, 36.4, 29.8, 20.6. HRMS (ESI/Q-TOF) *m/z*: [M-H₂O + H]⁺ calcd for C₁₉H₁₆O, 279.1174, found, 279.1164.



1-ethyl-1,2-dihydronaphtho[2,1-b]furan 15c and 1-methyl-2,3-dihydro-1H-benzo[f]chromene 15c'

Yield (15c + 15c') 82% (0.164 mmol, 32.4 mg).

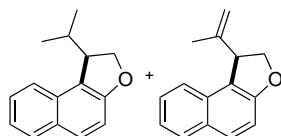
Physical form: Pale yellow oil.

15c:15c' > 95:5 Determined from ¹H-NMR of the reaction crude by integration of the proton(s) in benzylic position.

15c was obtained following the general procedure as stated above employing 0.2 mmol (55.4 mg, 1 equiv.) of **14c**.

The title compound was isolated by flash column chromatography (SiO₂, 3-5% EtOAc in hexane).

Spectroscopical data are in agreement with the reported literature.^[2]



1-isopropyl-1,2-dihydronaphtho[2,1-b]furan 15d and 1-(prop-1-en-2-yl)-1,2-dihydronaphtho[2,1-b]furan 15d'

Yield (15d+ 15d') 83% (0.083 mmol, 17.6 mg of **15d**, 0.083 mmol, 17.6 mg of **15d'**).

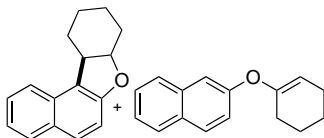
Physical form: White solid.

15d:15d' = 1:1 Determined from ¹H-NMR of the reaction crude by integration of the proton(s) in benzylic position.

15d:15d' were obtained employing 0.2 mmol (58.2 mg, 1 equiv.) of **14d** slightly modifying the general procedure. Meisenheimer adduct was prepared *in situ* combining 3 equivalents of **2** and 2.5 equivalents of *n*BuLi.

The title compound(s) were isolated by flash column chromatography (SiO₂, 2% EtOAc in hexane).

Spectroscopical data are in agreement with the reported literature.^[2,3]



7α,8,9,10,11,11a-hexahydrobenzo[b]naphtho[1,2-d]furan 15e and 2-(1-cyclohexenyl)oxynaphthalene 15e'

Yield 89% (0.097 mmol, 21.7 mg of **15e** and 0.080 mmol, 17.9 mg of **15e'**).

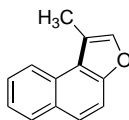
Physical form: Pale yellow oil.

15e:15e' = 1.2:1 Determined from ¹H-NMR of the reaction crude by integration of the benzylic proton of **15e** and vinylic proton of **15e'**.

15e was obtained following the general procedure as stated above employing 0.2 mmol 60.6 mg, 1 equiv.) of **14e**.

The title compound was isolated by flash column chromatography (SiO₂, 3-5% EtOAc in hexane).

Spectroscopical data are in agreement with the reported literature.^[15,16]



1-methylnaphtho[2,1-b]furan 15f

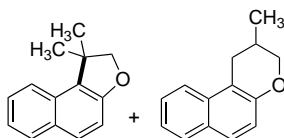
Yield 28% (0.056 mmol, 10.2 mg).

Physical form: White solid.

15f was obtained employing 0.2 mmol (52.2 mg, 1 equiv.) of **14f** slightly modifying the general procedure. Meisenheimer adduct was prepared *in situ* combining 3 equivalents of **2** and 2.5 equivalents of *n*BuLi.

The title compound(s) were isolated by flash column chromatography (SiO₂, 2% EtOAc in hexane).

Spectroscopical data are in agreement with the reported literature.^[17]



1,1-dimethyl-1,2-dihydronaphtho[2,1-b]furan 15g and 2-methyl-2,3-dihydro-1H-benzo[f]chromene 15g'

Yield 90% (0.180 mmol, 35.7 mg)

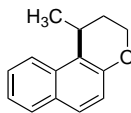
15g:15g' = 1.2:1 Determined from ¹H-NMR of the reaction crude by integration proton in a-position concerning the oxygen atom

Physical form: White solid

15g was obtained applying the general procedure as stated above employing 0.2 mmol (55.4 mg, 1 equiv.) of **14g**.

The title compound(s) were isolated by flash column chromatography (SiO₂, 3 - 6% EtOAc in hexane).

Spectroscopical data are in agreement with the reported literature.^[2]



1-methyl-2,3-dihydro-1H-benzo[f]chromene 15c'

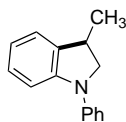
Yield > 95 % (0.195 mmol, 38.6 mg)

Physical form: White solid

15c' was obtained employing 0.2 mmol (55.4 mg, 1 equiv.) of **14h** slightly modifying the general procedure. Meisenheimer adduct was prepared *in situ* combining 3 equivalents of **2** and 2.5 equivalents of *n*BuLi.

The title compound(s) were isolated by flash column chromatography (SiO₂, 5% EtOAc in hexane).

Spectroscopical data are in agreement with the reported literature.^[18]



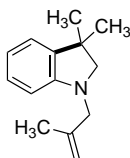
3-methyl-1-phenylindoline 15i

Yield 89 % (0.178 mmol, 37.2 mg).

Physical form: Yellowish solid.

15i was obtained employing 0.2 mmol (57.6 mg, 1 equiv.) of **14i** slightly modifying the general procedure. Meisenheimer adduct was prepared *in situ* combining 3 equivalents of **2** and 2.5 equivalents of *n*BuLi. After acid quenching **11i** was obtained ¹H- and ¹³C-NMR-pure without further purification after work-up.

Spectroscopical data are in agreement with the reported literature.^[19]



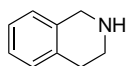
3,3-dimethyl-1-(2-methylallyl)indoline 15j

Yield > 95 % (0.195 mmol, 39.2 mg).

Physical form: Yellowish solid.

15j was obtained employing 0.2 mmol (56.0 mg, 1 equiv.) of **14j** slightly modifying the general procedure. Meisenheimer adduct was prepared *in situ* combining 3 equivalents of **2** and 2.5 equivalents of *n*BuLi. After acid quenching **15j** was obtained ¹H- and ¹³C-NMR-pure without further purification after work-up.

Spectroscopical data are in agreement with the reported literature.^[20]



1,2,3,4-tetrahydroisoquinoline 19a

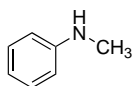
Yield 68% (0.136 mmol, 18 mg)

Physical form: pale yellow oil.

19a was obtained following the general procedure as stated above employing 0.2 mmol (57.4 mg, 1 equiv.) of **18a**.

The title compound was isolated by flash column chromatography (SiO₂, 15% EtOAc in hexane).

Spectroscopical data are in agreement with the reported literature.^[21]



N-methylaniline 19b

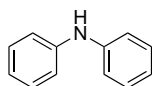
Yield 33% (0.066 mmol, 7.1 mg).

Physical form: pale yellow oil.

19b was obtained following the general procedure as stated above employing 0.2 mmol (52.2 mg, 1 equiv.) of **18b**.

The title compound was isolated by flash column chromatography (SiO₂, 20% EtOAc in hexane).

Spectroscopical data are in agreement with the reported literature.^[22]



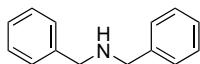
Diphenylamine 19c

Yield 86% (0.172 mmol, 29.1 mg)

Physical form: Yellow solid

19c was obtained following the general procedure as stated above employing 0.2 mmol (64.6 mg, 1 equiv.) of **18c**.

The title compound was isolated by flash column chromatography (SiO₂, 10% EtOAc in hexane). Spectroscopical data are in agreement with the reported literature.^[8]



Dibenzylamine 19d

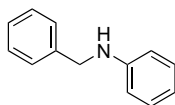
Yield 55% (0.172 mmol, 21.2 mg)

Physical form: yellow solid

19d was obtained following the general procedure as stated above employing 0.2 mmol (70.2 mg, 1 equiv.) of **14d**.

The title compound was isolated by flash column chromatography (SiO₂, 20% EtOAc in hexane).

Spectroscopical data are in agreement with the reported literature.^[23]



N-benzylaniline 19e

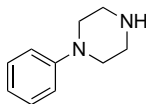
Yield 90% (0.180 mmol, 32.9 mg)

Physical form: white solid

19e was obtained following the general procedure as stated above employing 0.2 mmol (67.4 mg, 1 equiv.) of **18e**.

The title compound was isolated by flash column chromatography (SiO₂, 20% EtOAc in hexane).

Spectroscopical data are in agreement with the reported literature.^[10]



1-phenylpiperazine 19f

Yield 93% (186 mmol, 30.1 mg).

Physical form: white solid.

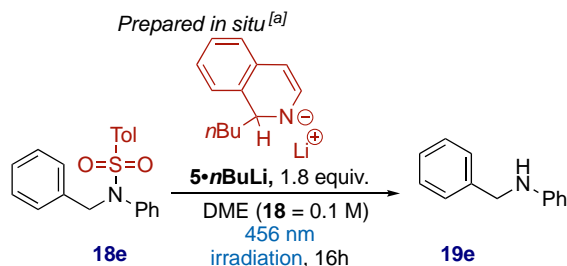
19f was obtained following the general procedure as stated above employing 0.2 mmol (63.2 mg, 1 equiv.) of **18f**.

The title compound was isolated by flash column chromatography (SiO₂, 30% EtOAc in hexane).

Spectroscopical data are in agreement with the reported literature.^[11]

Optimization for photoinduced detosylation of amines.

Table S2.



Entry ^[a]	Deviation from standard conditions	Yield (%) ^[b]
1	None	90
2	No light	NR
3	No <i>n</i> BuLi	NR
6	THF instead of DME	75
8	Et ₂ O instead DME	32
9	MTBA instead DME	NR
10	2 · <i>n</i> BuLi instead of 5 · <i>n</i> BuLi ^[c]	57
11	2 · <i>n</i> BuLi instead of 5 · <i>n</i> BuLi ^[d]	81
12	2 · <i>n</i> BuLi instead of 5 · <i>n</i> BuLi ^[e,f]	75

[a] Reaction performed on 0.2 mmol scale of **10a**. [b] Isolated yield after chromatographic purification. [c] Reaction performed in THF. [d] Reaction performed in Et₂O [e] Reaction performed in Et₂O [f] **2**·*n*BuLi 2.5equiv. (Prepared from 3 equiv. of **2** and 2.5 equiv. of *n*BuLi). NR = no reaction

Photophysical investigation.

UV/vis absorbance spectra were recorded with an Agilent Cary 300, using sealed quartz suprasil (QS) cuvettes with an optical path of 2 mm or 10 mm. Emission spectra were recorded on a Perkin Elmer LS55 or an Edinburgh FS5 equipped with a PMT980 detector for UV and visible range. Emission lifetime measurements in the range 0.5 ns - 1 μ s were performed by an Edinburgh FLS920 spectrofluorometer equipped with a TCC900 card for data acquisition in time-correlated single photon counting experiments (0.2 ns time resolution) with a 405 nm pulsed laser. The estimated experimental errors are 2 nm on the band maximum and 5% on the luminescence lifetime.

Emission quenching trials in the presence of compound **14g** have not demonstrated the oxidative quenching of ***5 \cdot nBuLi**, since changes in the emission intensity or lifetime of the latter originated from multiple factors, such as experimental difficulties to monitoring lifetime decays for highly concentrated solutions, and/or different excitation energy compared to the reaction conditions.

2 \cdot nBuLi, **4 \cdot nBuLi**, **5 \cdot nBuLi** were prepared as previously described in the section "General Procedures".

Photophysical investigation on 5 \cdot nBuLi and the role of concentration/aggregation.

Figure S6. Comparison between absorption spectra obtained from deaerated solutions of 5 \cdot nBuLi in THF at 0.1 mg/mL (grey line; optical path 10mm) and 25 mg/mL (orange line; optical path 2 mm).

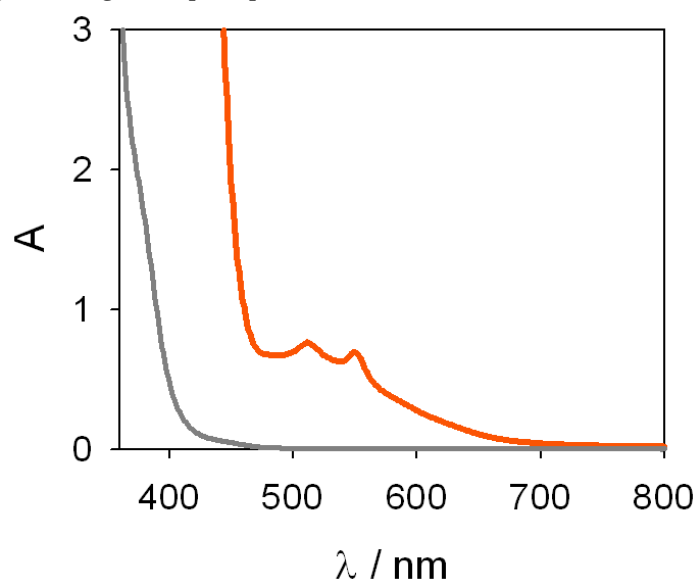


Figure S7. Deaerated solutions of 5 \cdot nBuLi in THF at different concentrations. Concentrations in the vials from left to right: 1 / 0.1 / 0.2 / 0.3 / 0.4 / 0.5 / 0.6 / 0.7 / 0.8 / 0.9 mg/mL.



Figure S8. (A) Comparison between emission spectra obtained from deaerated solutions of 5*n*BuLi in THF at 25 mg/mL upon excitation at different wavelengths (front-face configuration) and (B) corresponding normalized spectra. The excitation signal has been cut for the sake of clarity.

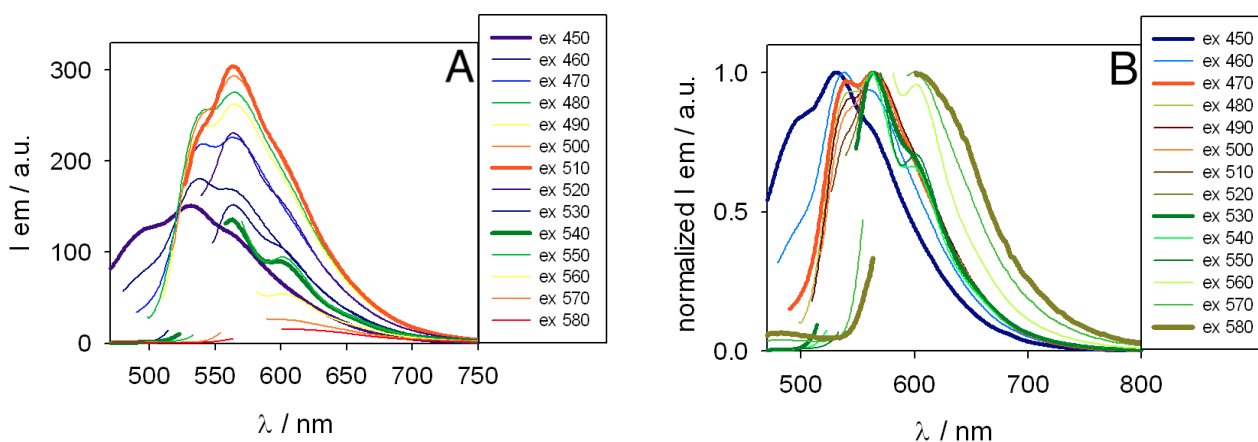
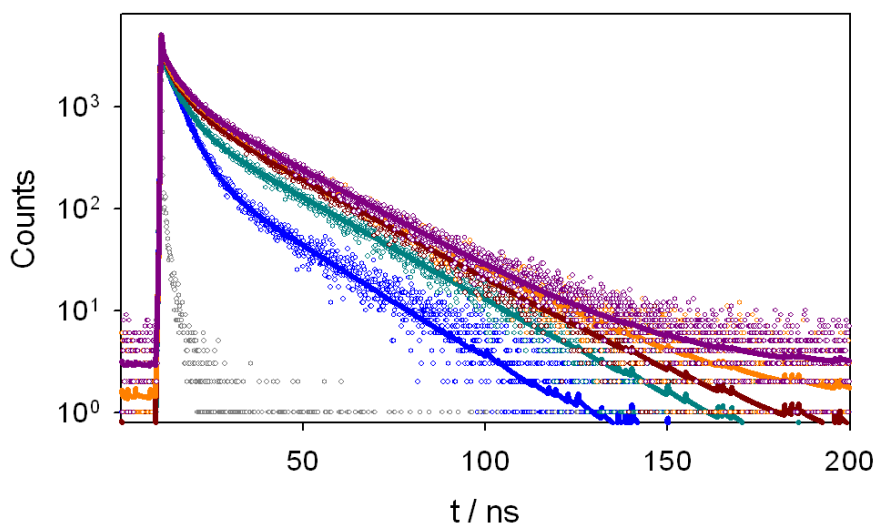


Figure S9. Comparison between emission decays obtained from deaerated solutions of 5*n*BuLi in THF at 25 mg/mL at different emission wavelengths ($\lambda_{em} = 470$ nm: blue; $\lambda_{em} = 500$ nm: green; $\lambda_{em} = 530$ nm: red; $\lambda_{em} = 565$ nm: orange; $\lambda_{em} = 590$ nm: purple) and corresponding multiexponential fitting functions. $\lambda_{ex} = 405$ nm; the instrumental response function (grey dots) is also shown. Decay constants ≤ 0.2 ns are not reported.



$$\lambda_{em} = 470 \text{ nm} : \tau_1 = 3.9 \text{ ns [64\%]}, \tau_2 = 19.1 \text{ ns [28\%]}; (\chi^2 = 0.945)$$

$$\lambda_{em} = 500 \text{ nm} : \tau_1 = 3.9 \text{ ns [35\%]}, \tau_2 = 21.3 \text{ ns [59\%]}; (\chi^2 = 1.004)$$

$$\lambda_{em} = 530 \text{ nm} : \tau_1 = 1.3 \text{ ns [6\%]}, \tau_2 = 5.3 \text{ ns [24\%]}, \tau_3 = 22.1 \text{ ns [66\%]}; (\chi^2 = 1.010)$$

$$\lambda_{em} = 565 \text{ nm} : \tau_1 = 1.1 \text{ ns [5\%]}, \tau_2 = 5.7 \text{ ns [24\%]}, \tau_3 = 22.8 \text{ ns [69\%]}; (\chi^2 = 1.132)$$

$$\lambda_{em} = 590 \text{ nm} : \tau_1 = 1.3 \text{ ns [5\%]}, \tau_2 = 5.7 \text{ ns [24\%]}, \tau_3 = 22.9 \text{ ns [69\%]}; (\chi^2 = 1.167)$$

Figure S10. (A) Comparison between emission spectra obtained from deaerated solutions of 5*n*BuLi in THF at 0.1 mg/mL upon excitation at different wavelengths and (B) corresponding normalized spectra. The excitation signal has been cut for the sake of clarity.

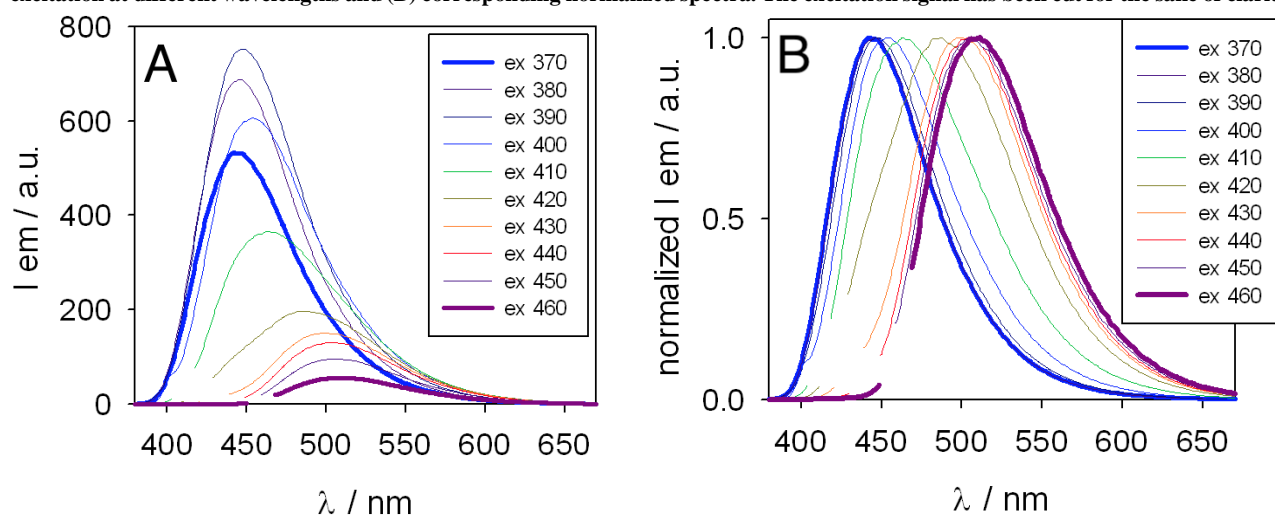
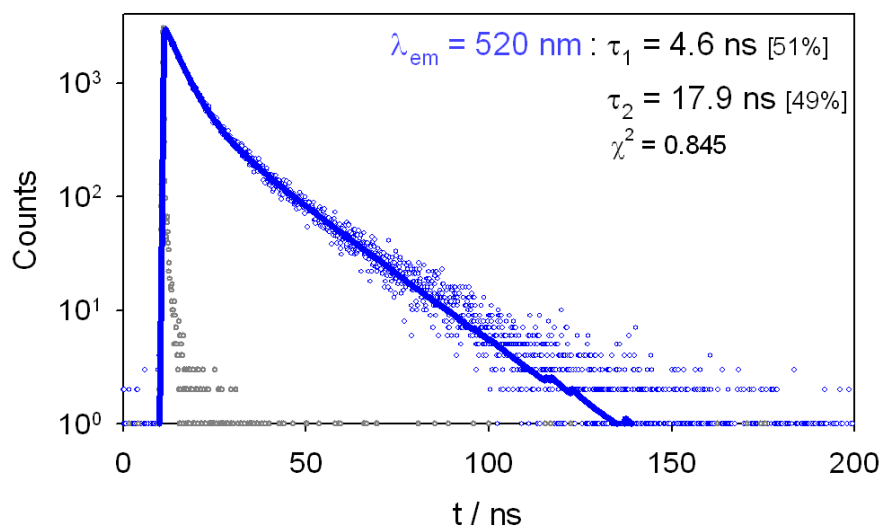


Figure S11. Emission decay was obtained from deaerated solutions of 5*n*BuLi in THF at 0.1 mg/mL at $\lambda_{em} = 520$ nm and the corresponding multiexponential fitting function. $\lambda_{ex} = 405$ nm; the instrumental response function (grey dots) is also shown.



Further photophysical investigation on different Meisenheimer's adducts.

Figure S12. Absorption spectra of $2\cdot n$ BuLi in deaerated THF solution at different concentrations.

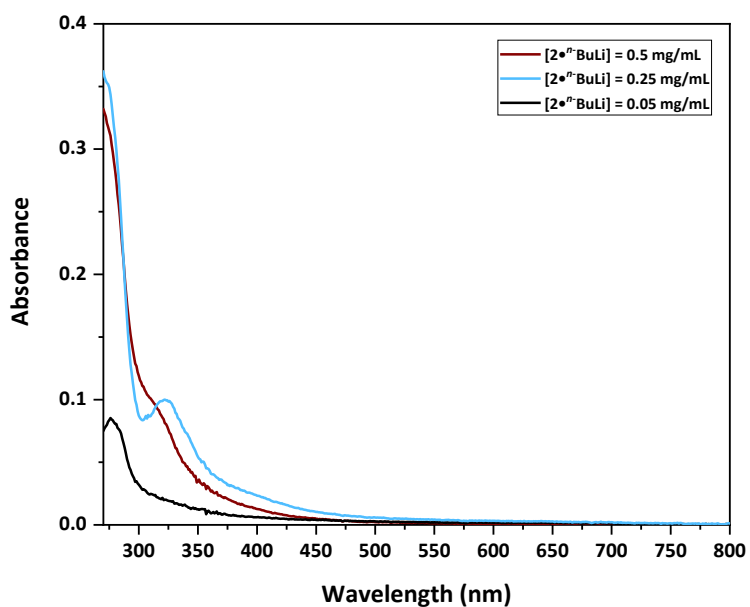


Figure S13. Absorption spectra of $4\cdot n$ BuLi in deaerated THF solution at different concentrations.

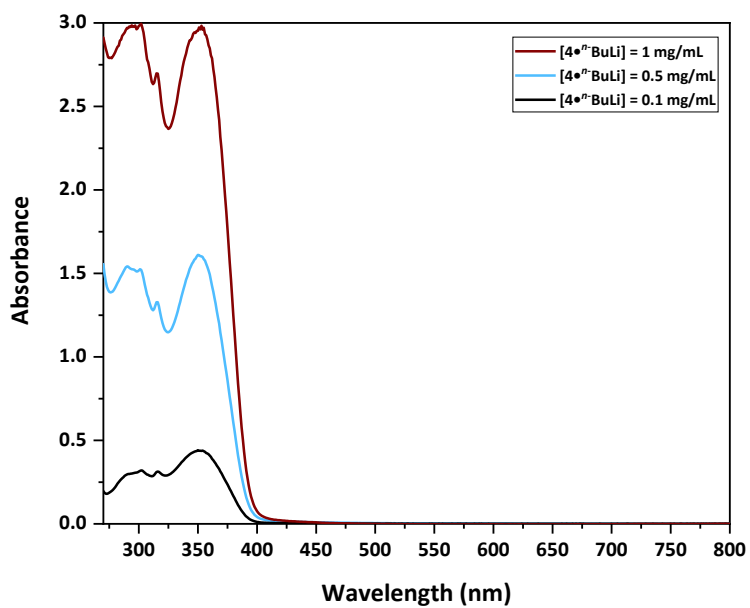


Figure S14. Emission map of a deaerated THF solution of 2·*n*BuLi at 0.5 mg/mL. Excitation range: 280 – 320 nm.

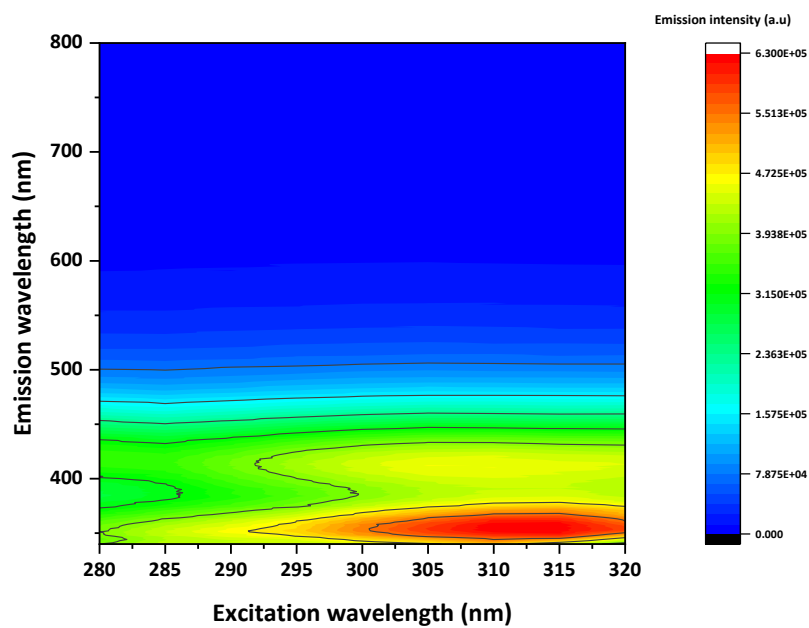


Figure S15. Emission map of a deaerated THF solution of 2·*n*BuLi at 0.5 mg/mL. Excitation range: 400 – 450 nm.

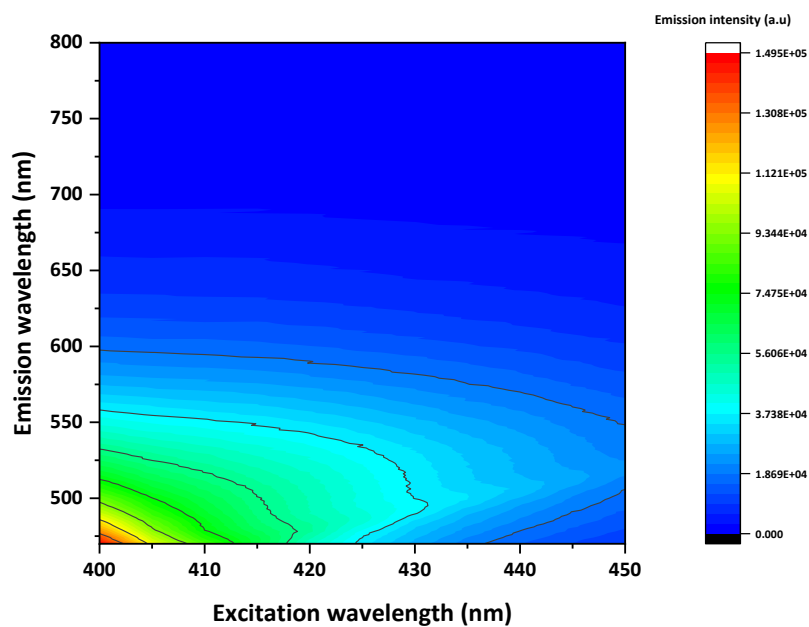


Figure S16. Emission map of a deaerated THF solution of 4*n*BuLi at 1 mg/mL. Excitation range: 300 – 360 nm

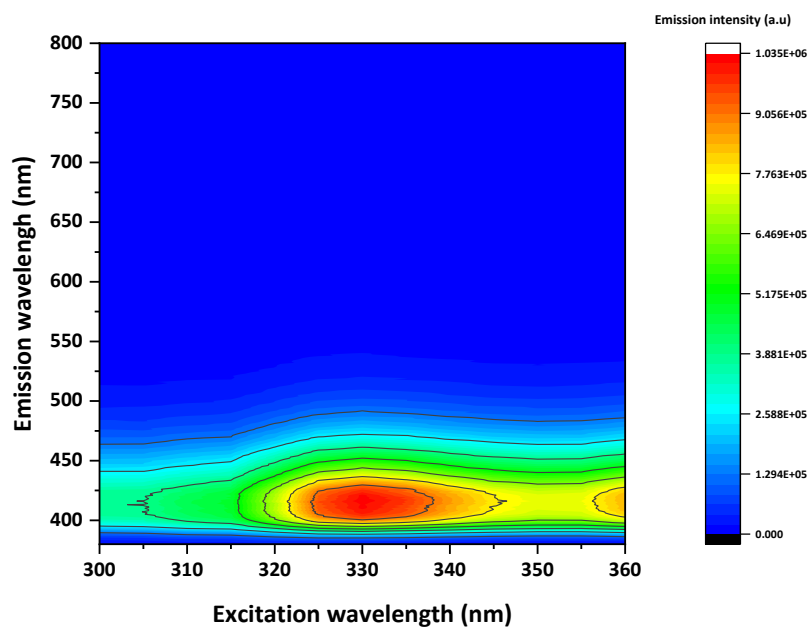


Figure S17. Emission map of a deaerated THF solution of 4*n*BuLi at 1 mg/mL. Excitation range: 410 – 450 nm.

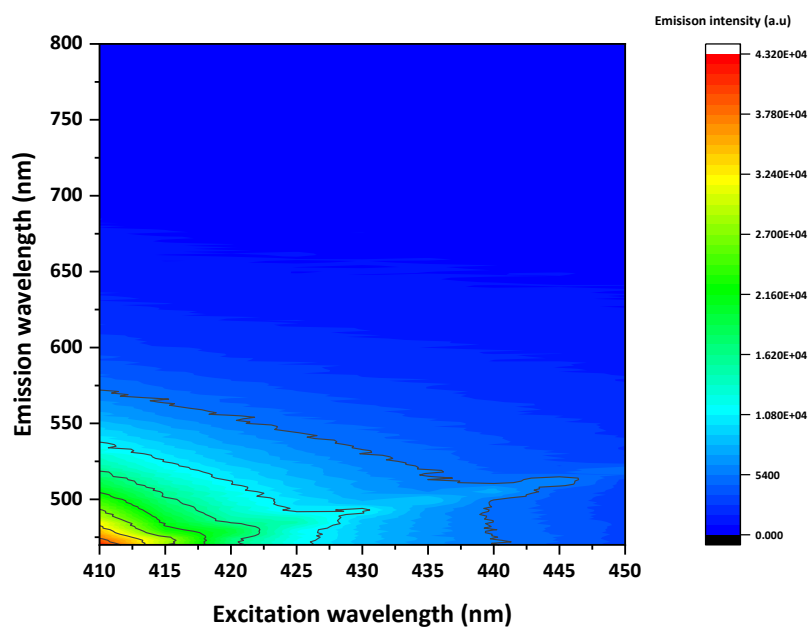


Figure S18. Emission decay of 2*n*BuLi in a deaerated THF at 0.5 mg/mL ($\lambda_{\text{ex}} = 405 \text{ nm}$, $\lambda_{\text{em}} = 600 \text{ nm}$).

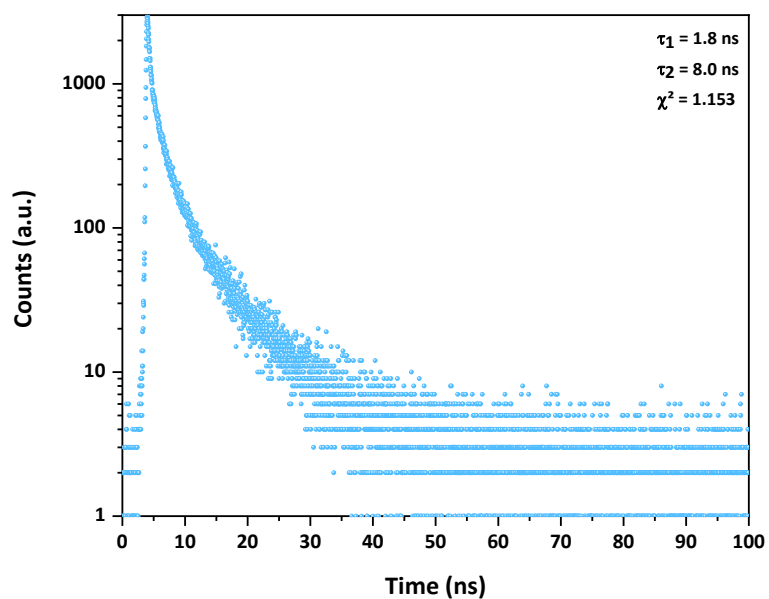
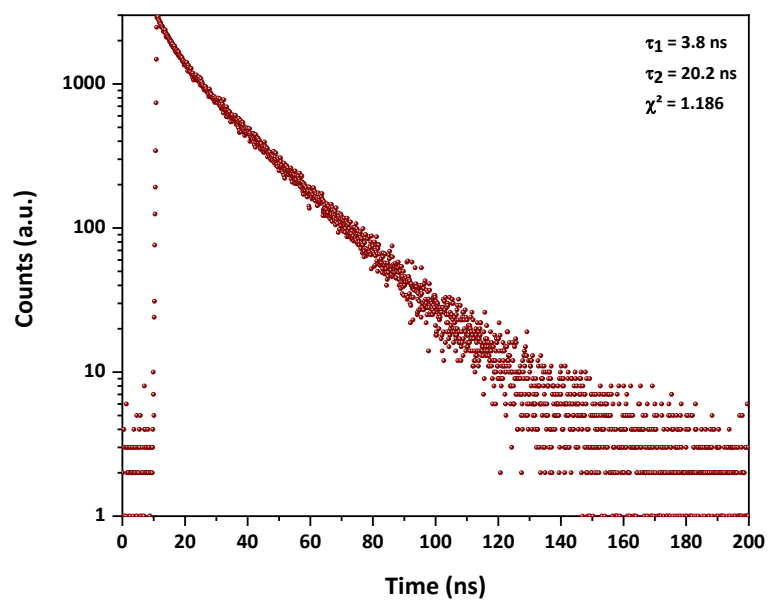


Figure S19. Emission decay of 4*n*BuLi in a deaerated THF at 1 mg/mL ($\lambda_{\text{ex}} = 405 \text{ nm}$, $\lambda_{\text{em}} = 450 \text{ nm}$).



Computational details.

Density functional theory (DFT) and time-dependent DFT (TD-DFT) calculations were carried out on **4*n*BuLi**, **5*n*BuLi**, and several aggregate structures of **5*n*BuLi**. Geometries were first optimized in their ground electronic state using the functional ω B97X-D and the def2-SVP basis set (Figures S21-S22 and S26-S33). TD-DFT calculations of excitation energies and oscillator strengths were performed at the ground state optimized geometries with the same functional including up to thirty excited electronic states. We also optimized the lowest singlet excited state for a few promising structures at the same level of theory (Figures S23 and S35). The ω B97X-D functional is known to overestimate excitation energies by ca 0.4-0.5 eV^[24,25] but it was selected because of its balanced description of charge transfer states in aggregates of polycyclic aromatic hydrocarbons.^[26] In the organolithium aggregates considered in this work, excited states dominated by charge transfer character, such as those describing charge transfer from N to Li, are therefore expected to be correctly described. For **5*n*BuLi**, we determined the ground and excited state optimized geometries not only in vacuo but also including implicit solvent effects with the polarizable continuum model (PCM)^[27], by keeping, in both cases, the two explicit THF molecules. Ground state equilibrium structures and excitation energies to the lowest singlet state were very close to those obtained without implicit solvent effects and therefore the calculations on aggregates were carried out only with explicit solvent molecules. All calculations were carried out with Gaussian 16^[28], and Gaussian 09^[29] software, while visualizations of molecular structures and molecular orbitals were obtained with the graphical software Avogadro^[30] and Gaussview^[31]

Table S3. The 5*n*BuLi aggregate structures were investigated.

Label	type of aggregate	geometry of Li—N patterns	number of THF molecules
A	dimer	Square	2
B	dimer	Square	4
C	tetramer	Cubic	4
D	tetramer	Planar	4
E	tetramer	Planar	6
F	tetramer	Ladder	2
G	tetramer	Bisquare	6
H	tetramer	Bisquare	6

Table S4. Ground and excited state TD- ω B97X-D/def2-SVP absolute energies for 4*n*BuLi, 5*n*BuLi and the aggregate structures of 5*n*BuLi investigated. From ω B97X-D/def2-SVP and TD- ω B97X-D/def2-SVP calculations.

System	S ₀ optimized geometry / a.u.	S ₁ optimized geometry / a.u.
4<i>n</i>BuLi + 2THF	-1031.24534718	-
5<i>n</i>BuLi + 2THF	-1031.24952351	-1031.11885217
Aggregate A	-1598.08879334	-
Aggregate B	-2062.56688382	-
Aggregate C	-3196.23583873	-
Aggregate D	-3196.18935055	-
Aggregate E	-3660.65935776	-
Aggregate F	-2731.72182613	-2731.60521494
Aggregate G	-3660.65656327	-3660.54798955
Aggregate H	-3660.66625944	-

Table S5. TD- ω B97X-D/def2-SVP computed excitation and emission energies for 4 n BuLi, 5 n BuLi and the aggregate structures of 5 n BuLi investigated.

System	$S_0 \rightarrow S_1$ Excitation energy @ S_0 state structure eV (nm)	S_1-S_0 Emission energy @ S_1 state structure eV (nm)
4 n BuLi + 2THF	3.24 (383)	
5 n BuLi + 2THF	3.85 (322) 3.80 ^a (326) ^[a]	3.23 (384) 3.23 ^a (384) ^[a]
Aggregate A	3.89 (319)	-
Aggregate B	3.88 (319)	-
Aggregate C	3.96 (313)	-
Aggregate D	3.92 (316)	-
Aggregate E	3.92 (316)	-
Aggregate F	3.83 (324)	2.54 (487)
Aggregate G	3.60 (344)	2.66 (466)
Aggregate H	3.64 (340)	-

[a] From TD- ω B97X-D/def2-SVP including PCM implicit solvent (THF) effects.

Figure S20. Possible organolithium aggregate structures as discussed in ref. 83^[32]

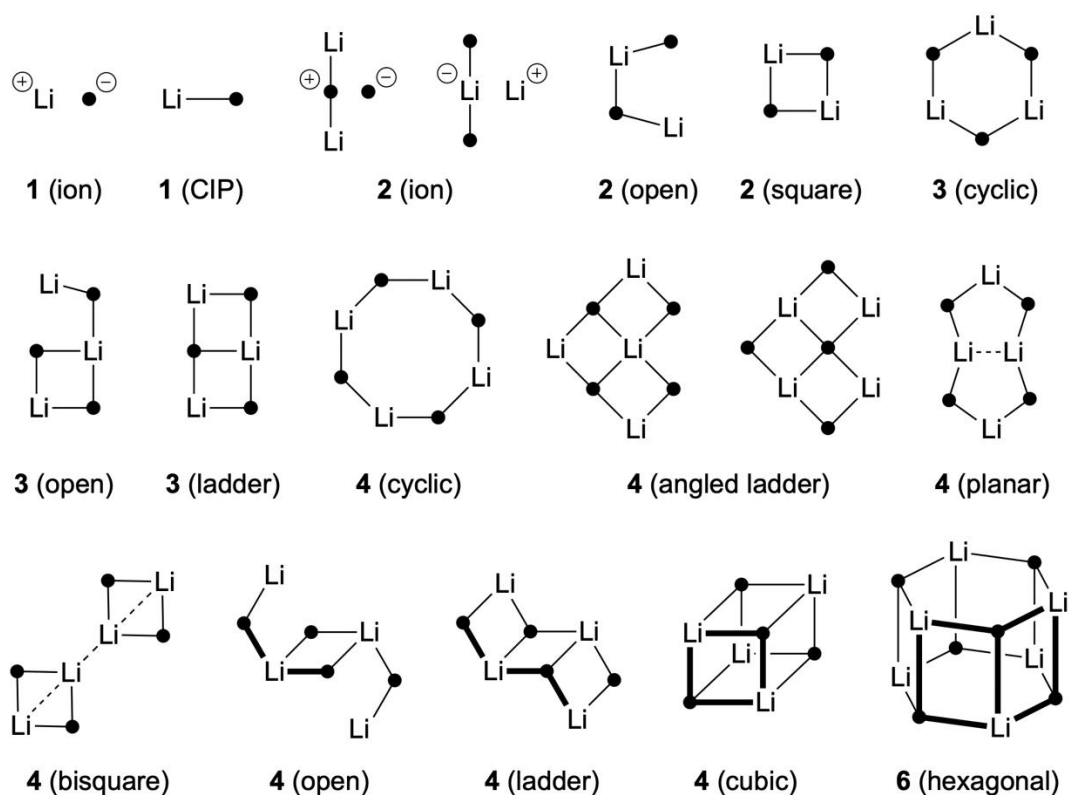


Figure S21. Ground state optimized geometry (ω B97X-D/def2-SVP) of 4•*n*BuLi featuring two THF solvent molecules.

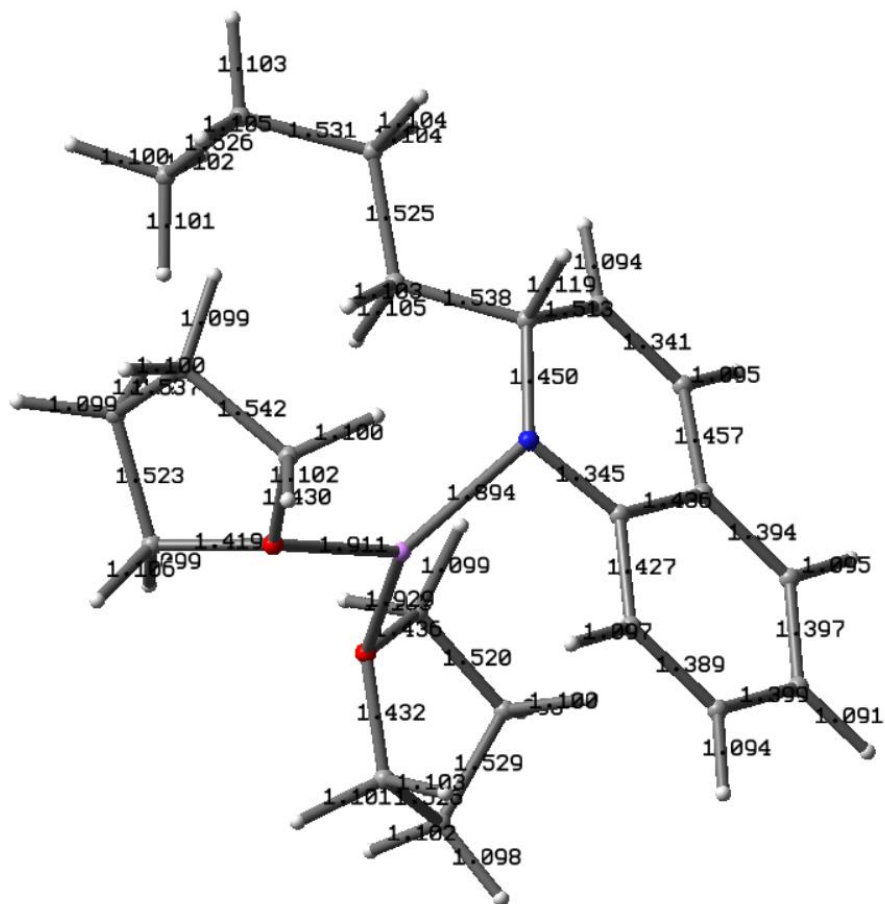


Figure S23. Optimized geometry (TD- ω B97X-D/def2-SVP) of the lowest singlet excited state of 5-*n*BuLi featuring two THF solvent molecules.

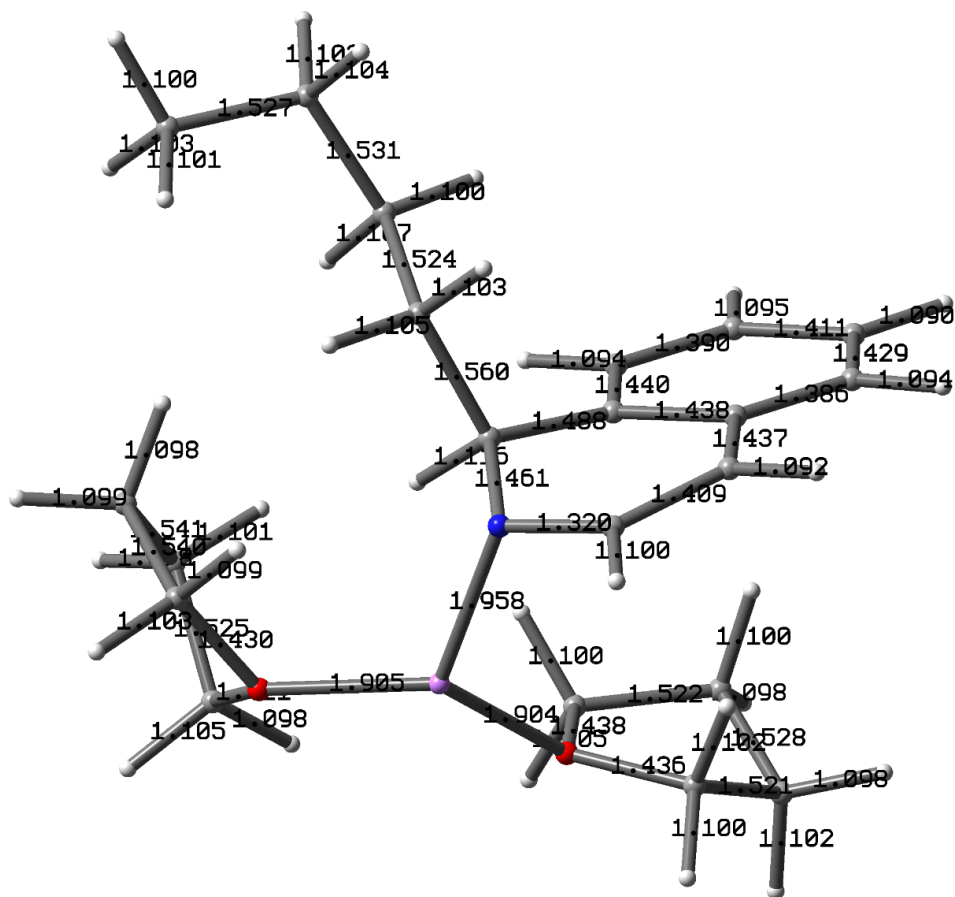


Figure S24. Comparison between (top) ground state optimized geometries (ω B97X-D/def2-SVP) and (bottom) lowest singlet excited state geometries of $5\cdot n$ BuLi featuring two THF solvent molecules with (right) or without (left) PCM solvent corrections.

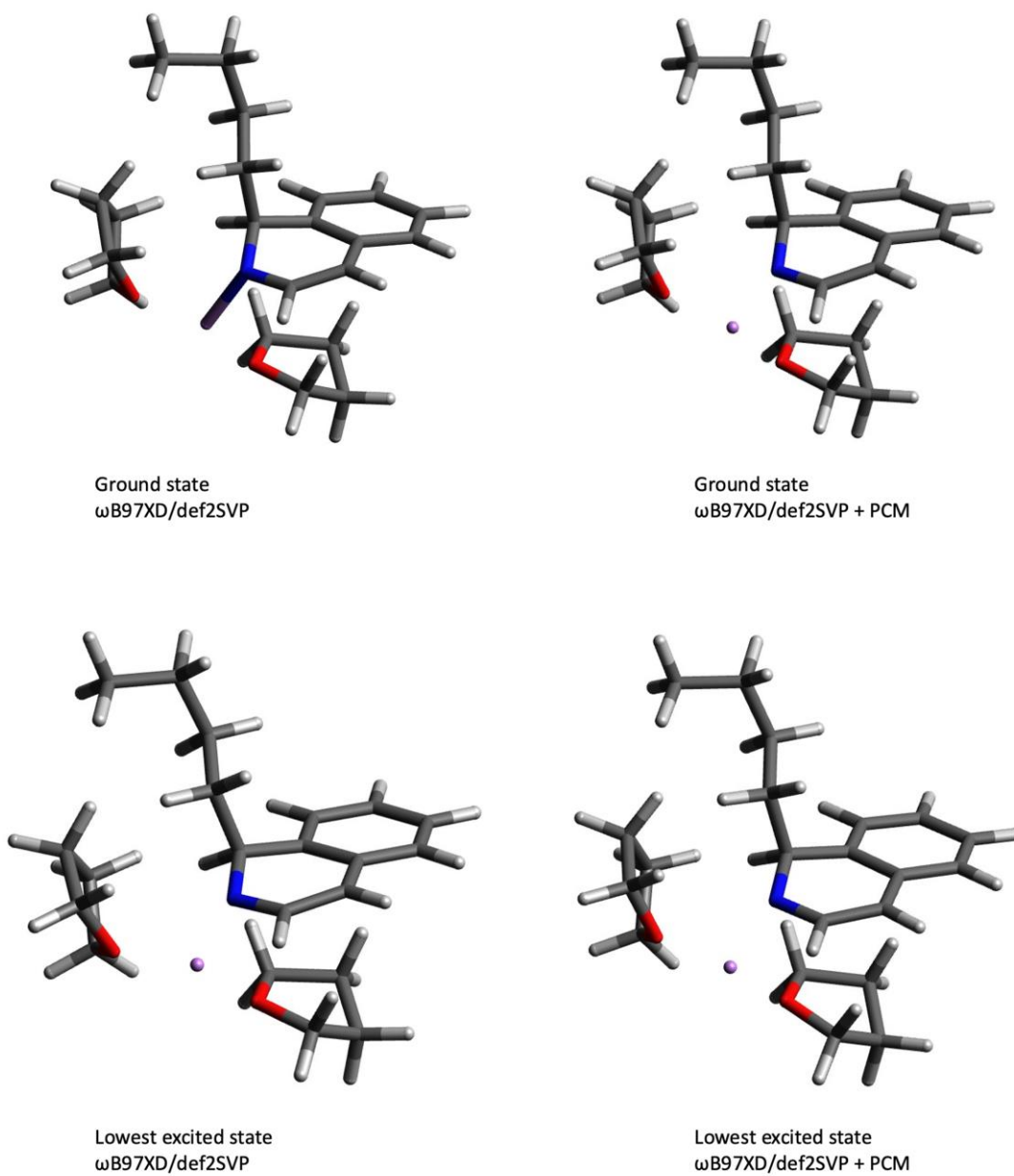


Figure S25. (Top) Frontier molecular orbitals and lowest excited states of $5\cdot n\text{BuLi}$ at the ground state optimized geometry. (Bottom) Electrostatic potential maps for the ground state (left), lowest excited state (center), and CT state (S3 in the list of states above) (right) of $5\cdot n\text{BuLi}$ with two THF solvent molecules (from $\omega\text{B97X-D/def2-SVP}$ and $\text{TD-}\omega\text{B97X-D/def2-SVP}$ calculations).

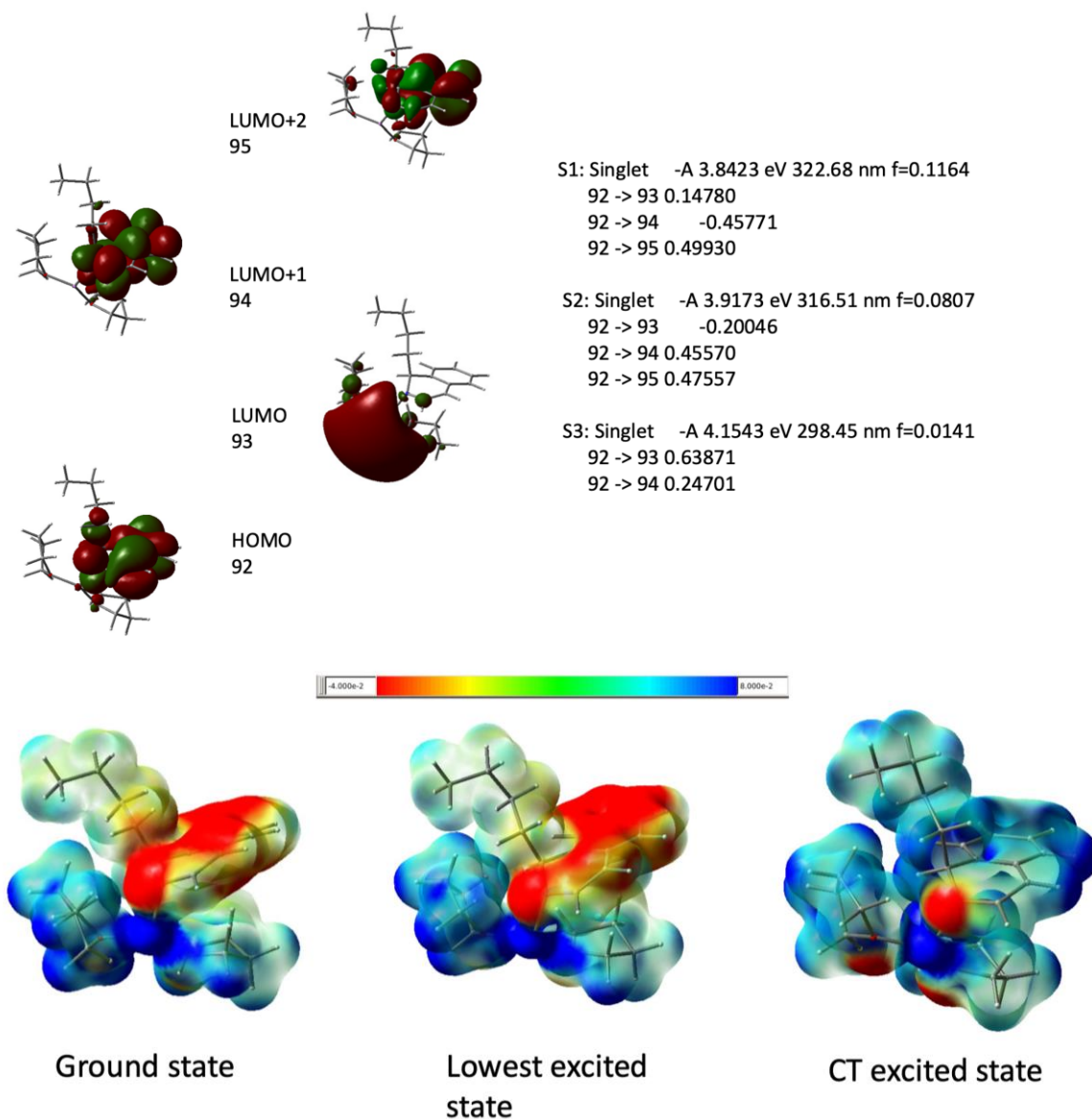


Figure S26. Schematic representation (inset) and two views of the ground state optimized geometry (ω B97X-D/def2-SVP) of 5-*n*BuLi dimer structure A featuring two THF solvent molecules.

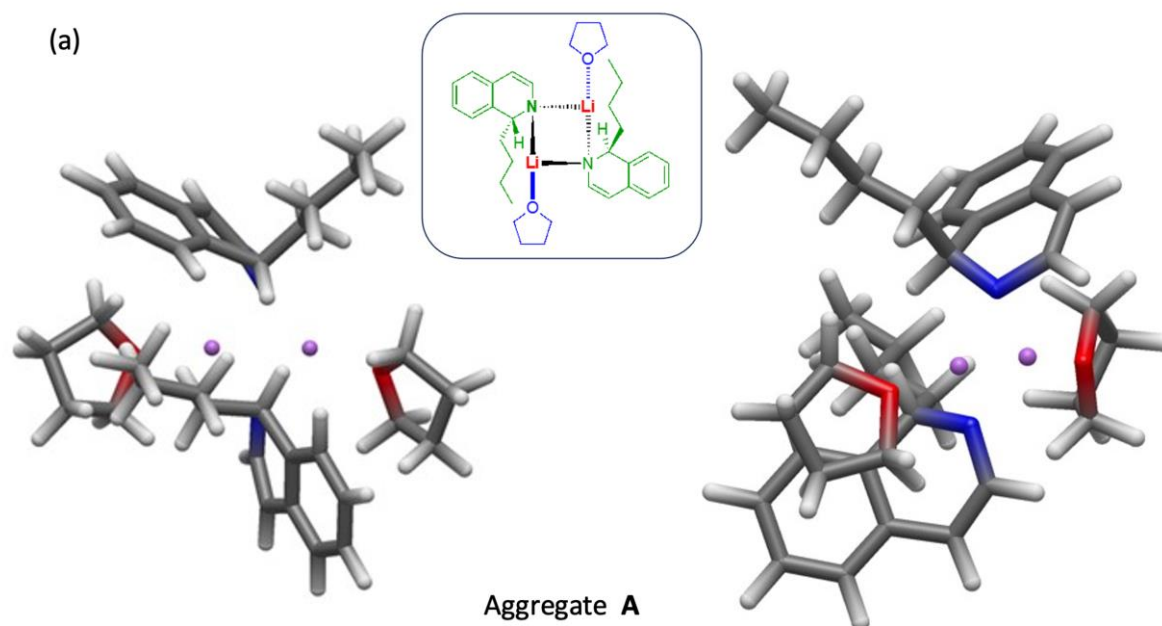


Figure S27. Schematic representation (inset) and two views of the ground state optimized geometry (ω B97X-D/def2-SVP) of 5-*n*BuLi dimer structure B featuring four THF solvent molecules.

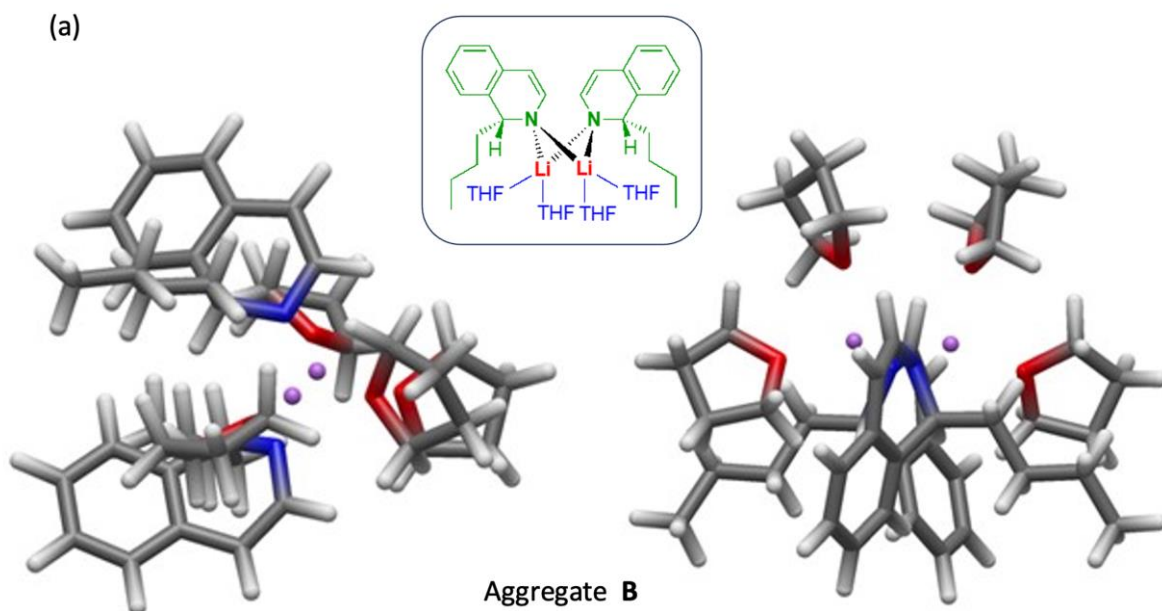


Figure S28. Schematic representation (inset) and two views of the ground state optimized geometry (ω B97X-D/def2-SVP) of 5-*n*BuLi tetramer structure C featuring four THF solvent molecules.

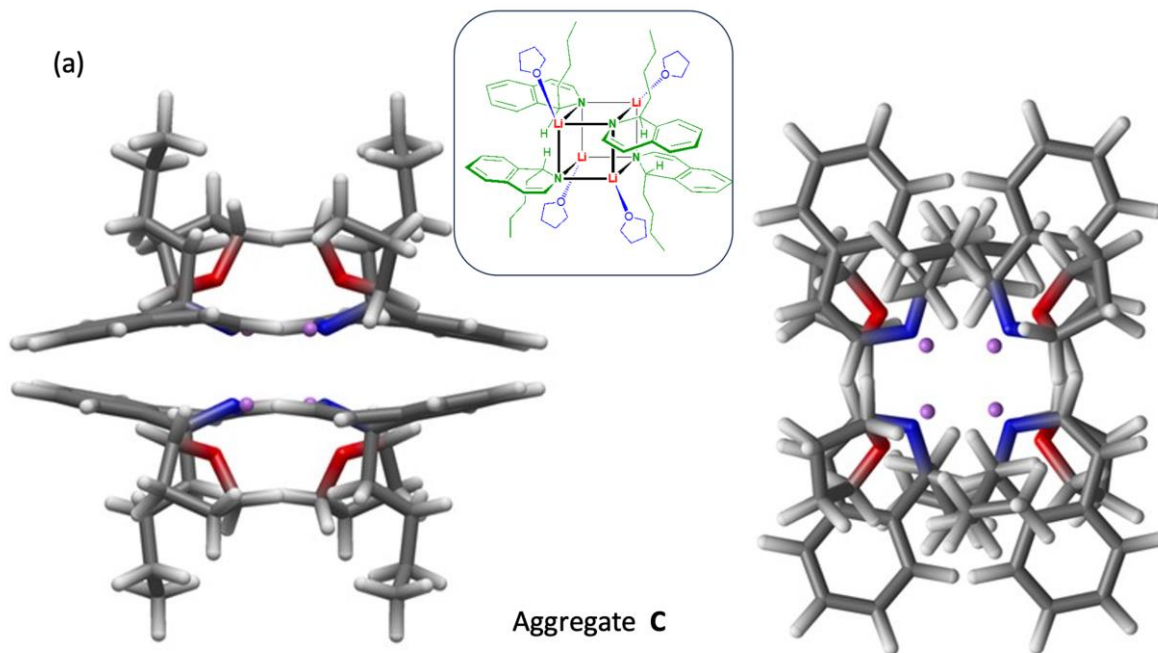


Figure S29. Schematic representation (inset) and two views of the ground state optimized geometry (ω B97X-D/def2-SVP) of 5-*n*BuLi tetramer structure D featuring four THF solvent molecules.

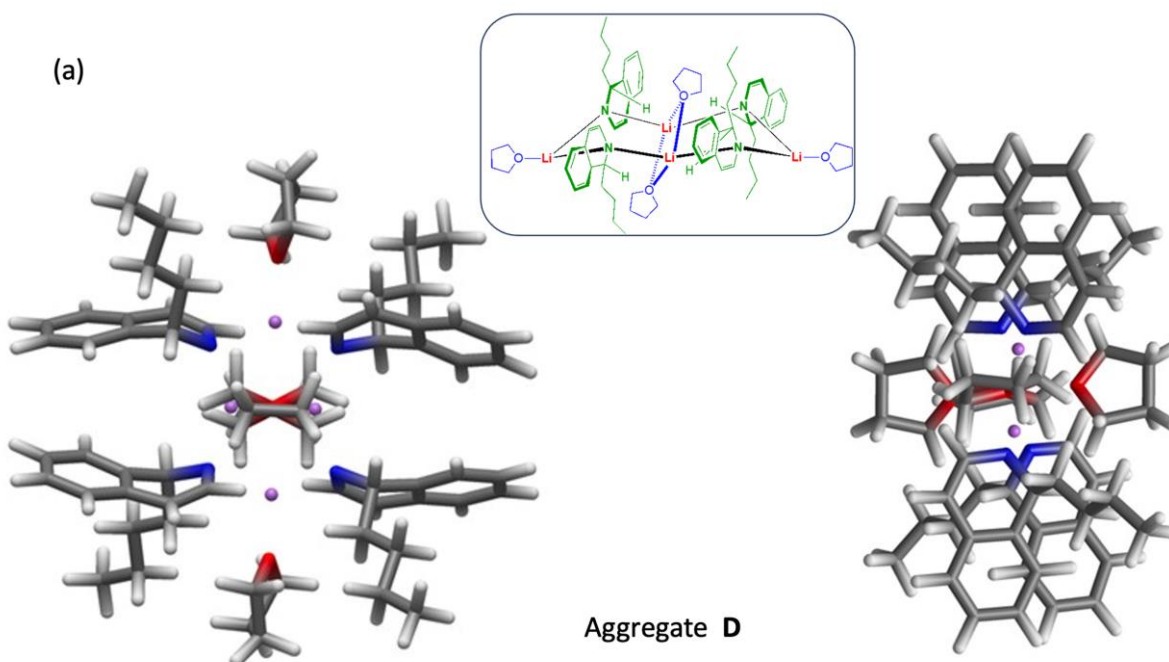


Figure S30. Schematic representation (inset) and two views of the ground state optimized geometry (ω B97X-D/def2-SVP) of 5-*n*BuLi tetramer structure E featuring six THF solvent molecules.

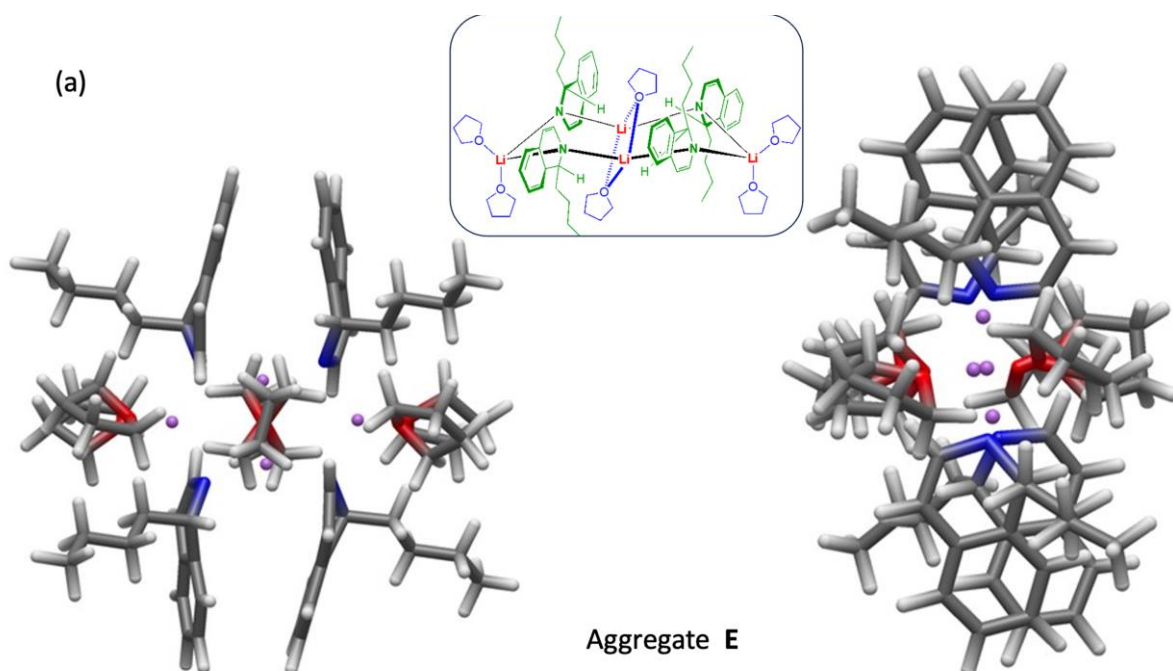


Figure S31. Schematic representation (inset) and two views of the ground state optimized geometry (ω B97X-D/def2-SVP) of 5-*n*BuLi tetramer structure F featuring two THF solvent molecules.

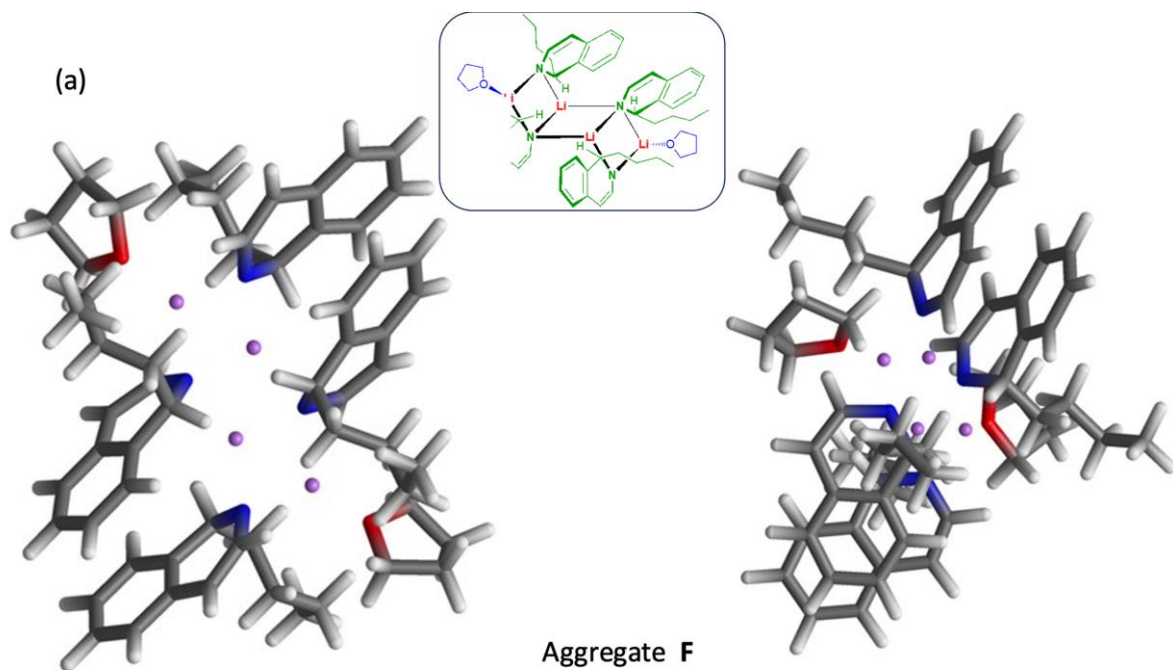


Figure S32. Schematic representation (inset) and two views of the ground state optimized geometry (ω B97X-D/def2-SVP) of 5-*n*BuLi tetramer structure G featuring six THF solvent molecules.

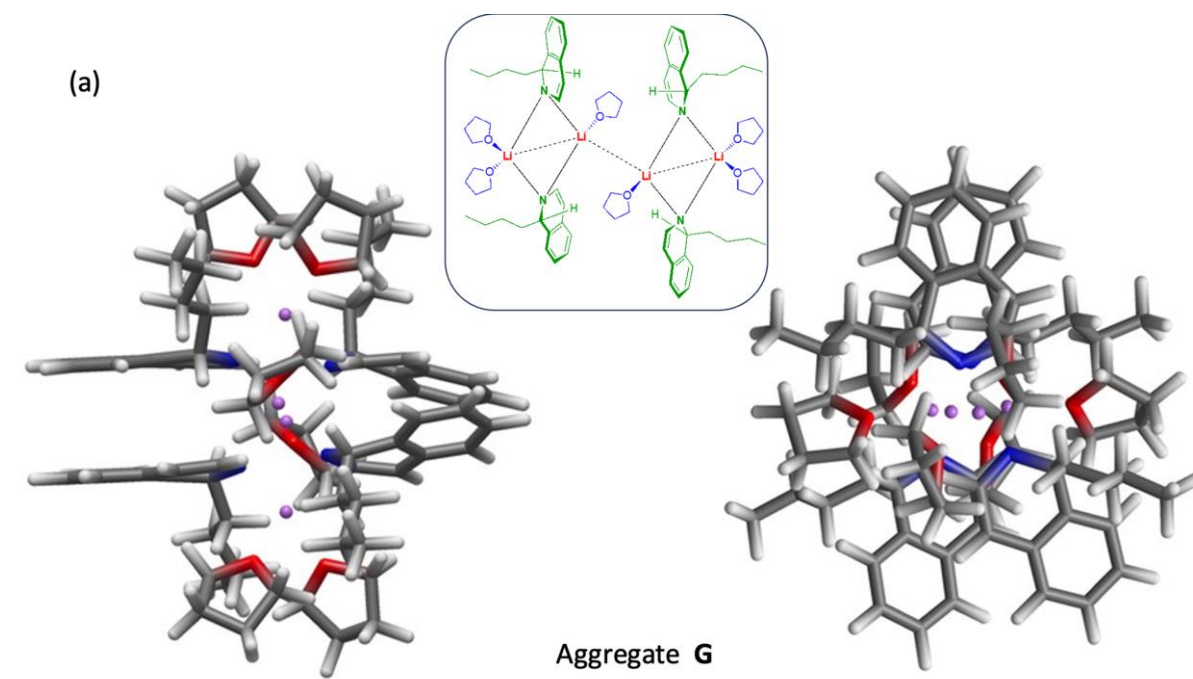


Figure S33. Schematic representation (inset) and two views of the ground state optimized geometry (ω B97X-D/def2-SVP) of 5-*n*BuLi tetramer structure H featuring six THF solvent molecules.

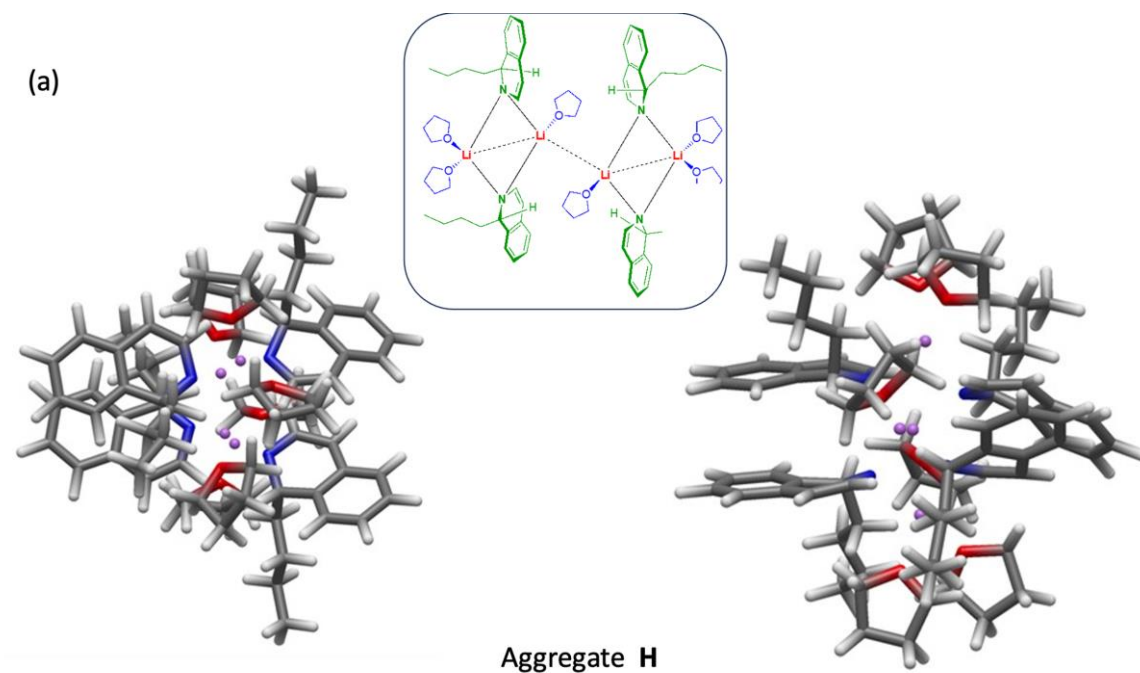


Figure S34. Simulated absorption spectra of the investigated oligomeric structures A-H and of the monomeric 5-*n*BuLi (black line). From TD- ω B97X-D/def2-SVP calculations at optimized ground state geometries.

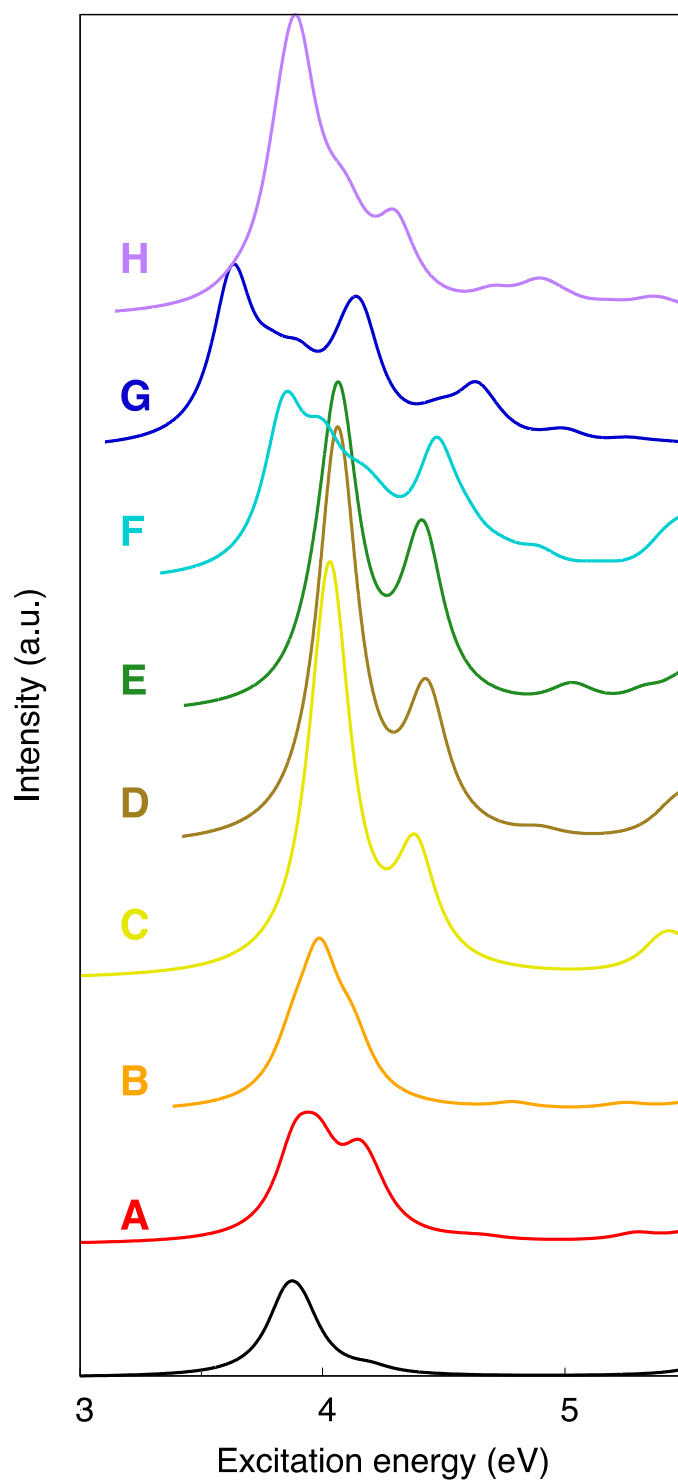
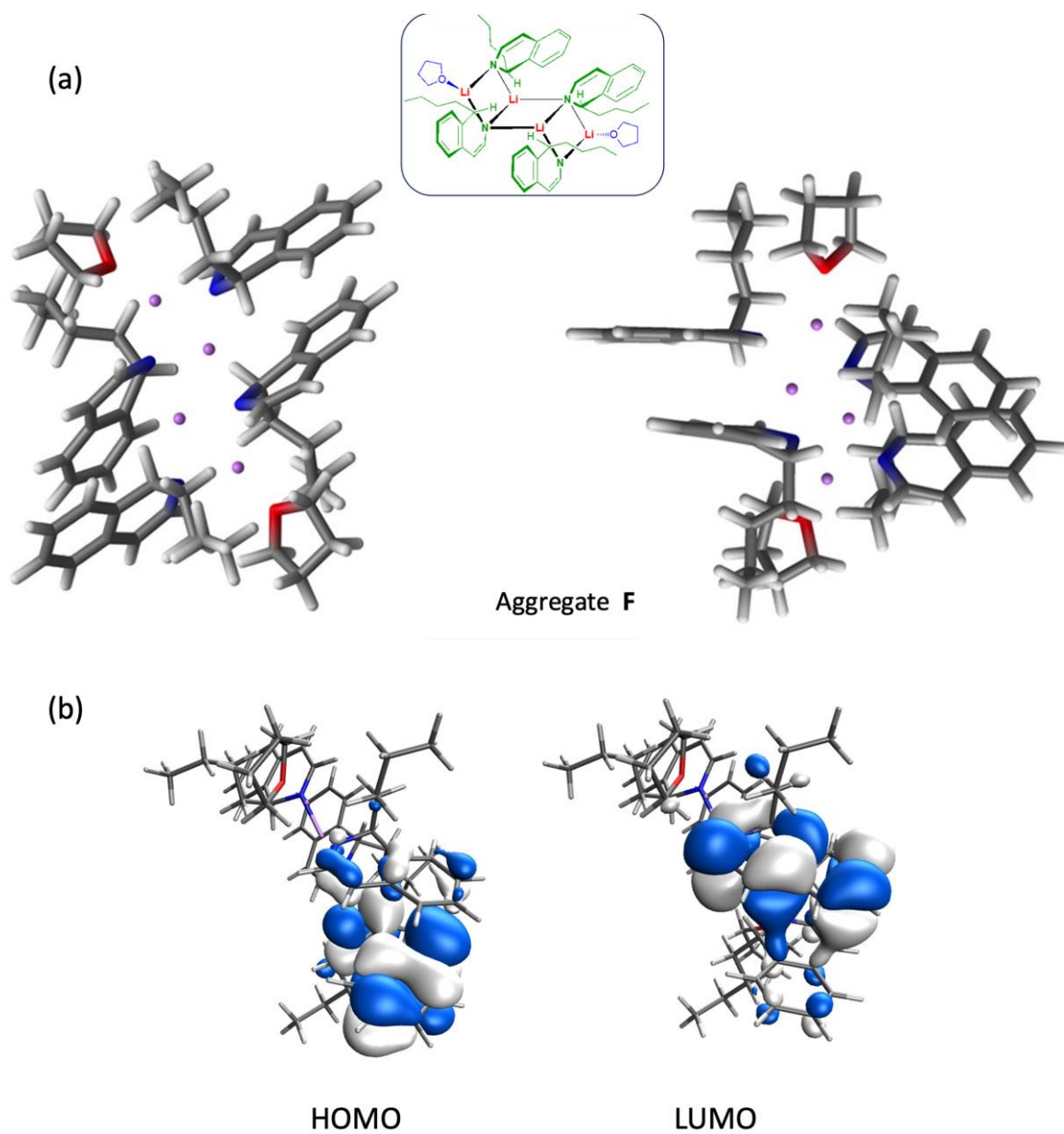


Figure S35. (a) Front and side views of the optimized excited state structure of the $5\cdot n$ BuLi aggregate F and (b) molecular orbitals involved in the excitation that characterizes the lowest singlet excited state responsible for red-shifted emission. From TD- ω B97X-D/def2-SVP calculations.



Calculation of excited state oxidation potentials.

To evaluate the excited state oxidation potentials E_{ox}^* we adopted a direct protocol and computed the Gibbs free energy change between the neutral (excited) form and the radical cation in solution-phase. Thus, the oxidation potential of the excited state was determined as the adiabatic Gibbs free energy difference ($\Delta G_a(THF)$) in the solution-phase (THF) associated with the process $MA^*(THF) \rightarrow MA^+(THF)$, where MA^* and MA^+ are the excited state and cationic form of one of the Meisenheimer Adducts. Specifically,

$$\begin{aligned}\Delta G_a(THF) &= G@geom(MA^+(THF)) - G@geom(MA^*(THF)) = \\ &= IP_a^* + G_{therm}@geom(MA^+(THF)) - G_{therm}@geom(MA^*(THF)) = \\ &= IP_a^* + \Delta G_{therm}\end{aligned}$$

where IP_a^* includes the electronic contribution to the adiabatic ionization potential of the excited state and $G_{therm} = ZPE + H - TS$ includes the zero point energy (ZPE) and the thermal contribution of enthalpy (H) and entropy (S) at room temperature to the total energy of each species (the excited state MA^* and the cationic species MA^+).

The excited state redox potentials are then obtained as

$$E_{ox}^* = \frac{\Delta G_a}{nF}$$

where $n = 1$ is the number of electrons involved and F is Faraday's constant.

Since experimental redox potentials are measured relative to the potential of a reference electrode, we subtracted the redox potential of the reference electrode (e.g. saturated calomel electrode, SCE)

$$E_{ox}^* = \frac{\Delta G_a(THF)}{F} - 4.35$$

where the last term is the standard redox potential of the SCE taken in DMF, a solvent of similar polarity.^[33] We note, finally, that it has recently been suggested that the direct calculation gives a slightly better agreement with the experiment, compared to the use of a thermodynamic cycle, for oxidation potentials.^[34] The excited state oxidation potentials were determined for **4-nBuLi**, **5-nBuLi**, and the G aggregate of **5-nBuLi**. For **4-nBuLi** and **5-nBuLi**, we determined the excited state and the cationic state optimized geometries including implicit solvent effects with the polarizable continuum model (PCM), by keeping, in both cases, the two explicit THF molecules. For the G aggregate of **5-nBuLi** the aggregate included six THF molecules and implicit solvent was not considered during the optimization of the excited state and cationic state. Furthermore, due to the large size of the aggregate and highly demanding calculation, excited state vibrational frequencies could not be computed, and we adopted the displaced harmonic oscillator approximation, which assumes that the contributions to G_{therm} are identical for both states so that $\Delta G_{therm} = 0$. The resulting computed oxidation potentials are collected in Table S6. It can be seen that all computed oxidation potentials are < -3 V vs SCE, with the lowest computed E_{ox}^* for the monomeric **5-nBuLi**. Furthermore, the assumption of the displaced harmonic oscillator approximation implies an overestimate (in absolute value) of ca. 0.1-0.15 V for **4-nBuLi** and **5-nBuLi**. Based on the above, we can thus deduce a more realistic prediction of -3.2 V for aggregate G of **5-nBuLi**. All these values support the super-reductant character of these *MA*.

Table S6. Computed excited state oxidation potentials of 4-nBuLi, 5-nBuLi, and the aggregate G of 5-nBuLi.

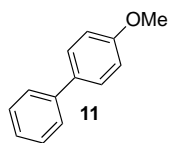
System	IP* / eV	E_{ox}^* / V (vs SCE)
4-nBuLi + 2THF	1.026	-3.22 -3.32 ^[a]
5-nBuLi + 2THF	0.378	-3.82 -3.97 ^[a]
Aggregate G (6 THF)	1.005	-3.20 ^[b] -3.35 ^[a]

[a] adopting the displaced harmonic oscillator approximation, which implies that $\Delta G_{therm}=0$ [b] assuming a $\Delta G_{therm} = 0.15$ eV as determined for **5-nBuLi + 2THF** (see the discussion in the text).

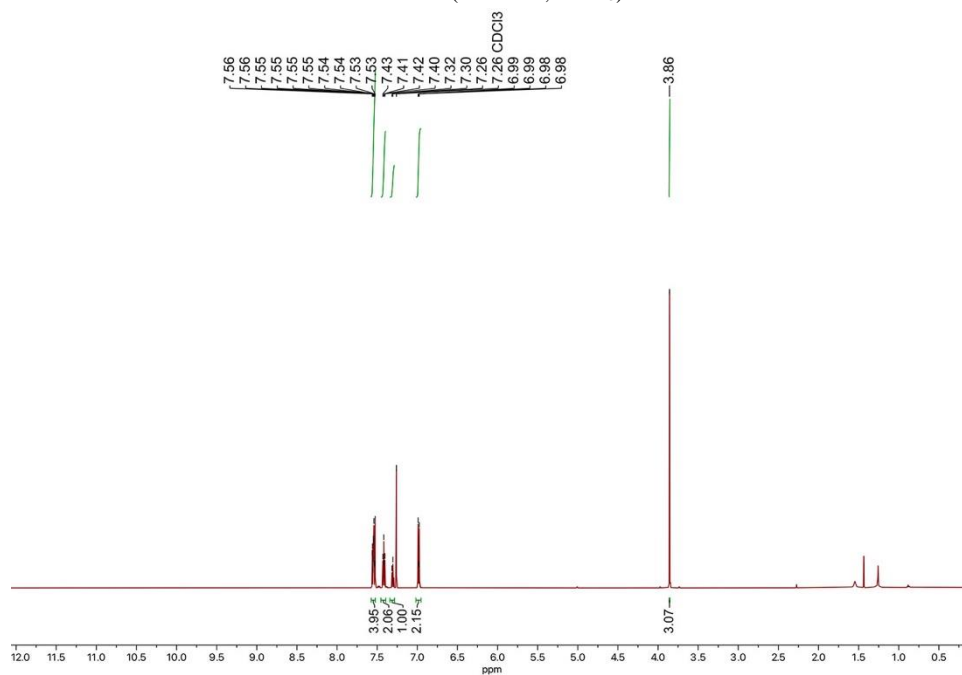
References.

- [1] <https://www.kessil.com/photoreaction/PR160L.php>.
- [2] R. D. Riley, B. S. N. Huchenski, K. L. Bamford, A. W. H. Speed *Angew. Chem. Int. Ed.*, **2022**, *61*, e202204088.
- [3] Y. Suzuki, Y. Okita, T. Morita, Y. Yoshimi *Tetrahedron Lett.*, **2014**, *55*, 22, 3355-3357.
- [4] J. Barluenga, F. J. Fañanás, R. Sanz, C. Marcos, M. Trabada *Org. Lett.*, **2002**, *4*, 1587-1590.
- [5] J. I. Bardagí, S. E. Vaillard, R. A. Rossi, *Tetrahedron Lett.*, **2006**, *47*, 3149-3152.
- [6] V. Papa, J. Fessler, F. Zaccaria, J. Hervochon, P. Dam, C. Kubis, A. Spannenberg, Z. Wei, H. Jiao, C. Zuccaccia, A. Macchioni, K. Junge, M. Beller *Chem.Eur.J.*, **2023**, *29*, e2022027.
- [7] R. D. Patil, S. Pratihari *J. Org. Chem.*, **2024**, *89*, 3, 1361-1378.
- [8] H. Talukdar, D. Gogoi, P. Phukan *Tetrahedron*, **2023**, *132*, 133251-133262.
- [9] S. Furukawa, N. Morishima, K.-I. Fujita *Eur. J. Org. Chem.*, **2024**, *27*, e202301105.
- [10] R. Mondal, S. Pal, A. K. Guin, L. Roy, N. D. Paul *J. Org. Chem.*, **2023**, *88*, 2, 771-787.
- [11] S.-D. Wang, B. Yang, H. Zhang, J.-P. Qu, Y.-B. Kang *Org. Lett.*, **2023**, *25*, 5, 816-820.
- [12] J. Du, H. Li, t. Wu, M. Wang, R. Cheng, D. Wu, Y. Yang, J. Lan *Chem. Commun.*, **2023**, *59*, 8957-8960.
- [13] D. Khan, I. Parveen *Eur. J. Org. Chem.* **2021**, 4946-4957.
- [14] T. Zhang, Y. Lv, Z. Zhang, Z. Jia, T.-P. Loh *Org. Lett.* **2023**, *25*, 24, 4468-4472.
- [15] K. Kobayashi, S. Komatsuzaki, S. Onozawa, K. Masuda, S. Kobayashi *Org. Biomol. Chem.*, **2023**, *21*, 8259-8262.
- [16] L. A. Adria, K. K. Hii *Chem. Commun.*, **2008**, 2325-2327.
- [17] Q. Zhang, J. Luo, B. Wang, X. Xiao, Z. Gan, Q. Tang *Tetrahedron Lett.*, **2019**, *60*, 1337-1340.
- [18] C. E. McDonald, H. D. Bendorf, J. R. Mauck, C. C. McAtee, A. I. Green, D. J. Ciccarelli, C. A. Bendyk, B. J. Conrad, A. T. Delgado *Org. Lett.*, **2020**, *22*, 14, 5685-5689.
- [19] C. H. M. Zheng, D. A. Balatsky, R. C. DiPucchio, L. L. Schafer *Org. Lett.*, **2022**, *24*, 36, 6571-6575.
- [20] K. Ramesh, G. Satyanarayana, *J. Organomet. Chem.*, **2019**, *902*, 120963-120968.
- [21] T. Bhatt, K. Natte *Org. Lett.*, **2024**, *26*, 4, 866-871.
- [22] C. C. Suarez, I. Colomer *Chem. Sci.*, **2023**, *14*, 12083-12090.
- [23] A. Kaithal, B. Chatterjee, C. Gunanathan *J. Org. Chem.*, **2016**, *81*, 22, 11153-11161.
- [24] J. Liang, X. Feng, D. Hait, M. Head-Gordon *J. Chem. Theory Comput.*, **2022**, *18*, 6, 3460-3473.
- [25] D. Jacquemin, B. Mennucci, C. Adamo *Phys. Chem. Chem. Phys.*, **2011**, *13*, 16987-16998.
- [26] U. Salzner, A. Aydin *J. Chem. Theory Comput.*, **2011**, *7*, 8, 2568-2583.
- [27] J. Tomasi, B. Mennucci, R. Cammi *Chem. Rev.*, **2005**, *105*, 8, 2999-3094.
- [28] Gaussian 16, Revision C.01, M. J. Frisch, G. W. Trucks, H. B. Schlegel, G. E. Scuseria, M. A. Robb, J. R. Cheeseman, G. Scalmani, V. Barone, G. A. Petersson, H. Nakatsuji, X. Li, M. Caricato, A. V. Marenich, J. Bloino, B. G. Janesko, R. Gomperts, B. Mennucci, H. P. Hratchian, J. V. Ortiz, A. F. Izmaylov, J. L. Sonnenberg, D. Williams-Young, F. Ding, F. Lipparini, F. Egidi, J. Goings, B. Peng, A. Petrone, T. Henderson, D. Ranasinghe, V. G. Zakrzewski, J. Gao, N. Rega, G. Zheng, W. Liang, M. Hada, M. Ehara, K. Toyota, R. Fukuda, J. Hasegawa, M. Ishida, T. Nakajima, Y. Honda, O. Kitao, H. Nakai, T. Vreven, K. Throssell, J. A. Montgomery, Jr., J. E. Peralta, F. Ogliaro, M. J. Bearpark, J. J. Heyd, E. N. Brothers, K. N. Kudin, V. N. Staroverov, T. A. Keith, R. Kobayashi, J. Normand, K. Raghavachari, A. P. Rendell, J. C. Burant, S. S. Iyengar, J. Tomasi, M. Cossi, J. M. Millam, M. Klene, C. Adamo, R. Cammi, J. W. Ochterski, R. L. Martin, K. Morokuma, O. Farkas, J. B. Foresman, and D. J. Fox, Gaussian, Inc., Wallingford CT, **2016**.
- [29] Gaussian 09, Revision A.02, M. J. Frisch, G. W. Trucks, H. B. Schlegel, G. E. Scuseria, M. A. Robb, J. R. Cheeseman, G. Scalmani, V. Barone, G. A. Petersson, H. Nakatsuji, X. Li, M. Caricato, A. Marenich, J. Bloino, B. G. Janesko, R. Gomperts, B. Mennucci, H. P. Hratchian, J. V. Ortiz, A. F. Izmaylov, J. L. Sonnenberg, D. Williams-Young, F. Ding, F. Lipparini, F. Egidi, J. Goings, B. Peng, A. Petrone, T. Henderson, D. Ranasinghe, V. G. Zakrzewski, J. Gao, N. Rega, G. Zheng, W. Liang, M. Hada, M. Ehara, K. Toyota, R. Fukuda, J. Hasegawa, M. Ishida, T. Nakajima, Y. Honda, O. Kitao, H. Nakai, T. Vreven, K. Throssell, J. A. Montgomery, Jr., J. E. Peralta, F. Ogliaro, M. Bearpark, J. J. Heyd, E. Brothers, K. N. Kudin, V. N. Staroverov, T. Keith, R. Kobayashi, J. Normand, K. Raghavachari, A. Rendell, J. C. Burant, S. S. Iyengar, J. Tomasi, M. Cossi, J. M. Millam, M. Klene, C. Adamo, R. Cammi, J. W. Ochterski, R. L. Martin, K. Morokuma, O. Farkas, J. B. Foresman, and D. J. Fox, Gaussian, Inc., Wallingford CT, **2016**.
- [30] M. D. Hanwell, D. E. Curtis, D. C. Lonie, T. Vandermeersch, E. Zurek, G. R. Hutchison; *J. of Cheminformatics*, **2012**, 4-17.
- [31] R. Dennington, T. A. Keith, J. M. Millam, Semichem Inc., Shawnee Mission, KS, **2016**.
- [32] H. J. Reich, *Chem. Rev.*, **2013**, *113*, 7130-7178.
- [33] A. A. Isse, A. Gennaro, *J. Phys. Chem. B* **2010**, *114*, 7894-7899.
- [34] A. Gualandi, A. Nenov, M. Marchini, G. Rodeghiero, I. Conti, E. Paltanin, M. Balletti, P. Ceroni, M. Garavelli, P. G. Cozzi, *ChemCatChem* **2021**, *13*, 981-989.

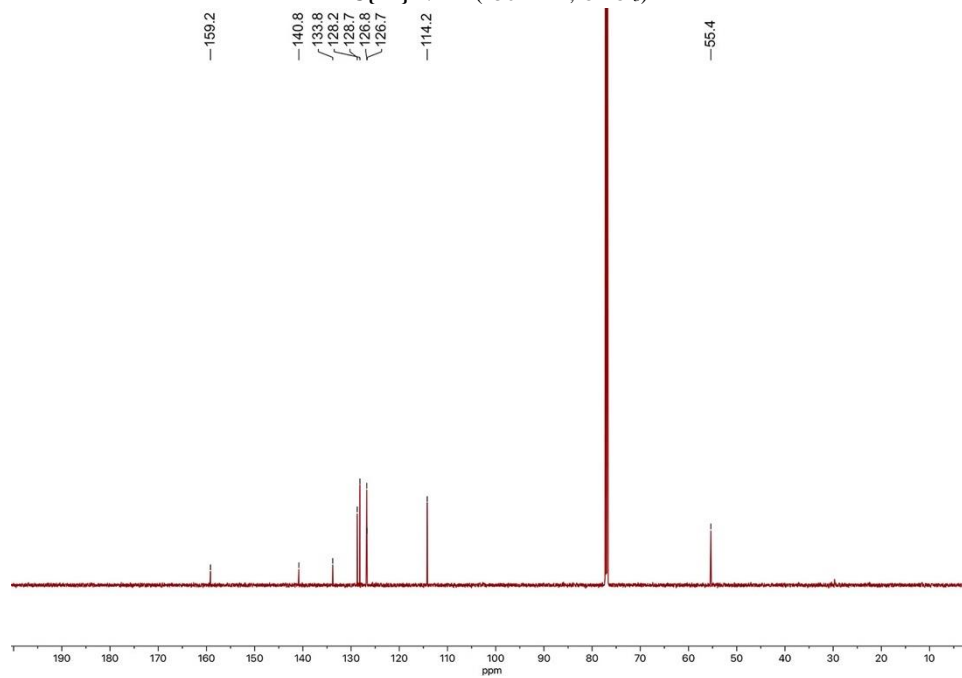
NMR Traces.

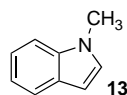


^1H NMR (600 MHz, CDCl_3)



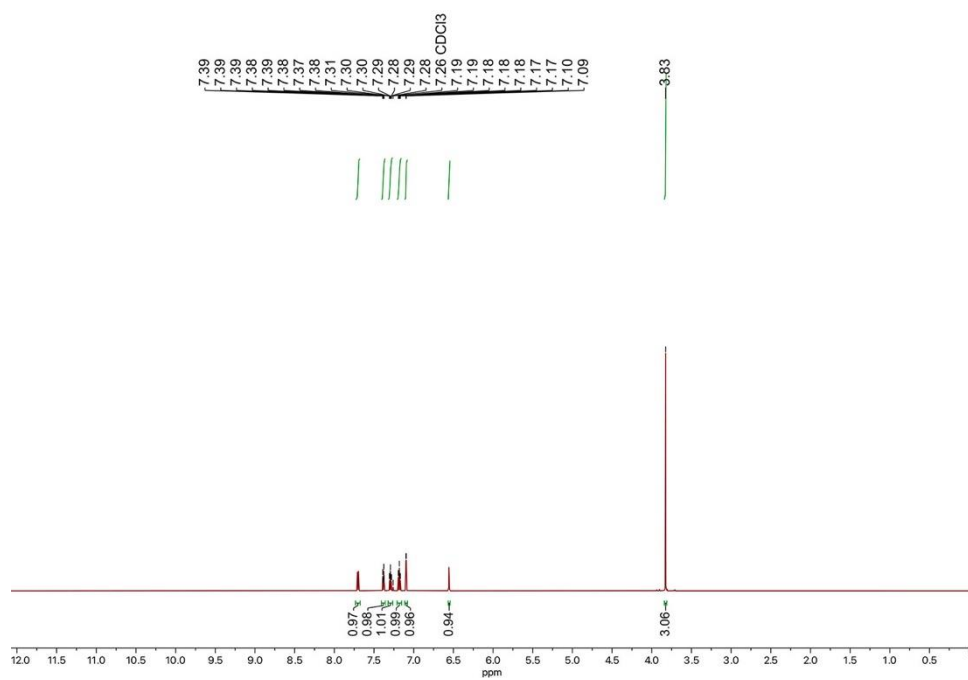
$^{13}\text{C}\{^1\text{H}\}$ NMR (150 MHz, CDCl_3)



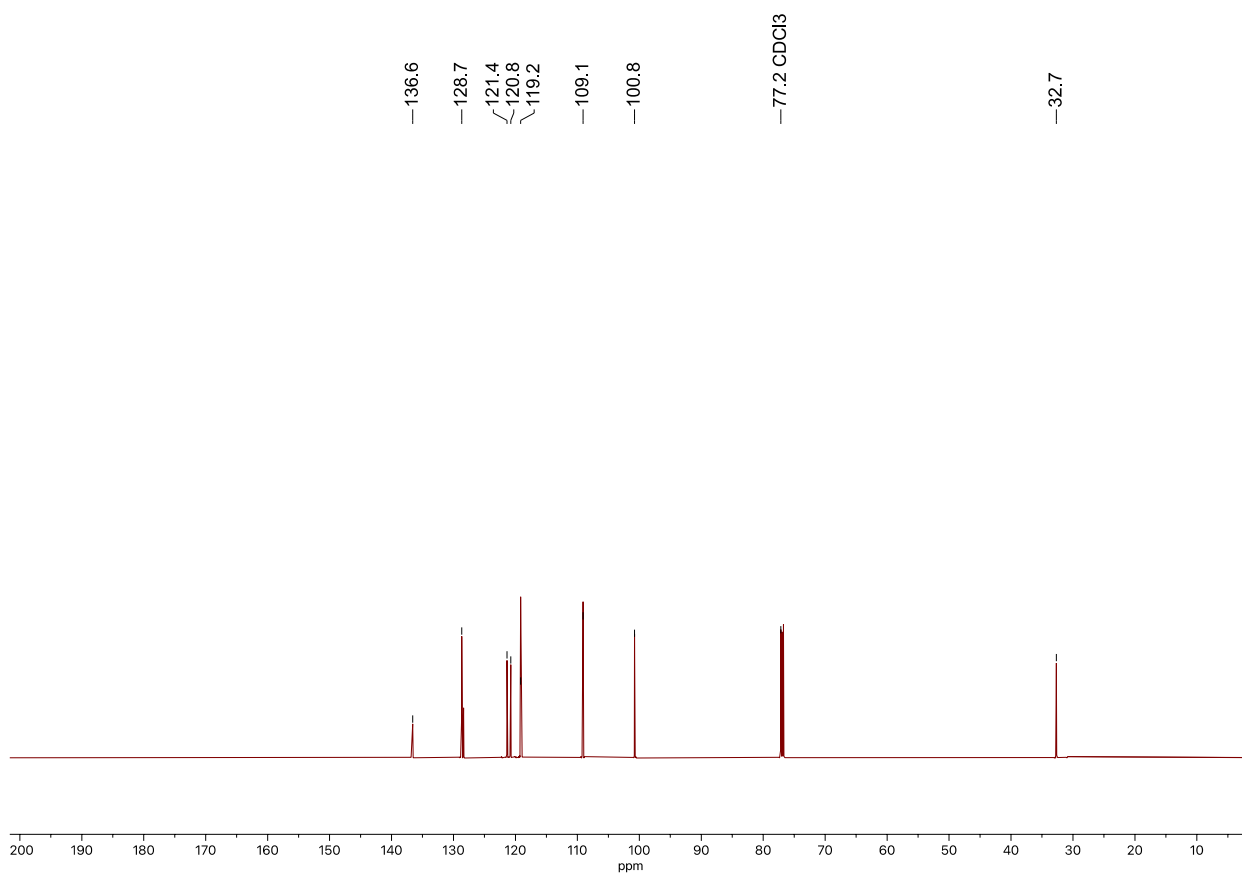


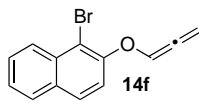
13

¹H NMR (600 MHz, CDCl₃)

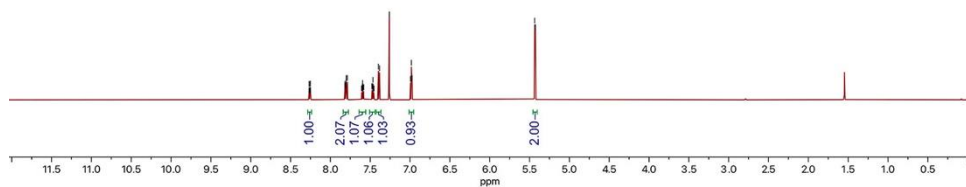
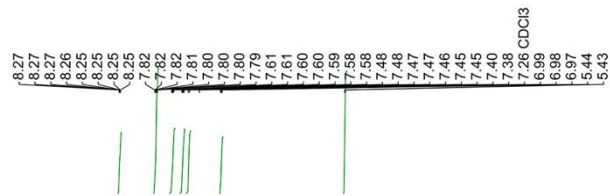


¹³C{¹H} NMR (150 MHz, CDCl₃)

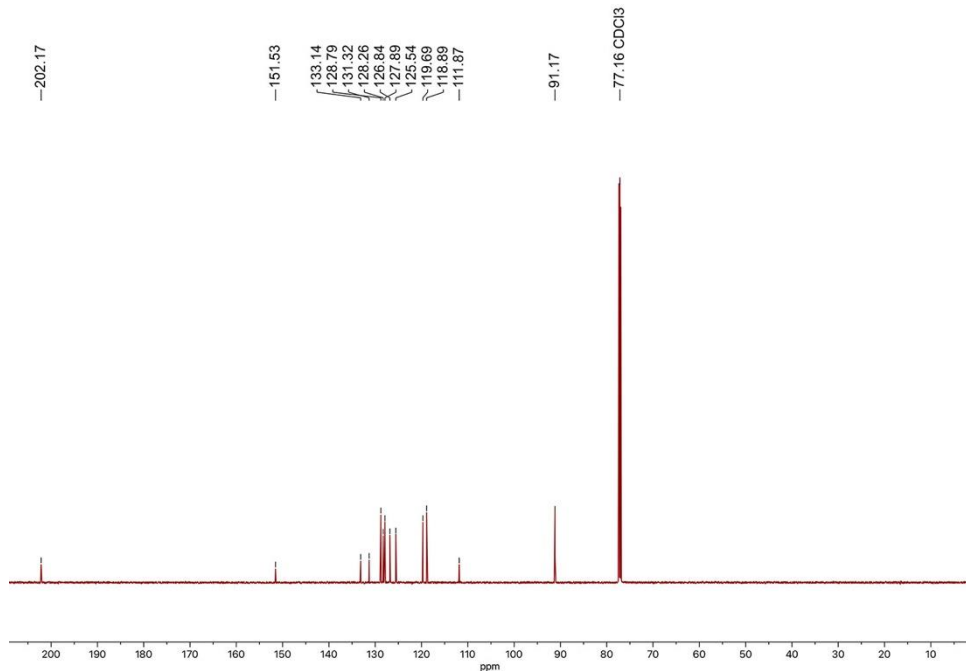


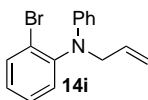


$^1\text{H NMR}$ (400 MHz, CDCl_3)

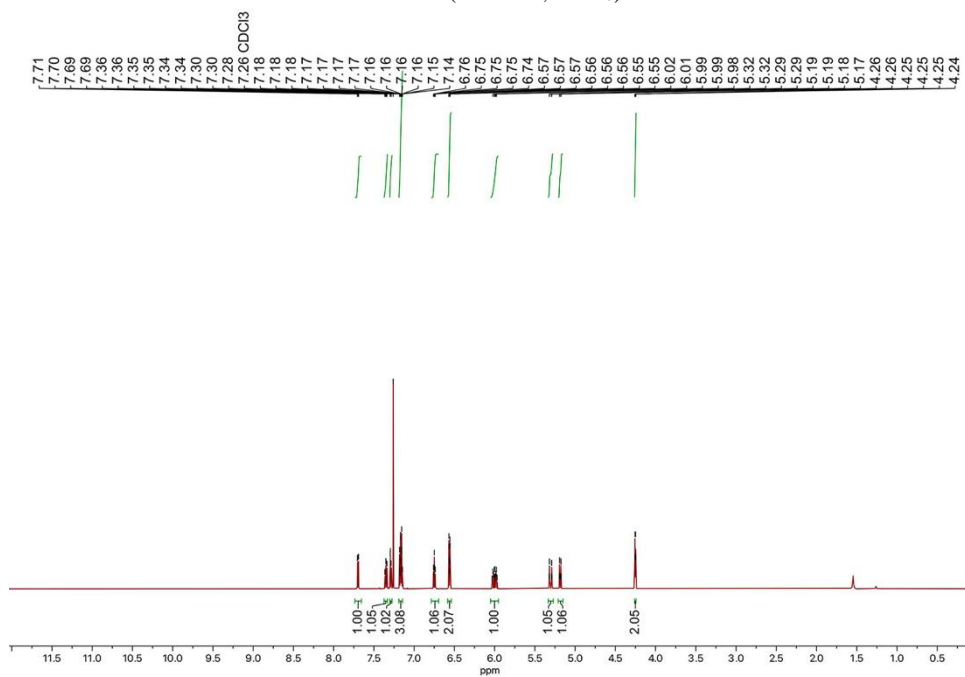


$^{13}\text{C}\{^1\text{H}\}$ NMR (100 MHz, CDCl_3)

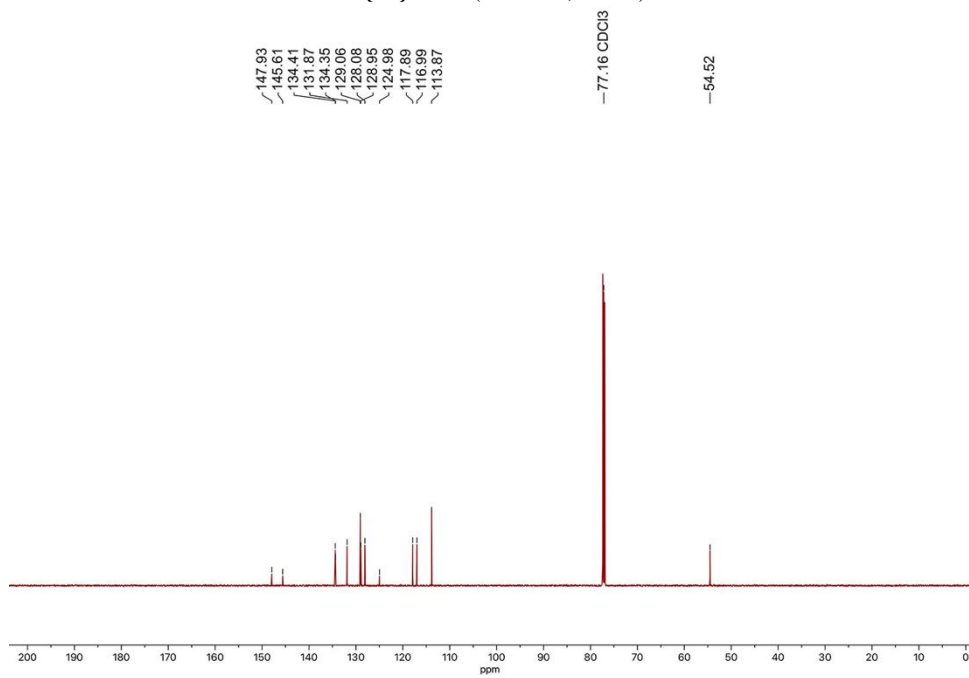


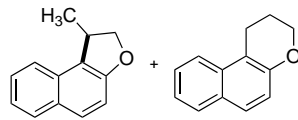


¹H NMR (400 MHz, CDCl₃)



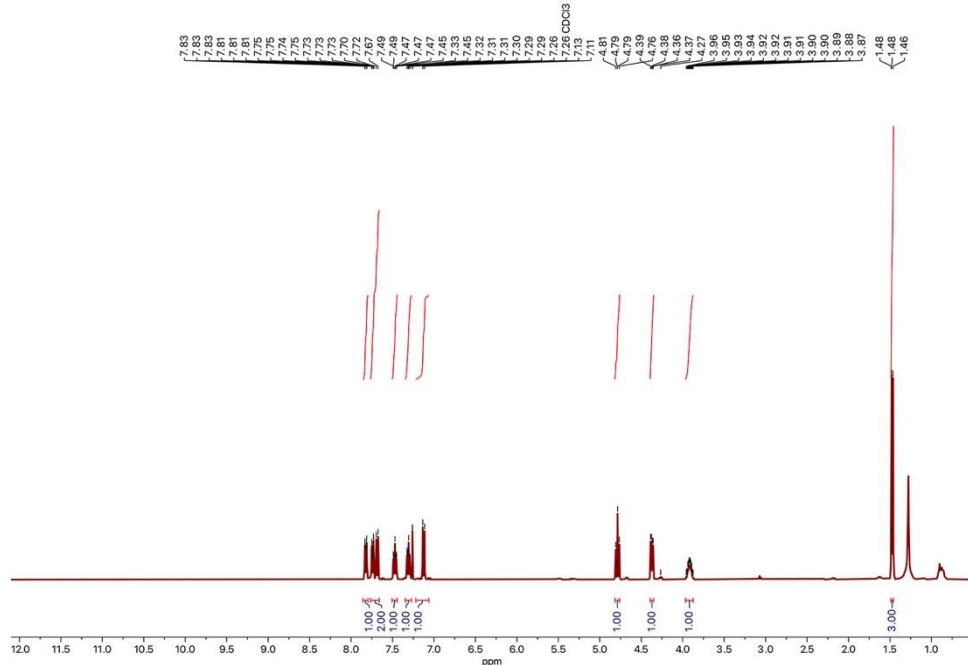
¹³C{¹H} NMR (100 MHz, CDCl₃)



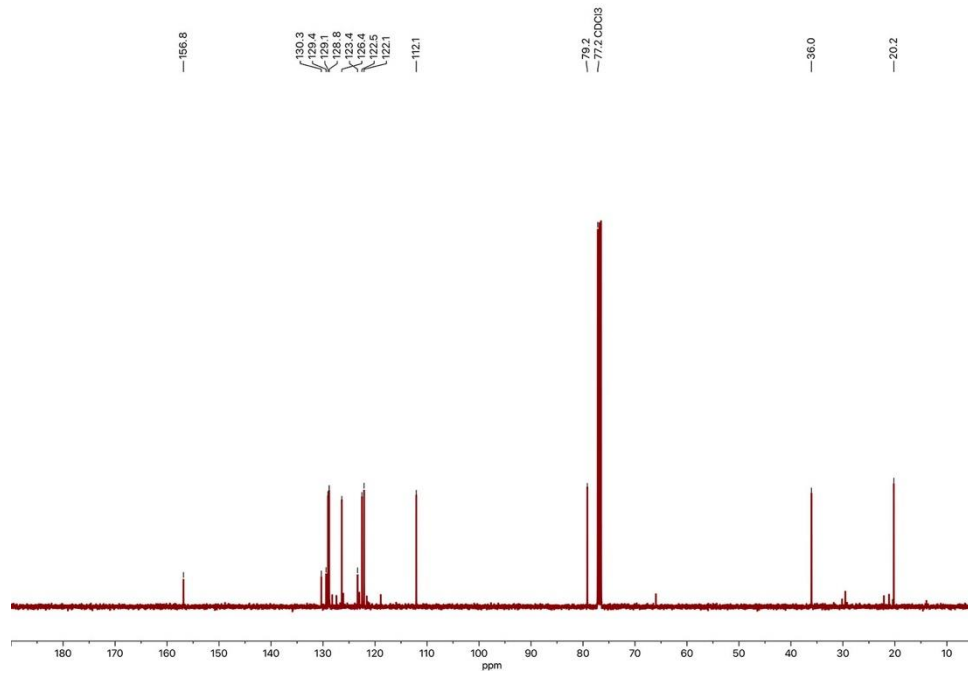


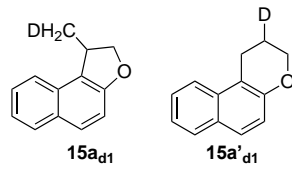
15a **15'a**

¹H NMR (400 MHz, CDCl₃)

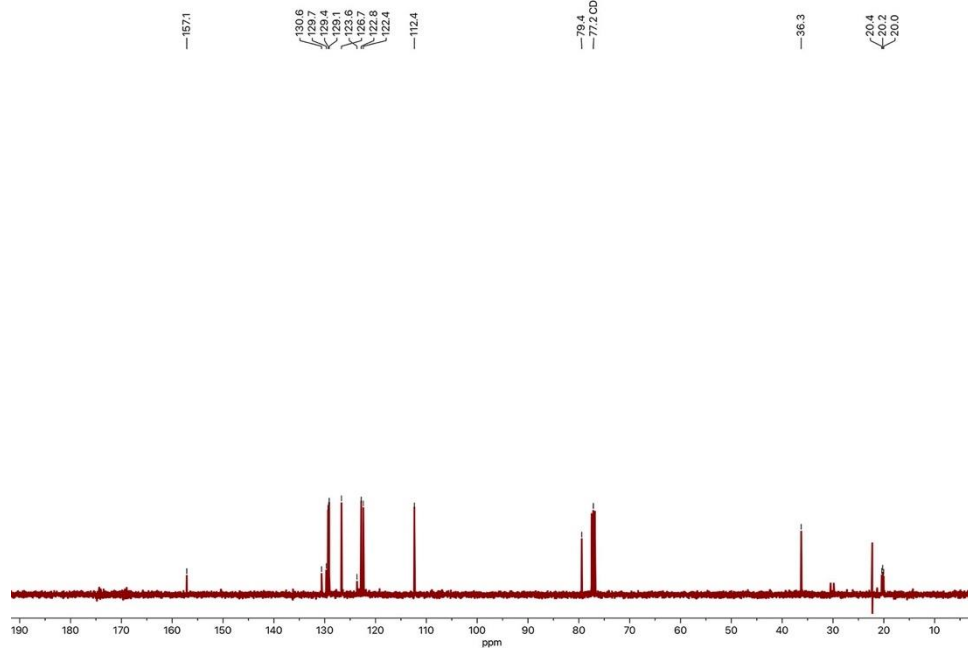
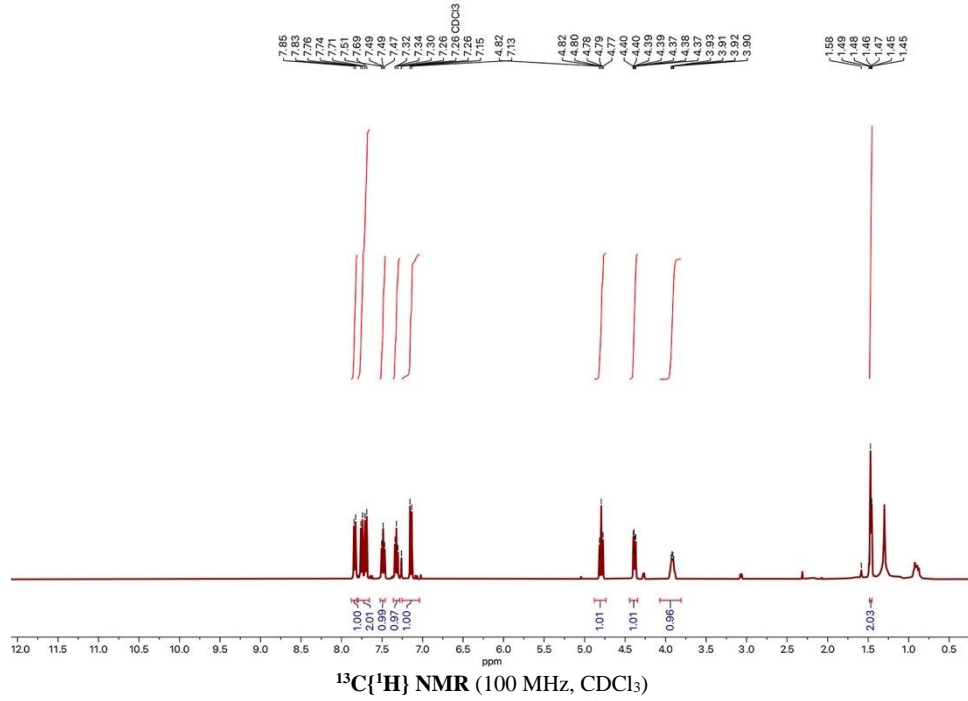


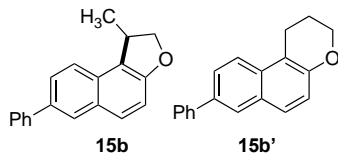
¹³C{¹H} NMR (100 MHz, CDCl₃)



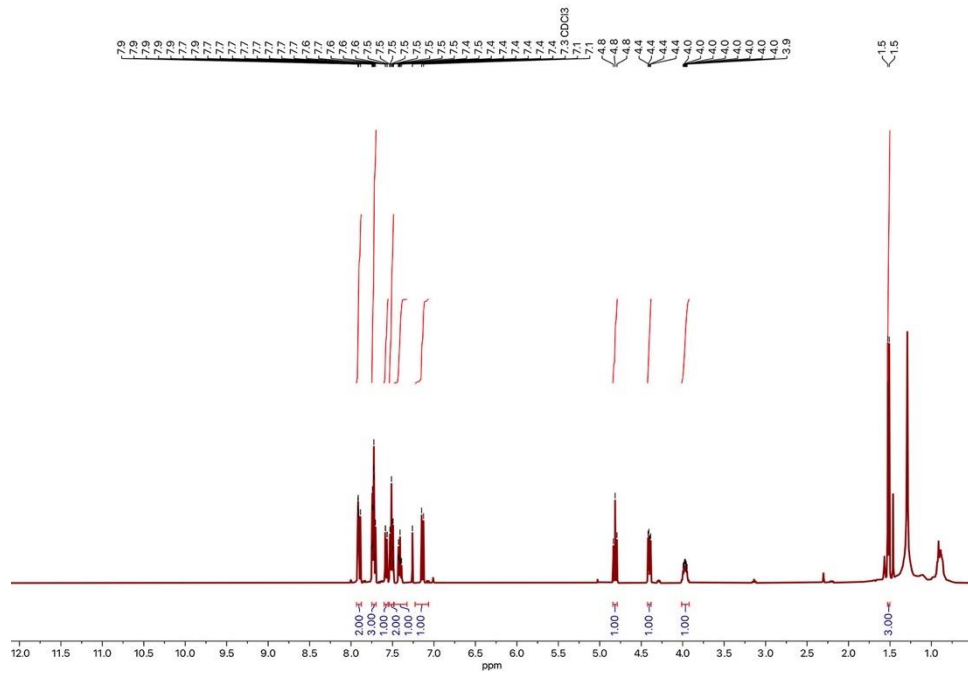


¹H NMR (400 MHz, CDCl₃)

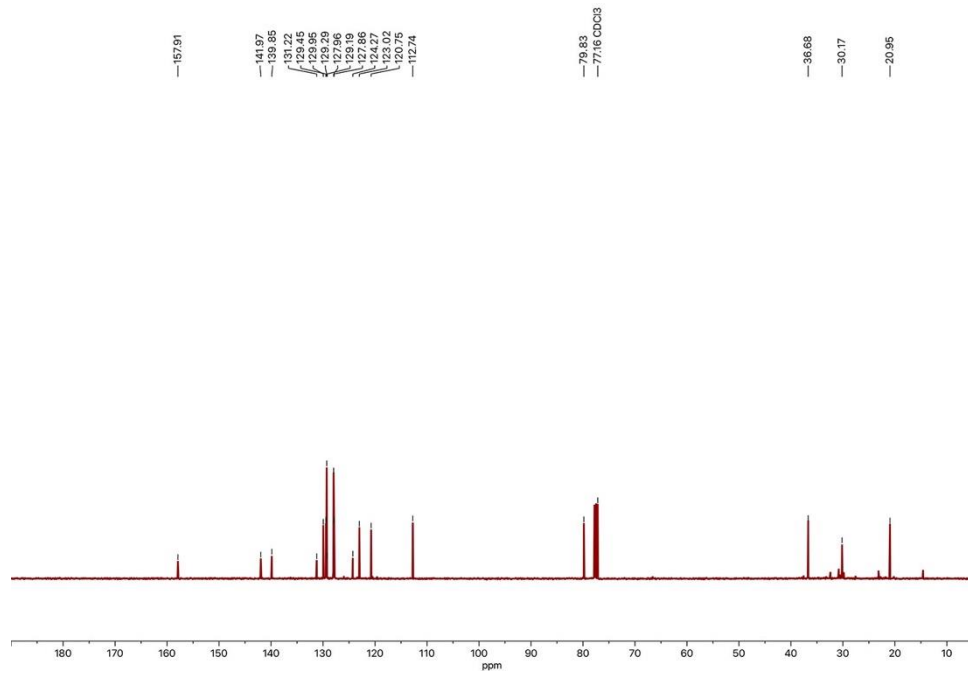


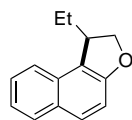


¹H NMR (400 MHz, CDCl₃)

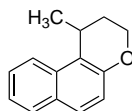


¹³C{¹H} NMR (100 MHz, CDCl₃)



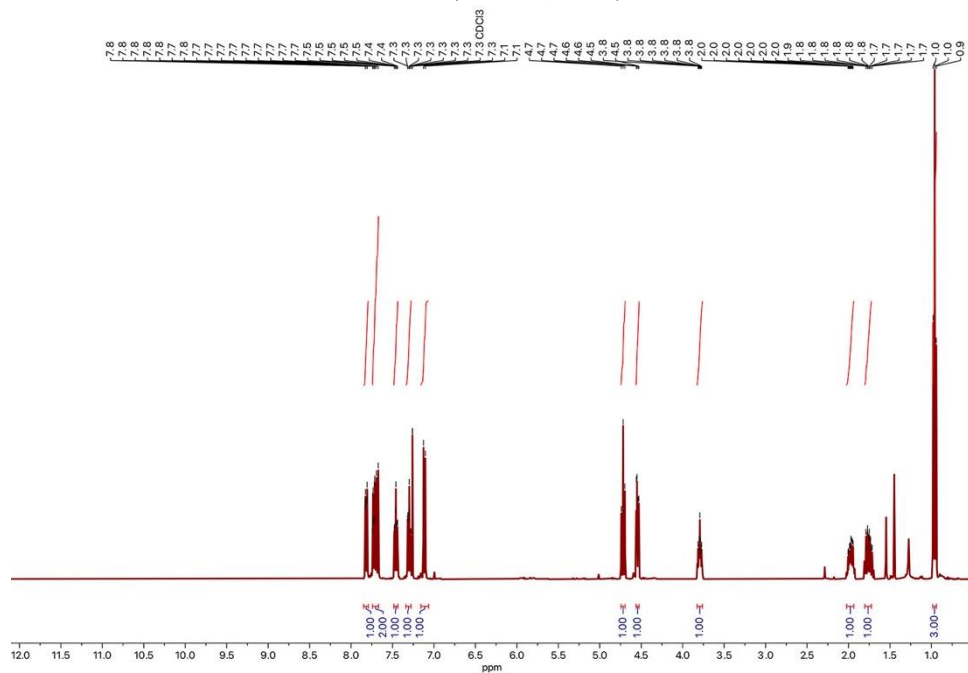


15c

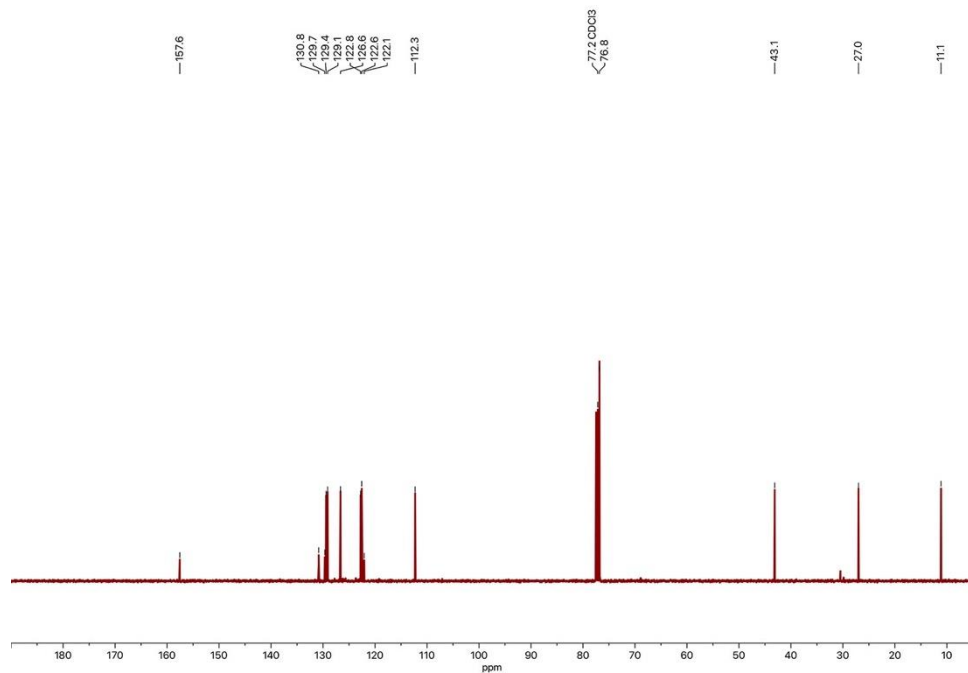


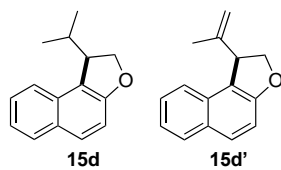
15c'

¹H NMR (400 MHz, CDCl₃)

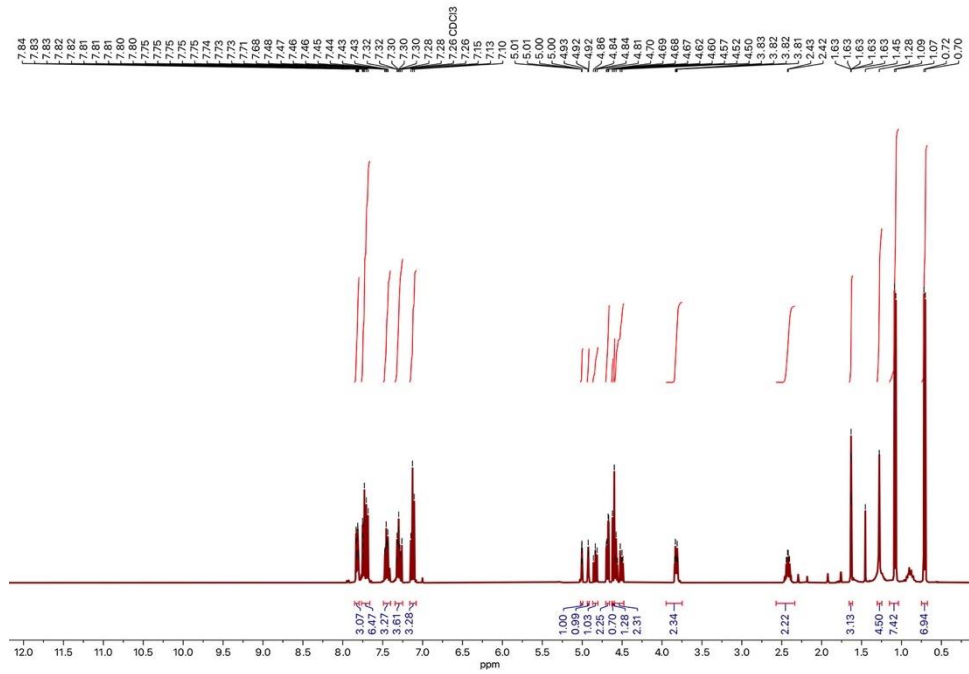


¹³C{¹H} NMR (100 MHz, CDCl₃)

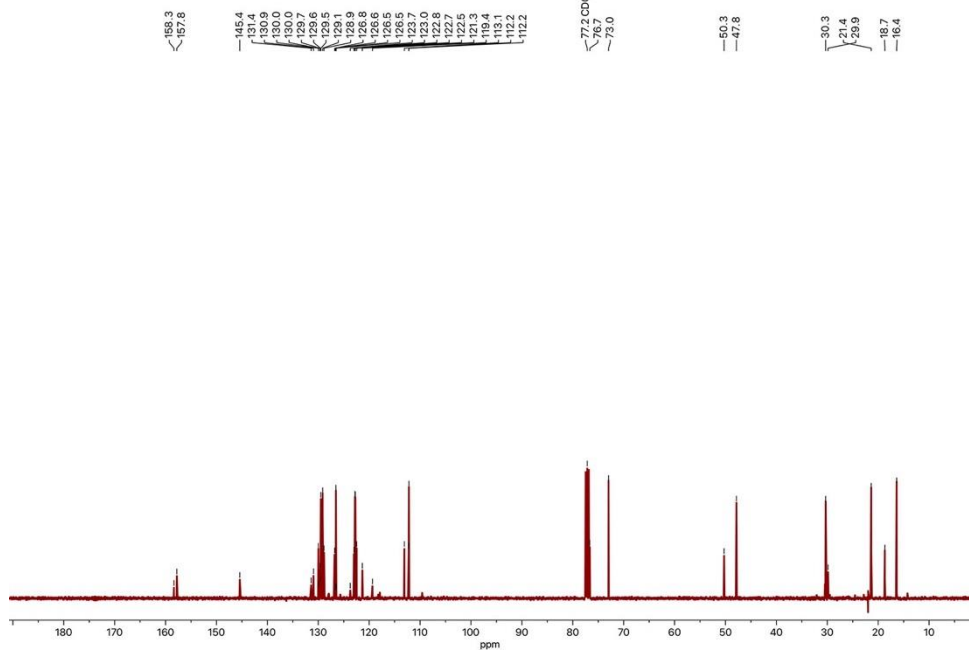


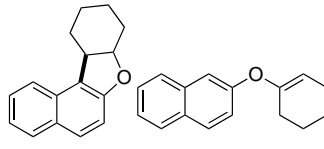


¹H NMR (400 MHz, CDCl₃)

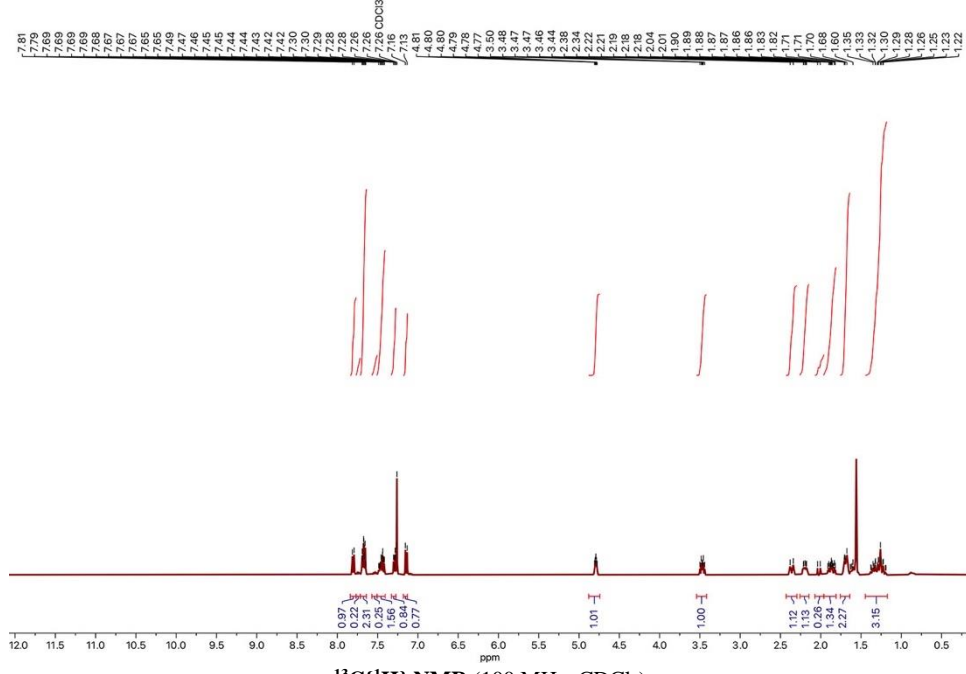


¹³C{¹H} NMR (100 MHz, CDCl₃)

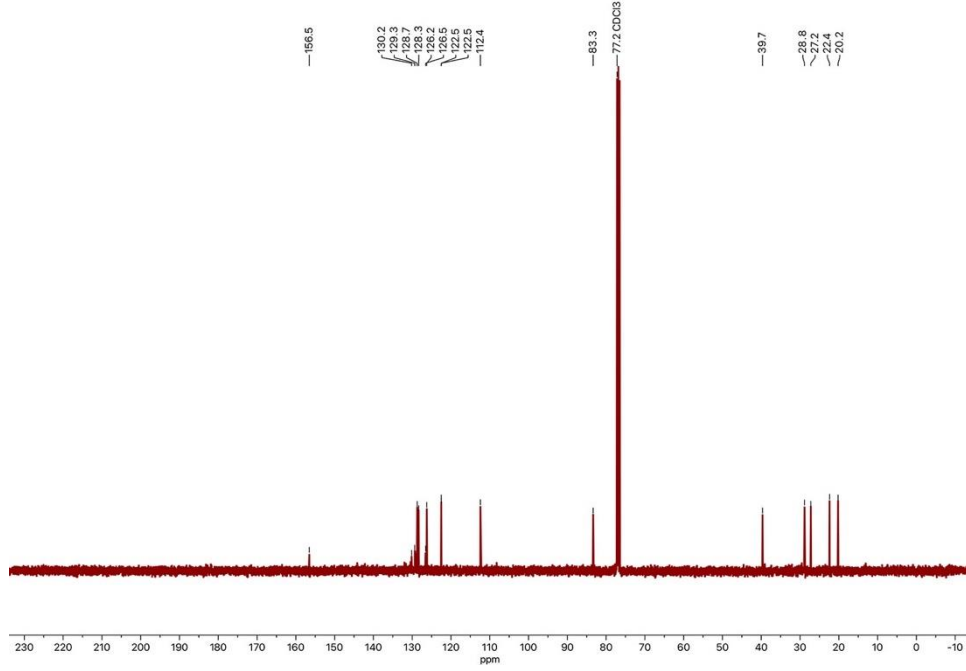


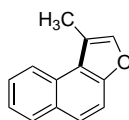


¹H NMR (400 MHz, CDCl₃)



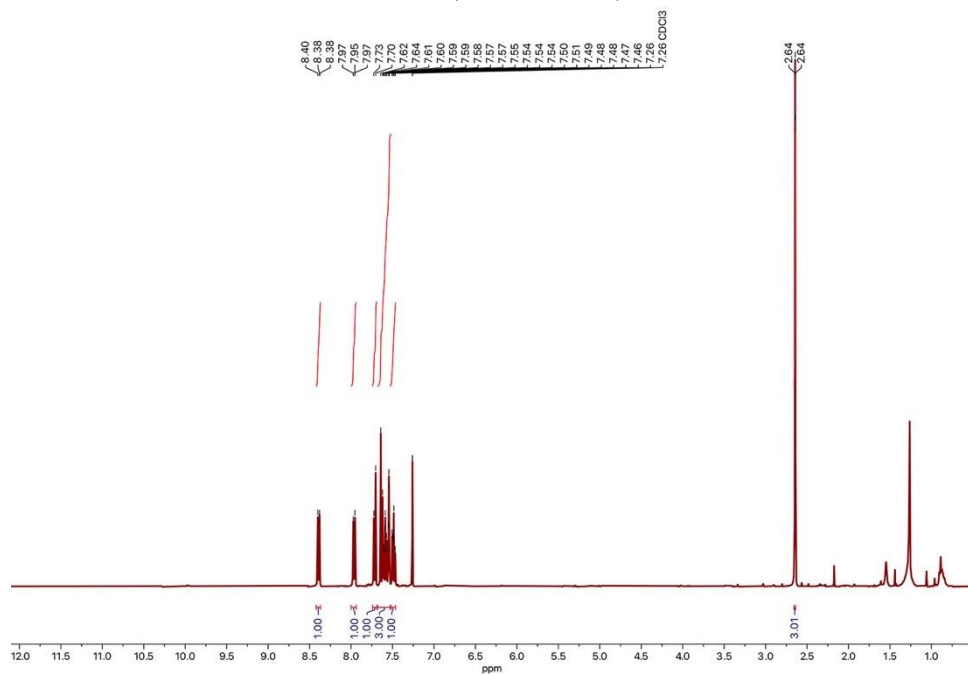
¹³C{¹H} NMR (100 MHz, CDCl₃)



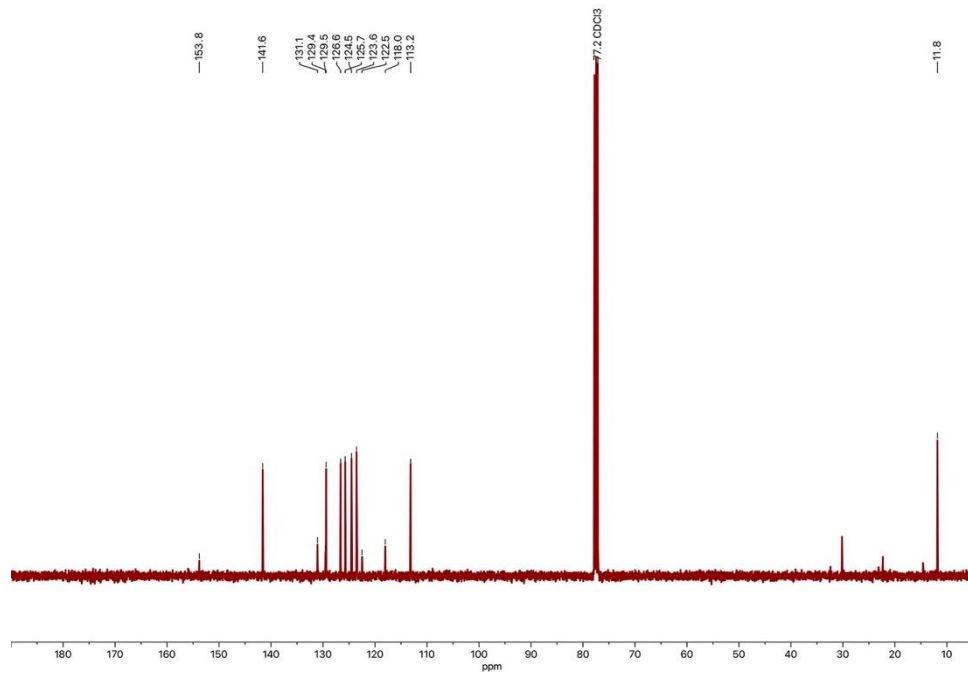


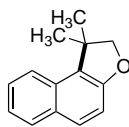
15f

$^1\text{H NMR}$ (400 MHz, CDCl_3)



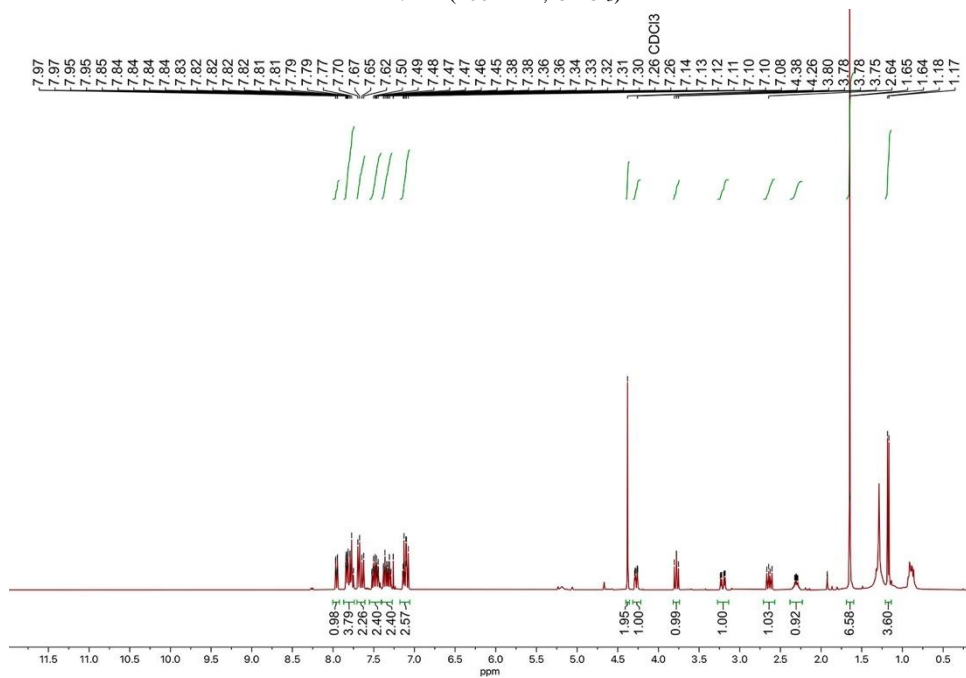
$^{13}\text{C}\{^1\text{H}\}$ NMR (100 MHz, CDCl_3)



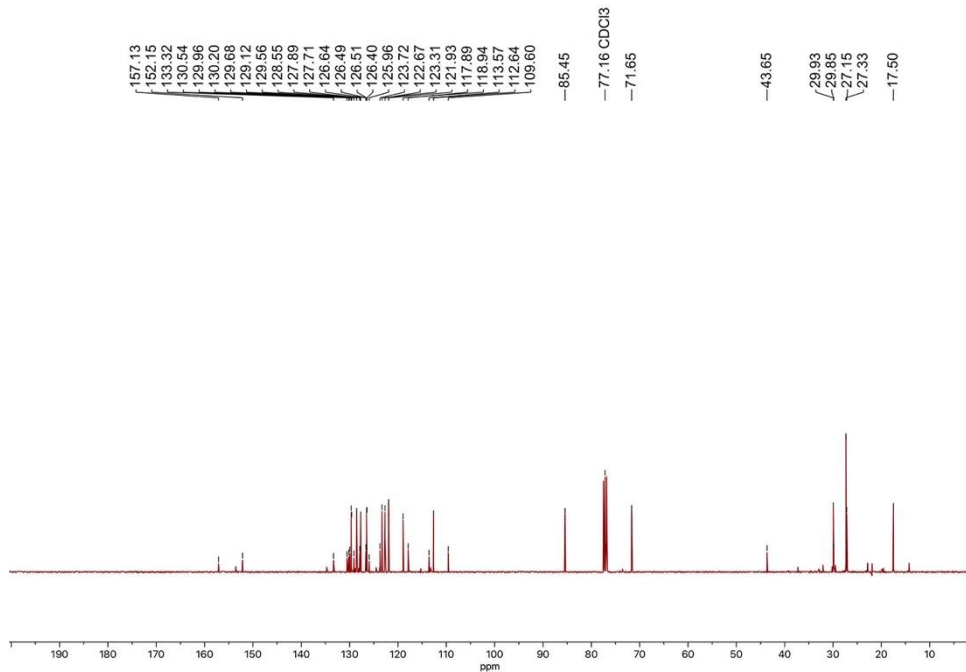


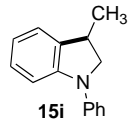
15g

$^1\text{H NMR}$ (400 MHz, CDCl_3)

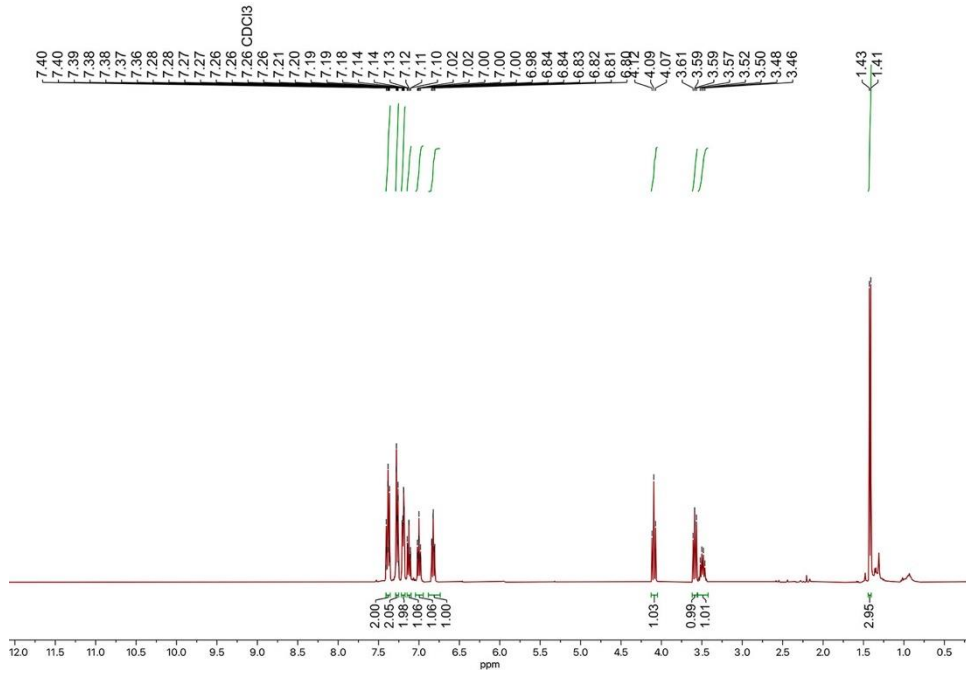


$^{13}\text{C}\{^1\text{H}\}$ NMR (100 MHz, CDCl_3)

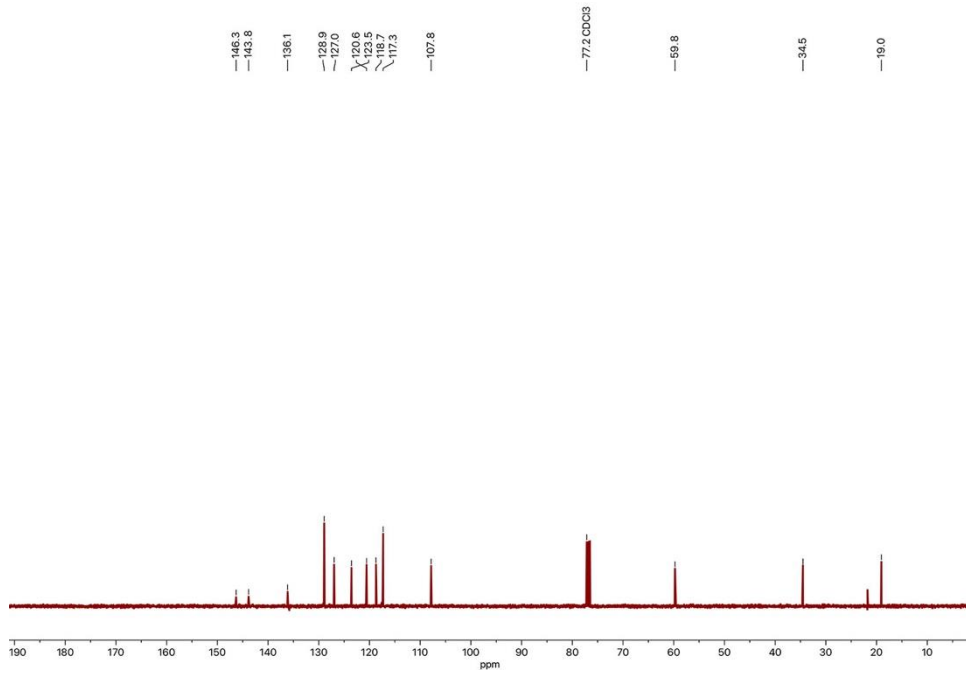


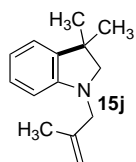


¹H NMR (400 MHz, CDCl₃)

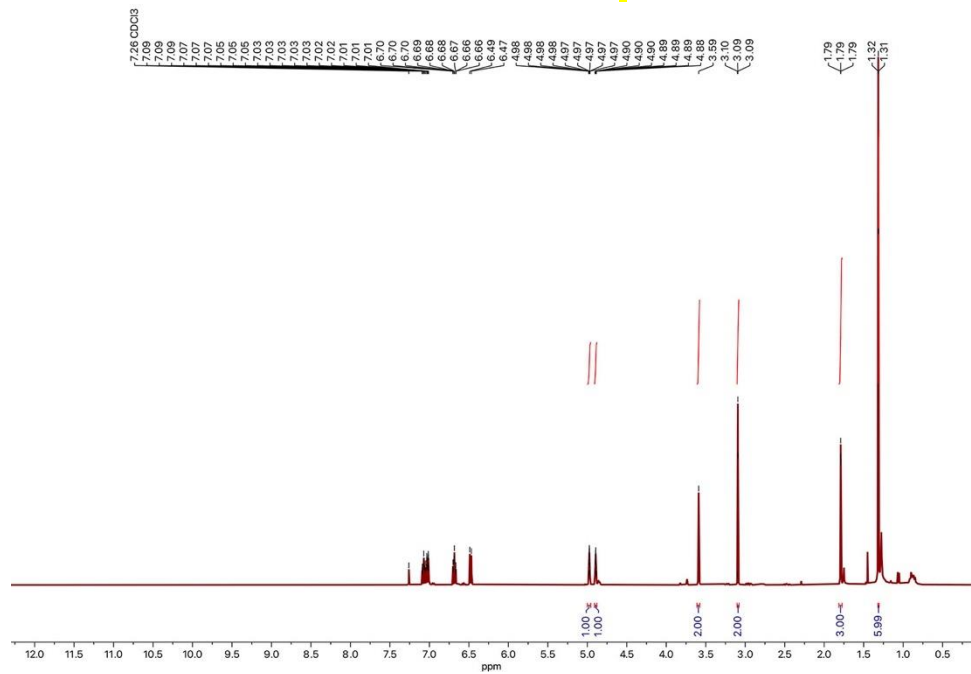


¹³C{¹H} NMR (100 MHz, CDCl₃)

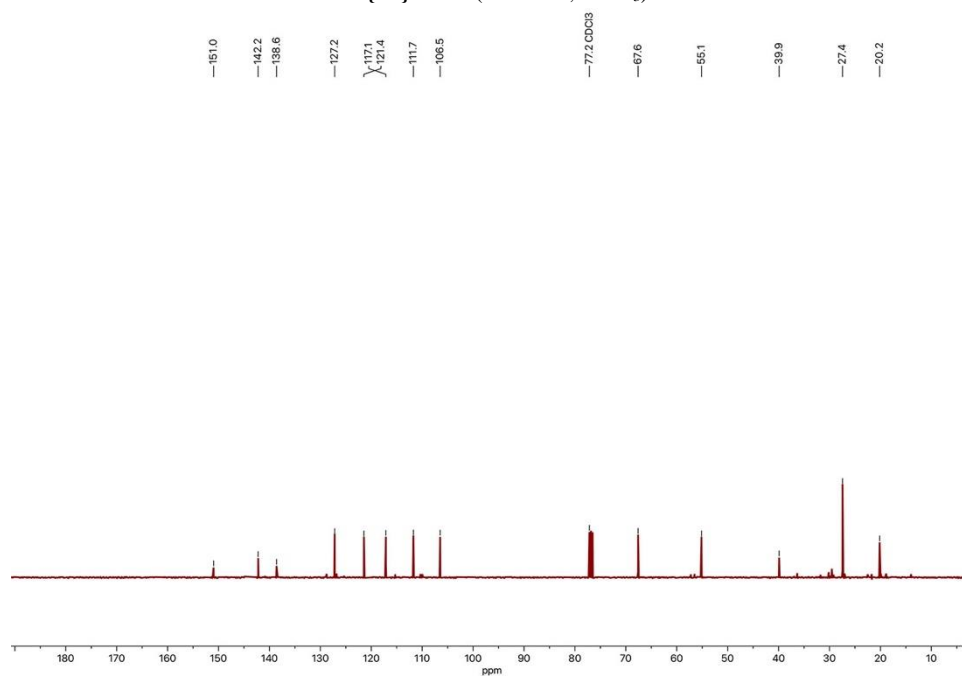


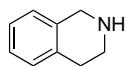


¹H NMR (400 MHz, CDCl₃)



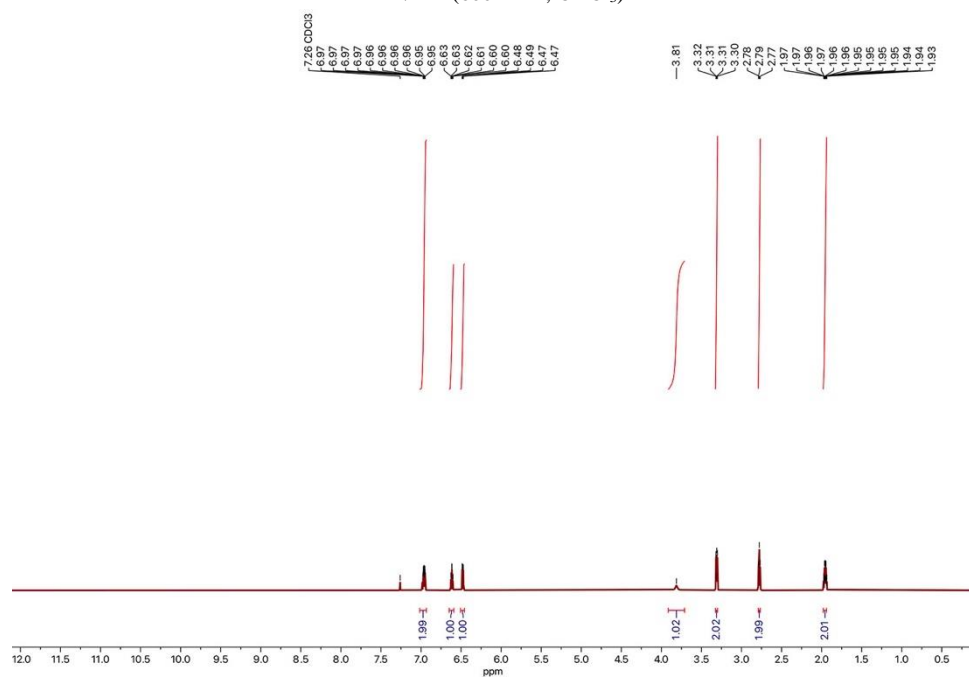
¹³C{¹H} NMR (100 MHz, CDCl₃)



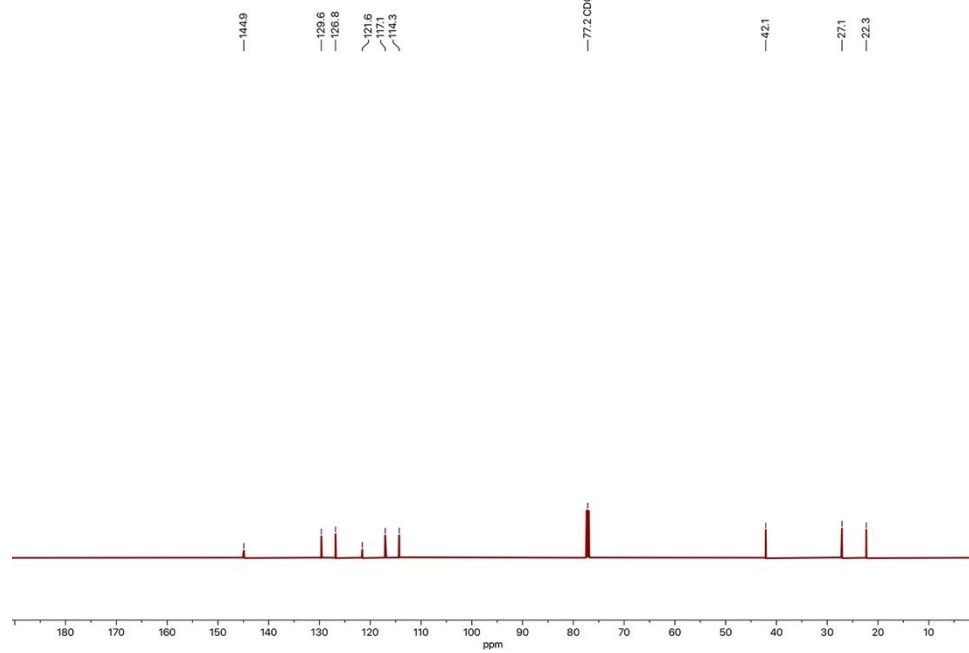


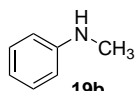
19a

^1H NMR (600 MHz, CDCl_3)



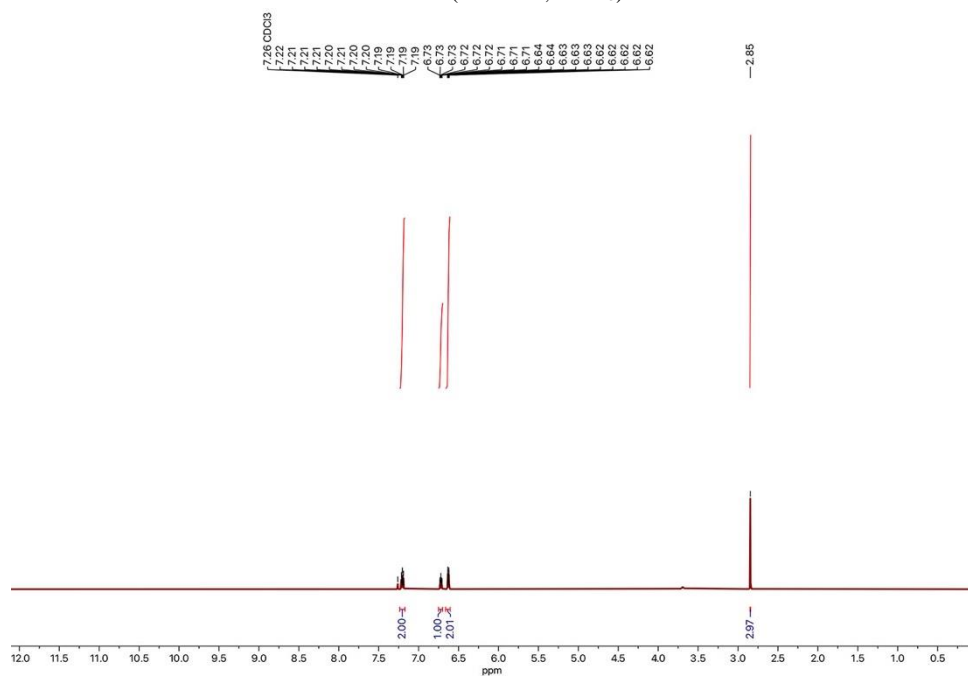
$^{13}\text{C}\{^1\text{H}\}$ NMR (150 MHz, CDCl_3)



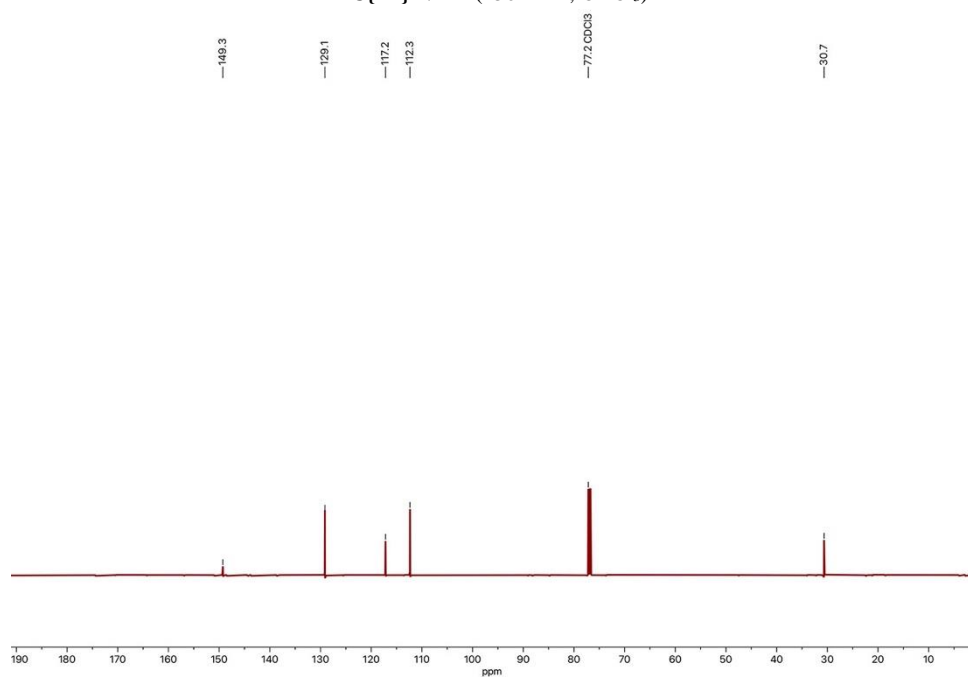


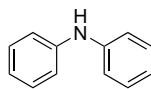
19b

¹H NMR (600 MHz, CDCl₃)



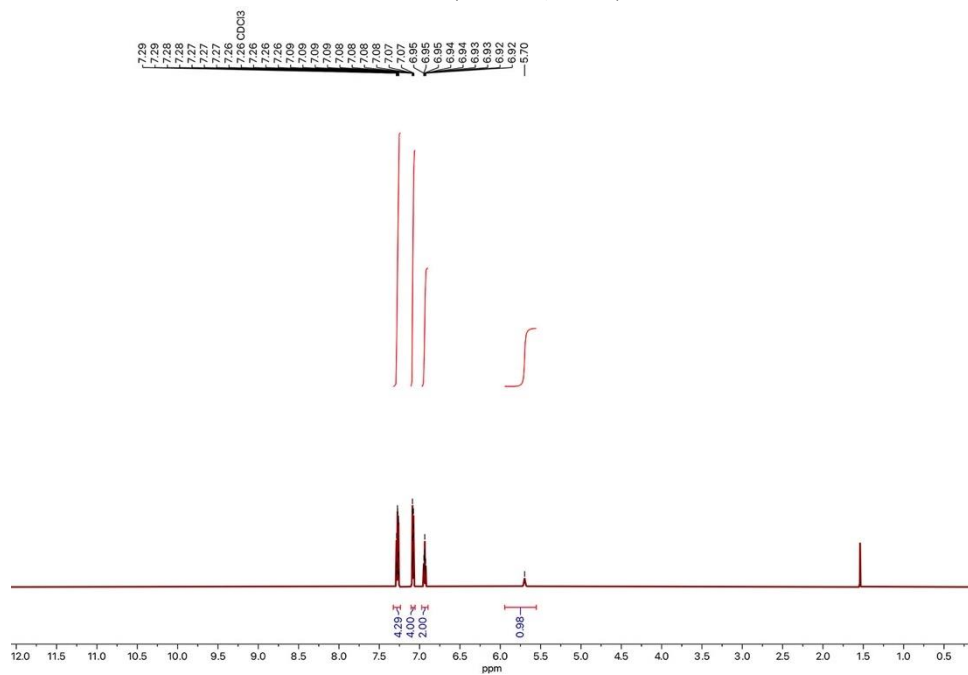
¹³C{¹H} NMR (150 MHz, CDCl₃)



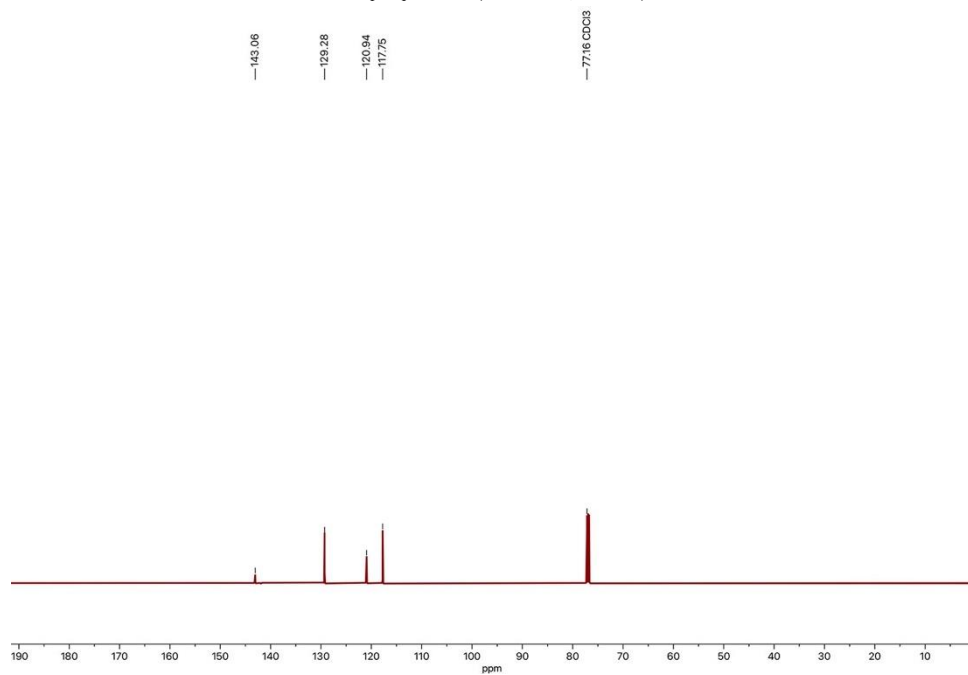


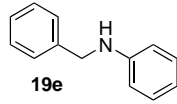
19c

¹H NMR (600 MHz, CDCl₃)



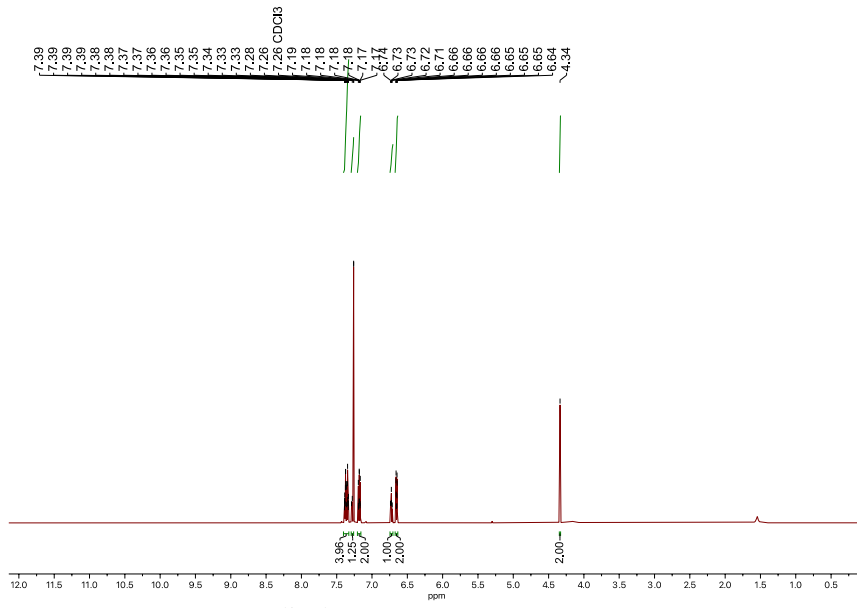
¹³C{¹H} NMR (150 MHz, CDCl₃)



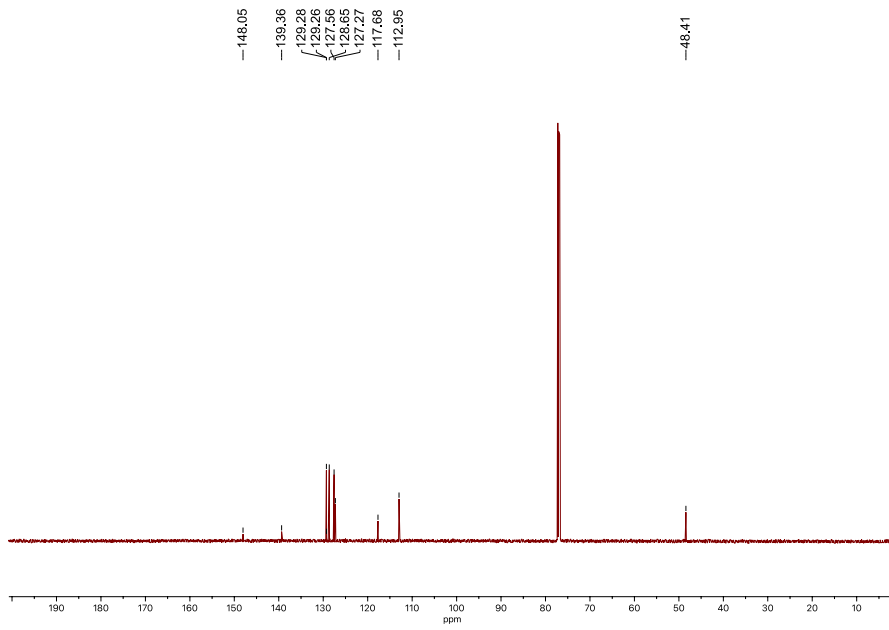


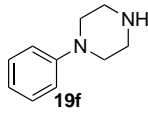
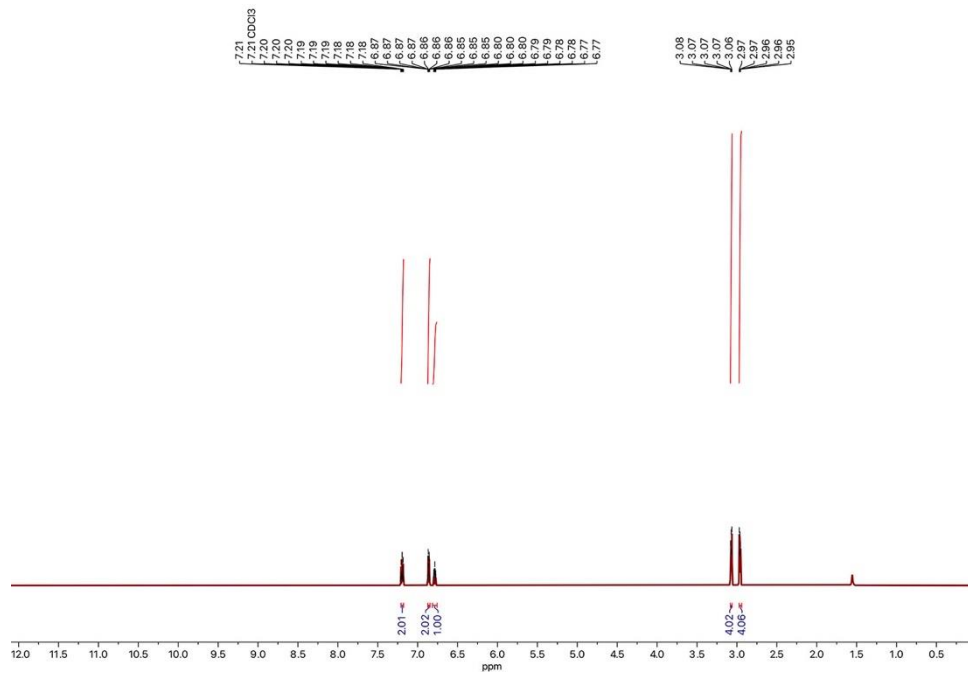
19e

$^1\text{H NMR}$ (600 MHz, CDCl_3)



$^{13}\text{C}\{^1\text{H}\}$ NMR (150 MHz, CDCl_3)



**19f****¹H NMR (600 MHz, CDCl₃)****¹³C{¹H} NMR (150 MHz, CDCl₃)**